DESIGN AND DEVELOPMENT OF MICROSTSRIP PATCH ANTENNA FOR DETECTION OF BREAST CANCER

A Dissertation Submitted in Partial Fulfillment of the Requirement for the Award of the Degree of

MASTER OF ENGINEERING

in

Wireless Communications

Submitted By

ARASHPREET KAUR SOHI

Roll No. 801563001

Under Supervision of

Dr. Amanpreet Kaur

Assistant Professor, ECED

ELECTRONICS AND COMMUNICATION ENGINEERING DEPARTMENT

THAPAR UNIVERSITY, PATIALA, PUNJAB

JUNE, 2017

DECLARATION

I, Arashpreet Kaur Sohi hereby declare that the work presented in this thesis entitled "Design and Development of Microstrip Patch Antenna for Detection of Breast Cancer" in partial fulfillment of the requirement for the award of degree of Master of Engineering(Wireless Communications) submitted at Electronics and Communication Engineering Department, Thapar University, Patiala is an authentic record of work carried out under supervision of Dr. Amanpreet Kaur (Assistant Professor), ECED, Thapar University from 2016 to 2017. The matter presented in this has not been submitted either in part or full to any other university or institute for the award of any other degree.

Arashpreet Kaur Sohi

Date: 15-07-2017

(Arashpreet Kaur Sohi)
(801563001)

It is certified that the above statement made by the candidate is correct to the best of my knowledge and belief.

Amanpreet Kaur

Date: 15/7/17

(Dr. Amanpreet Kaur)
(Assistant Professor)

ACKNOWLEDGEMENT

First and foremost, I evince my profound reverence and deep regards to my guide **Dr. Amanpreet Kaur, Assistant Professor**, Electronics and Communication Engineering Department, Thapar University, Patiala for her exemplary guidance and constant encouragement throughout the course of this thesis. I consider it my good fortune to have consociated with her.

I would also like to evince a deep sense of gratitude to **Head of Department of Electronics and Communication Engineering, Dr. Alpana Agarwal for** providing me adequate environment in carrying the work. I would like to extend my gratitude to entire staff and faculty of Electronics and Communication Engineering Department who directly or indirectly assisted me in the process and contributed towards this work.

Also, I would give special thanks to **Dr. Rajesh Khanna, Professor,** Electronics and Communication Engineering Department, for sharing his knowledge and allowing me to use the experimental facilities to test my fabricated antennas.

Finally, I would like to pay high regards to my family for their tireless love, sincere encouragement and continuous support throughout my research work and lifting me uphill this phase of life.

Arashpreet Kaur Sohi

Arashpreet Kaur Sohi

801563001

ABSTRACT

The utility of ultra wideband technology in the field of wireless communication systems has attained much attention in recent years due to its inherent advantages of large bandwidth, low power consumption and high speed short distance data transmissions. UWB antennas can be used for the detection of tumors and cancer using Radar based Microwave Imaging technique. Here the same antenna is made to transmit to an affected area and receive back from the same area. Based upon the difference between the received reflected signals from the normal and malignant breast tissues, tumors can be detected. Therefore, this thesis documents the development and analysis of four microstrip patch antennas with an overall aim to achieve ultra wideband (3.1GHz to 10.6GHz) and miniaturization characteristics using different patch geometries and defected ground structure. The first antenna geometry presented here consists of a staircase shaped slotted patch antenna with a reduced DGS which operates in the frequency band from 3.11GHz to 12.93GHz with bandwidth of 9.82GHz. The second antenna geometry is an extended semicircular microstrip patch antenna with a reduced DGS which covers the frequency range from 3.09GHz to 9.7GHz with bandwidth of 6.61GHz. The third antenna geometry is a fork shaped microstrip patch antenna with a reduced DGS which covers an operational band from 3.71GHz to 11.48GHz with bandwidth of 7.77GHz. The fourth antenna geometry is a stub loaded rectangular microstrip patch antenna with a reduced DGS which occupies the frequency band from 0.17GHz to 7.25GHz with bandwidth of 7.08GHz. A generalized parametric study of various antenna design parameters is executed to investigate the antenna performance and achieve optimum results. All UWB antennas are designed and simulated using CST MWS'14. To validate the simulated results for practical applications, prototype of antennas is fabricated using photolithography process and tested experimentally tested using a VNA.

The UWB fork shaped and rectangular microstrip fed patch antennas provides acceptable gains and can be used for breast cancer detection using mono-static radar based microwave imaging. A 3D planar breast phantom is modeled and simulations are carried out for by varying the distance between the breast phantom surface and UWB antenna for tumor radius of 10mm. It is observed that the reflected signals from an affected area show a lesser return loss for the same band as compared to the one without a tumor. This is because tumors have more water content and show more reflections. Therefore, the proposed UWB antennas can be successfully employed for the detection of breast cancer and tumors.

TABLE OF CONTENTS

LISTS OF FIGURES

LISTS OF TABLES

LISTS OF ABBREVIATIONS

MRI	Magnetic Resonance Imaging
UWB	Ultra wideband
RF	Radio Frequency
GPS	Global Positioning System
WLAN	Wireless Local Area Network
DGS	Defected Ground Structure
GSM	Global System for Mobile Communications
IEEE	Institute of Electrical and Electronics Engineers
WiMAX	Worldwide Interoperability for Microwave Access
IMT	International Mobile Telecommunications
NASA	National Aeronautics and Space Administration
Wi-Fi	Wireless Fidelity
HIPERLAN	High Performance Radio Local Area Network
INSAT	Indian National Satellite System
CST MWS'14	Computer Simulation Tool Microwave Studio version 2014
MSA	Microstrip Antenna
CPW	Coplanar Waveguide
USB	Universal Serial Bus
FR4	Flame Retardant-4
WPAN	Wireless Personal Area Network
PCB	Printed Circuit Board
UV	Ultra Violet
SMA	SubMiniature version A
VNA	Vector Network Analyzer
PSO	Particle Swarm Optimization

CHAPTER 1

INTRODUCTION

1.1 OVERVIEW

In the present world, breast cancer is the most common malignancy and second leading cause of death amongst women. Females are at higher risk of developing cancer with the advancing age as compared to males. Figure 1.1 illustrates the comparative scenario of developing cancer in males and females in India and U.S.A in year 2001. According to World Health Organization, in every minute a woman dies of breast cancer across the world and incidence of breast cancer is rising rapidly in the developed countries. It is reported that $1/8^{th}$ of U.S women, $1/12^{th}$ of European women and $1/40^{th}$ of Asian women are likely to develop invasive breast cancer during their lifetime. According to the report presented by International Agency for Research on Cancer in 2012, about 2, 32,000 breast cancer women were diagnosed in U.S and 1, 45,000 new breast cancer cases were detected and 70,000 women died of this disease in India. Indian women at younger age of 30s and 40s are more prone to breast cancer as compared to the older women [1].

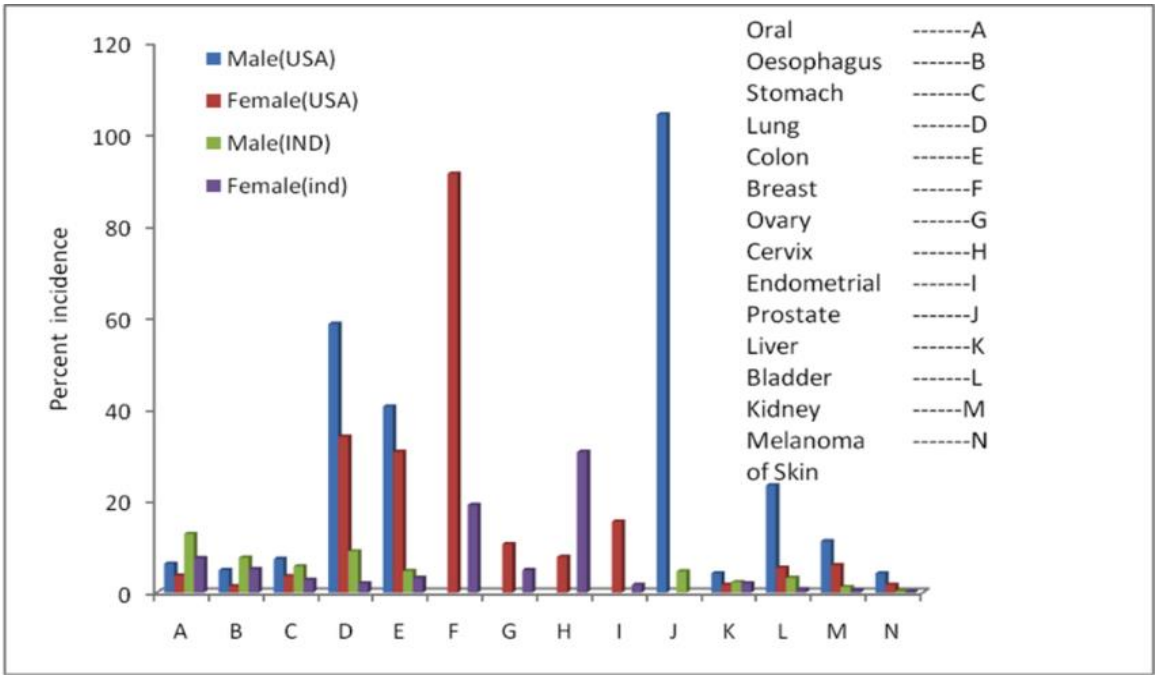

Figure 1.1 Comparison of Cancer Scenario in India and U.S.A in year 2001[1]

Breast cancer occurs when malignant cells in the breast tissue begins to grow uncontrollably. These cells result in the formation of life threatening tumors which can be felt as lump in the breast or can be observed on X-ray. It can be of invasive (spreading) or non-invasive

(localized) nature. The major cause of this prime killer disease is still unknown but extensive research works suggest that genetics, stress, family history, birth control pills, over consumption of alcohol, smoking, menstruation at an early age, giving birth to first child at old age or having no child, dense breast tissue, hormonal replacement therapy and use of estrogen and progesterone hormones can be considered as the causes for occurrence of breast cancer [2]. It can be dangerous to a level of causing death in patients too. Various stages of breast cancer are discussed as follows:

- Stage 0: Non-invasive breast cancer, no cancerous cells have spread outside the duct or lobule.
- Stage 1: Invasive breast cancer, Tumor ≤ 2cm, invasion is limited to breast.
- Stage 2a: No tumor/ Tumor ≤ 2cm, Cancerous cells in the lymph nodes, does not spread to other parts of body.
- Stage 2b: 2cm ≤Tumor ≤ 5cm, Cancerous cells in the lymph nodes, does not spread to other parts of body.
- Stage 3: Tumor can be of any size, Cancer has spread to lymph nodes near breast bone and chest wall
- Stage 4: Tumor can be of any size, Cancer has spread to other organs of the body like liver, lungs, brain or bones [3].

Early diagnosis of the breast cancer is considered to be the best way for prevention and results in more chances of survival when tumor is small in size. The type of treatment for curing breast cancer depends upon the overall health of the patient and stage of breast cancer [4]. It can turn out to be deadly if not taken seriously. Several techniques are available for its detection which is discussed in the next section.

1.2 VARIOUS TECHNOLOGIES FOR BREAST CANCER DETECTION

According to data collected by U.S Institute of Medicine in 2001, the ideal requirements for diagnostic imaging system for breast cancer should exhibit properties such as non ionizing radiations, provide minimum discomfort, earliest possible detection of malignant tumors, inexpensive, easy procedure and provide excellent tissue differentiation results. When choosing a technology for the breast imaging following goals should be kept in mind:

- Detect abnormal tissues.
- Identify the exact location of the abnormal tissue and provide its proper treatment.
- Characterize the abnormalities for the decision making process.

The techniques used for detection of breast cancer are mentioned as below:

1.2.1 X-ray mammography

Currently X-ray mammography is the most commonly used technique for the early detection of breast cancer in women who have no visible signs. X-rays are ionizing electromagnetic radiations that produce inside images of the breast called a mammogram which predicts the abnormalities in the tissue based on the differences in tissue density. Though it is a promising technique but also offers some disadvantages. Mammography uses ionizing radiation which can further increase the risk of cancer in the person undergoing the diagnosis. It requires uncomfortable and painful compression of breast which gives poor tissue contrast difference between benign and malignant tumor with high false positive and false negative results [5].

1.2.2 Ultrasound

Ultrasound is recommended for women who have dense breast tissue and are unable to undergo MRI screening or for pregnant women who should not be exposed to x-rays used in mammography due to its potential risks. Ultrasound imaging is carried out by transmitting sound waves of high frequency over the surface of tissue and recording the echoes that are reflected back by the tissue with different dielectric properties. This method of diagnosis is painless and makes use of sound waves [5]. However in many cases, it is unable to detect calcifications in breast. Hence it cannot replace mammography but can be used along with it.

1.2.3 Magnetic Resonance Imaging

MRI (Magnetic Resonance Imaging) is diagnostic procedure which is recommended for women who are at a higher risk of developing breast cancer because of a strong family cancer history. The principle of MRI is based upon the excitation of the hydrogen atoms present in the tissue when exposed to strong static magnetic field to produce images of high resolution. The tumor cells have more abundance of hydrogen atoms due to higher water content as compared to the normal tissue. So depending upon the number of hydrogen atoms present, the images of breast are recorded on the computer for detecting the tissue abnormalities. Like x-ray mammography, it is not limited by the tissue density. MRI provides excellent tissue contrast and has non-ionizing radiations. But before performing MRI screening, patient undergoing examination is given gadolinium injection in the vein to enhance tissue contrast which in turn causes headache and nausea in the patient. Though MRI is more sensitive in

detecting cancers as compared to x-ray mammography and ultrasound but it has higher false positive rate. In addition it is an expensive, time consuming and an invasive procedure [5].

1.2.4 Microwave Imaging

In order to overcome the shortcomings of above mentioned techniques, researchers are motivated to develop better alternatives for breast cancer detection. The microwave imaging is the most promising technique due to its inherent advantages such as low cost, non-ionizing radiations, does not require uncomfortable compression of breast, easily available, high sensitivity in detecting tumors and produces high resolution image which helps in differentiating between healthy and malignant tissues at microwave frequencies (300MHz-30GHz). Microwave frequencies are preferred for breast cancer detection because malignant tumors have high water content which results in larger microwave scattering as compared to than normal breast tissues with low-water content [5].

The working principle of microwave imaging is based on the significant contrast in dielectric properties (permittivity and conductivity) between the cancerous and normal tissue. The antenna is placed over the breast skin. As shown in the Figure 1.2, the amount of signal reflected back from the breast phantom in the presence of tumor is higher as compared to the normal breast tissue. In the presence of tumor, the more energy is scattered due to the difference in electrical properties between the normal and cancerous tissue which results in poor impedance matching and poor return loss characteristics when compared to normal breast tissue [6].

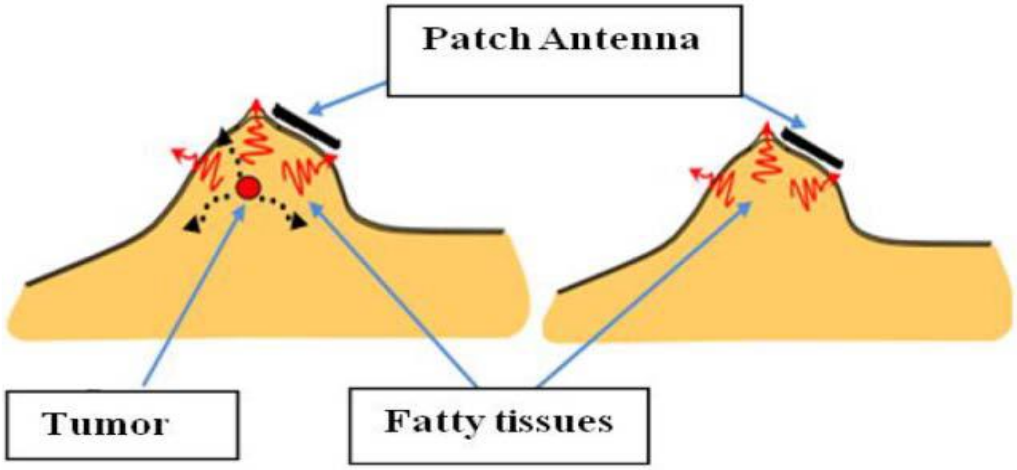

Figure 1.2 Microwave imaging concept in breast cancer detection when energy is transmitted into the breast and the reflected energy is detected in the presence and absence of cancerous cell [6]

Microwave imaging for breast cancer diagnosis can be classified in three categories:

- Passive method: This method is based upon the use of microwave radiometry which increases the temperature of tumor. This helps us to distinguish between healthy and malignant tissue [7].
- Hybrid method: This method makes use of microwaves for heating and expanding the tumor. An ultrasonic transducer is used to detect the presence of pressure waves exerted by the expanded tumor to locate the tumor [7].
- Active method: This is most preferred method as it radiates the UWB (Ultra wideband) pulse into the breast and gathers the reflected energy to construct the image of breast and detect the presence of tumor. It is further classified into two categories: tomography and radar-based technique. In tomography, single transmitter is used to transmit the waves into the breast and number of other antennas is placed around the breast to receive any scattered wave. This method is repeated to record data based upon different locations of transmitter around the breast to produce an image of breast. In radar based approach, single UWB antenna is used to transmit short-pulsed signal into the breast and the same antenna is used to receive any back-scattered wave. This method is repeated for different positions of the antenna around the breast and the travel time of signals is also recorded. When tumor is present, more energy is reflected back. This method is widely adopted as it does not require complex image reconstruction algorithms. Both microstrip patch antenna and horn antenna can be used for microwave imaging applications but microstrip patch antenna is widely preferred as it is easier to design and implement to achieve UWB characteristics [7].

1.2.4.1 Challenges in the design of Microwave Imaging System

Microwave imaging system has faced many significant difficulties in its design for biomedical applications. At microwave frequencies, a tissue with high conductivity suffers from the problem of high attenuation of the incident electromagnetic waves. Phase distortion takes place inside the biological tissues and in the surrounding regions. As a result many losses take place in the normal breast tissue and microwave imaging is used to detect tumors of small size. Such losses result in a tradeoff between spatial resolution and depth of penetration. In order to achieve better spatial resolution, high frequencies and small sized antennas are employed which in turn results in a small penetration depth inside the biological tissue. In addition it also increases the computational time required for imaging procedure. Some anatomical features of the patient also increase the complexity to construct the image [8].

1.2.4.2 Antenna for Microwave Imaging

For breast imaging, antennas with wide bandwidth, low side lobes and less mutual coupling is the preferred choice. The breast is illuminated with an ultra wideband pulse and back scattered signals are collected to produce high resolution images. In microwave breast tumor detection technique, the frequency band between 1GHz to 10GHz is desired to achieve better spatial resolution (higher frequencies) and better depth of penetration (lower frequencies). In addition, small sized antennas are required as they need to be placed on or near the breast [9]. Such requirements limit the availability of antennas. Generally antennas provide limited bandwidth and low efficiency. In literature, many UWB antennas are designed and studied for microwave imaging system such as stacked patch antenna [10], dipole [11], monopole [12], vivaldi [13], bowtie antenna [14], horn [15] and many more in order to achieve UWB characteristics. The pyramidal horn antenna provides an operational spectrum from 1GHz to 18GHz for commercial wireless applications but due large size and high cost it is less preferred to use it for diagnosis of breast cancer [15].

Microstrip patch antenna is ideally a suitable practical choice for diagnostic microwave imaging systems due to its many inherit advantages. It allows the integration of the any additional circuitry such as RF (Radio Frequency) switching, transmission lines etc required for the microwave imaging on the same board on which the antenna is fabricated. Due to small size, low cost, easy fabrication and low profile geometry, it can be used to form the imaging chamber. Using different photo etching techniques, multiple antennas can be integrated form an array on the same printed circuit board. Due to low manufacturing cost and high level of precision, it can be used in many hand held devices also. It offers both linear and circular polarization which can be obtained by selecting suitable feed position. Multiple frequency operation and radiation mechanism are also attractive qualities of microstrip patch antenna which makes it a good candidate for microwave imaging system [16]. On the other hand, microstrip patch antennas also face many challenges such as narrow bandwidth, low radiation efficiency, low gain and poor power handling capacity which can be overcome by carefully choosing appropriate antenna geometry [17].

1.3 STUDY OF MICROSTRIP PATCH ANTENNA

A Microstrip patch antenna is conventionally a narrow band wide beam antenna which is composed of two thin metallic layers, upper layer is radiating patch of any planar or non planar geometry with ground plane at the lower end and a thick dielectric substrate with low dielectric constant is added between them for better radiation due to the presence of more

loosely bound fields, higher efficiency and wide bandwidth. Figure 1.3 shows the configuration of microstrip patch antenna. Microstrip patch antenna is also called Printed patch antenna. It works similar to the parallel plate capacitor and can be used at microwave frequencies. They have numerous advantages such as small dimensions, low manufacturing cost, easily fabricated and can be directly printed on circuit boards. The radiating patch is fed along centerline of symmetry which minimizes the excitation of undesirable modes [18]. A thin patch is selected such that thickness of patch $t << \lambda$ where is wavelength in free space. Substrate can be made of different dielectric materials with dielectric constant ranging from $2.2 \leq \varepsilon_r \geq 12$ and height of substrate ranging from $0.003\lambda \leq h \geq 0.05\lambda$ where λ is wavelength in free space [19].

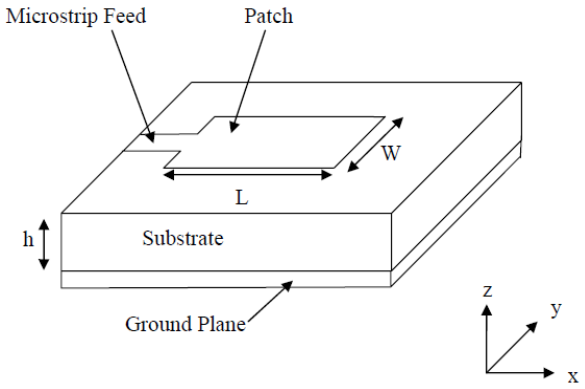

Figure 1.3 Configuration of Micro strip patch antenna [19]

Patch is made up of some high conductivity metal such as copper and can be designed with any shape such as square, rectangular, triangular, annular ring, circular etc. but rectangular and circular configurations are commonly preferred [19]. Figure 1.4 shows different patch shapes for microstrip patch antenna.

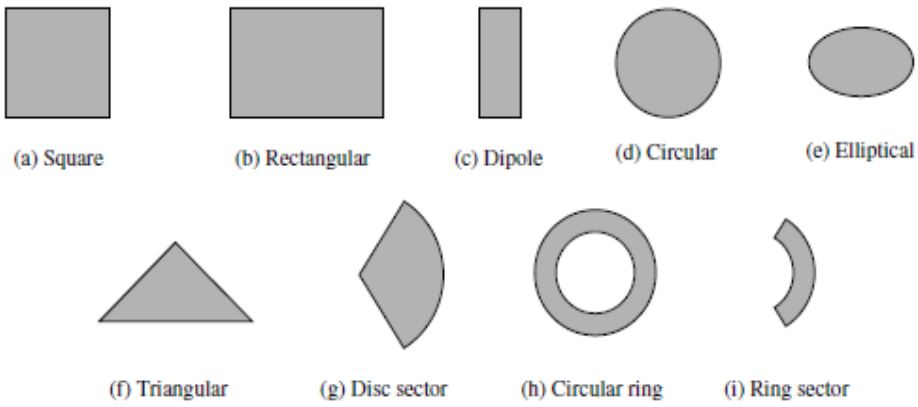

Figure 1.4 Different patch designs of Microstrip patch antenna [19]

1.3.1 Advantages of Microstrip patch antenna

Microstrip patch antenna has gained much antenna in past years as it has better prospects and numerous advantages over conventional microwave antenna which are as follows:

- Simple two dimensional physical geometry
- Light weight and Compact size
- Provides Multiple frequency operation
- Ease of fabrication and conformity
- Low manufacturing cost
- Provides both linear and circular polarization by selecting appropriate feed position.
- Mechanically robust
- Easy to integrate with monolithic microwave integrated circuits [20].

The major limitations of microstrip patch antenna are narrow bandwidth and low gain. In recent years, researchers have reported different techniques to overcome the limitations imposed by microstrip patch antenna by using appropriate antenna geometry. Some of techniques are as follows:

- By choosing appropriate feed dimensions and by adding a tuning stub to the feed line provides good impedance matching performance of antenna [21].
- Defected ground structure and staircase shaped geometry provides improvement in bandwidth and gain [22].
- Fractal antenna with multilayer configuration can used to increase the operational bandwidth [23].
- Proper array configuration to improve gain and power handling capacity [24].
- Using appropriate feeding technique and slotted patch structure [25].
- Thick dielectric substrate with lower dielectric constant is used to enhance the bandwidth [26].
- Surface wave losses can be eliminated using photonic band gap structure [27].

1.3.2 Radiation Mechanism of Microstrip patch antenna

When power is provided to half wavelength long rectangular microstrip patch, it establishes the charge concentration on the upper and lower surfaces of patch as well as on the ground plane surface. The current (magnetic field) is maximum at the center, zero at end (open circuit) and zero at the beginning (theoretically) of the half wavelength patch while the

voltage (electric field) is zero at the center of the patch, minimum and maximum at the two edges of the patch which change continuously according to the instantaneous value of signal applied. The electric field lines do not stop abruptly near the patch edges but they start to bend outwards in the free space at the patch edges. Such field extensions add up in phase and are responsible for the radiation of the micro strip patch antenna. Therefore, patch antenna is act as a voltage radiator. Figure 1.5 illustrates the radiation mechanism of microstrip patch antenna. The fringing fields can be enhanced by increasing the width of the patch, by increasing substrate thickness or by decreasing the dielectric constant of the substrate. Due to fringing effect, the effective electrical length of the patch is longer than its physical length [28].

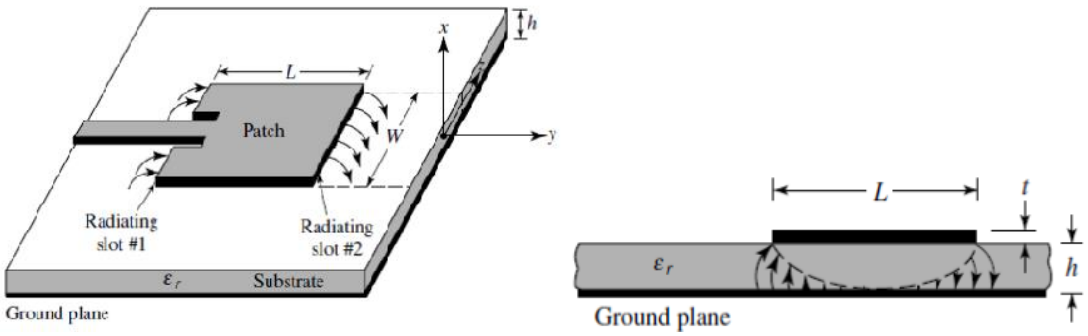

Figure 1.5 Front and side view of the Microstrip antenna showing radiation mechanism [28]

1.3.3 Feeding Techniques

Variety of Contacting and non-contacting feeding methods are available to excite microstrip patch antenna. In contacting feeding scheme, there is a direct transfer of the power to the radiating patch through a connecting element. In non-contacting scheme, power transfer between connecting element and radiating patch takes place through electromagnetic field coupling [29]. The most widely used methods of feeding are microstrip line, coaxial probe, aperture coupling and proximity coupling which are discussed in this section.

- Microstrip Line Feed: It is one of the simplest feeding techniques as it consists of conducting strip which is directly connected to the edge of microstrip patch as shown in the Figure 1.6 (a).The major disadvantage of this technique is narrow bandwidth and increased surface wave radiations [29].
- Coaxial or Probe Feed: In this technique, the inner conductor of the coaxial cable is soldered to the radiating patch of the antenna through the dielectric substrate and the outer conductor is attached to the ground plane as shown in Figure 1.6(b). It provides

low spurious radiations but has disadvantage of narrow bandwidth and difficult to design in case of thick substrate [29].

- Aperture Coupled Feed: In this technique, the radiating patch is etched on the upper substrate and microstrip feed line is etched on lower substrate with a slot on the ground plane as shown in the Figure 1.6(c). It provides wide bandwidth but most difficult to fabricate due to increase in overall thickness of antenna [29].
- Proximity Coupled Feed: It consists of two dielectric substrates which feed line sandwiched in between them and the radiating patch is etched on the upper substrate as shown in Figure 1.6(d). It offers largest bandwidth and reduced spurious feed radiations. But it is difficult to fabricate and increases the overall antenna thickness [29].

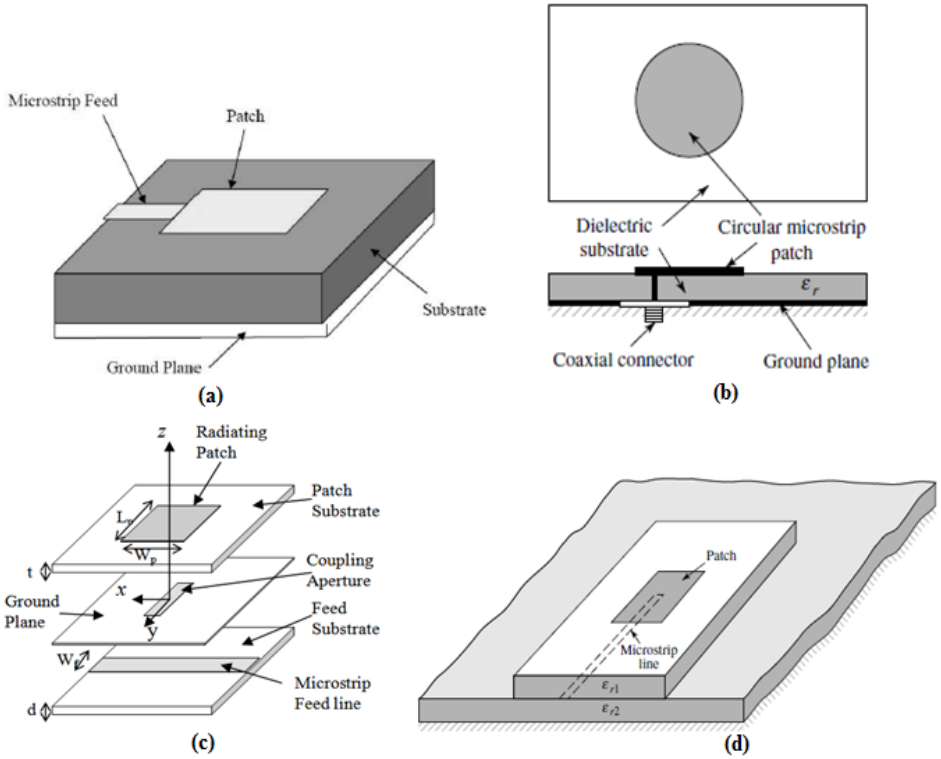

Figure 1.6 Feeding Techniques (a) Microstrip Line Feed (b) Coaxial or Probe Feed (c) Aperture Coupled Feed (d) Proximity Coupled Feed [29]

1.3.4 UWB Antenna

UWB technology have gained much attention in wireless communication systems in past few years due to the increasing demand of high speed and high data rate applications. UWB is a promising solution due to its numerous advantages such as high bandwidth, short range wireless propagation with high data rates, low power consumption with simple hardware and

reduced fading from multipath propagation. The UWB signal is defined as a signal which occupies a bandwidth ranging from 500MHz to 7.5GHz or fractional bandwidth is more than 0.2 [30]. The basic concept of UWB radio system is to transmit and receive pulses very short duration which gives a large instantaneous bandwidth as compared to narrowband radio system which transmit and receive sinusoidal waveforms with narrow frequency spectrum. Figure 1.7 shows the comparison of UWB and narrowband communications in frequency and time domain. Since 2002, U.S Federal Communications Commission has allocated the band from 3.1-10.6GHz with transmission power limited to 41.3dBm/MHz for commercial UWB wireless applications. UWB technology is suitable for large number of services such as satellite communication, weather measurements, GPS (Global Positioning System), medical sensing, military purposes, home electronics and WLAN (Wireless Local Area Network) devices [31]. Variety of techniques is available to enhance the bandwidth of the Microstrip antenna to obtain UWB characteristics from it. These include slotted patch antenna [32], use of DGS (Defected Ground Structure) [33], U-slot technique [34], staircase shaped geometry [35], probe-feeding [36], adding stub [37], increase height of the substrate [38] etc.

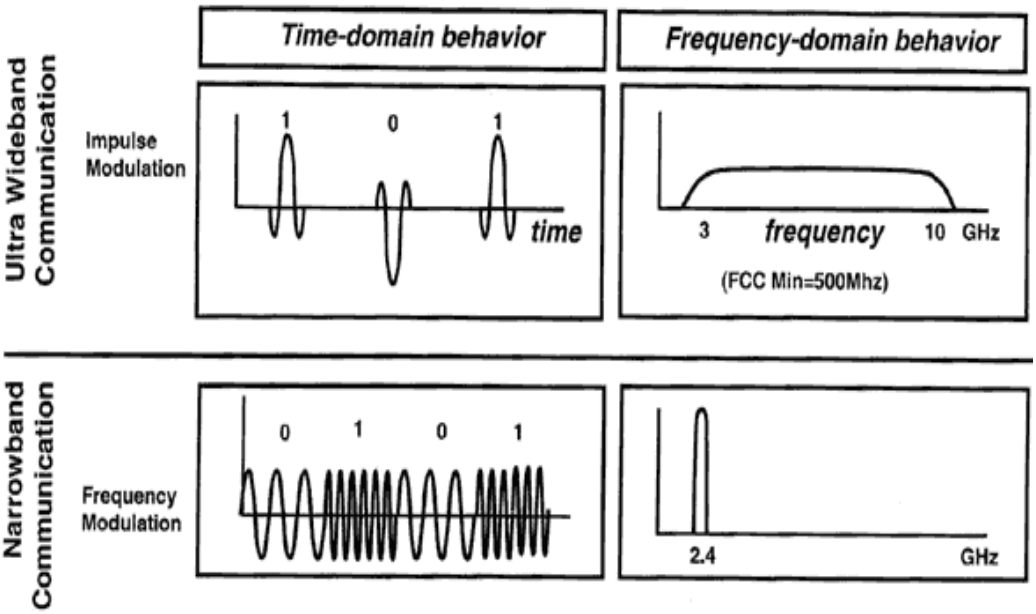

Figure 1.7 UWB versus Narrowband Communication [31]

1.4 TECHNIQUES TO ACHIEVE UWB CHARACTERISTICS USING MICROSRTIP PATCH ANTENNA

A brief insight about the numerous methods adopted to overcome the inherent disadvantages of low gain and narrow bandwidth of microstrip patch antenna and to achieve UWB characteristics are presented in this section.

1.4.1 Dielectric Substrate

For good performance of microstrip patch antenna, choosing an appropriate substrate is a crucial task as it is affects the radiation properties of the antenna and provides mechanical strength to antenna. Thin dielectric substrate with high dielectric constant is preferred for conventional microwave antenna. For microstrip patch antenna, it is preferred to use thick dielectric substrate with low dielectric constant because it makes antenna more mechanically strong and produce more fringing which in turn provides increase radiated power and improve the impedance bandwidth. But if the thickness of substrate is increased too much, it leads to large antenna dimensions and loss in accuracy [38].

1.4.2 Modified Patch Shape

In this technique, the bandwidth of conventional microstrip patch antenna can be improved by modifying the shape of the radiating patch. The rectangular and circular patch configurations can be replaced by rectangular ring [39], circular ring [40], U-shaped patch [41], Hexagonal shaped patch [42], diamond shaped patch [43], E-shaped patch [44], staircase shaped patch [45], semicircular patch [46], elliptical ring [47] etc to achieve wide bandwidth. Such modified configurations provides low quality factor as less energy is stored under the patch and provides better radiation .The current density along the edges of modified radiating patch excites additional resonances that adds up to enhance the bandwidth. It is suggested to choose the width of patch (W) larger than its length with proper excitation [48]. Figure 1.8 shows a typical staircase shaped patch antenna geometry. Staircase shaped patch antenna also provides optimized performance of Micro strip patch Antenna as it leads to the significant reduction of size of antenna, provides high gain and larger bandwidth [49].

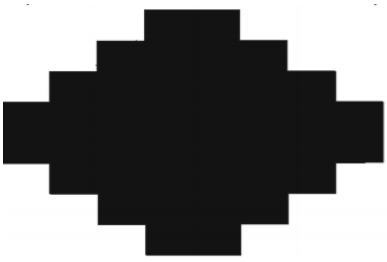

Figure 1.8 Staircase shaped patch [49]

1.4.3 Use of Slots, Notches and Tuning Stubs

Etching slot from the radiating patch is considered as effective way to improve the impedance matching performance of antenna especially at higher frequencies. The notch can be etched to

make antenna work below -10dB range, improve the peak return loss and to enhance impedance bandwidth [50]. In literature, results are presented to prove that there is substantial improvement in impedance bandwidth and impedance matching performance of antenna with addition of a tuning stub to the feeding network [51]. Figure 1.9 shows slots of irregular geometries etched from the radiating patch. Each slot affects the flow of current in the patch and excites an additional resonance which on proper optimization adds up to yield a continuous ultra wideband [52].

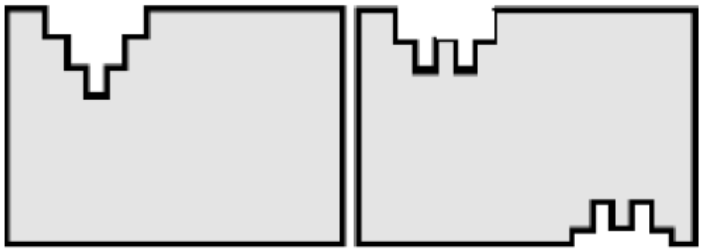

Figure 1.9 Slots with irregular geometries [52]

1.4.4 Defected Ground Structure

The concept of DGS is based upon etching some compact structures of any shape and dimension in form of single defect or periodic configuration from the ground plane according to the desired performance of microstrip patch antenna. Figure1.10 illustrates different geometries for DGS. Such geometry disturbs the shielded current distribution across the ground plane and does not require any additional circuit for its implementation [53]. This technique improves the front to back ratio of the antenna, provides compact antenna geometry and suppresses the propagation of unwanted surface waves across the substrate layer over a frequency band. It also excites additional resonance which in turn improves the bandwidth, return loss and gain of the antenna [54].

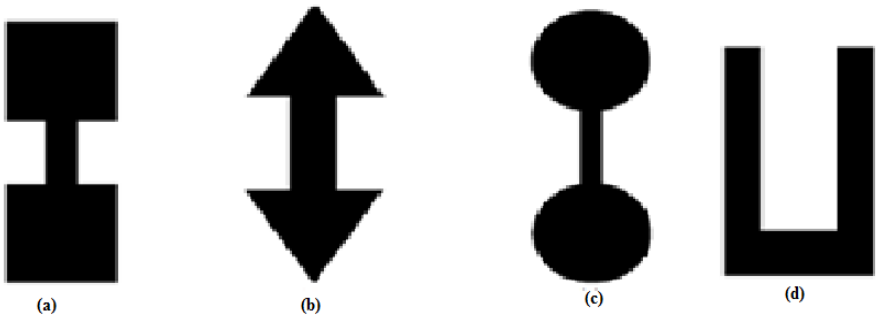

Figure 1.10 Defected ground structure geometries (a) Dumbbell shape [55] (b) Arrow head dumbbell shape [56] (c) Circular dumbbell shape [57] (d) U-shaped [58]

1.4.5 Parasitic Patch Configuration

This technique has two different configurations: Coplanar and Stacked antenna geometry which is an effective method to enhance the overall bandwidth and gain of the microstrip patch antenna. In coplanar technique, there are different types of patches printed on a single plane above substrate layer out of which only patch is connected to the feed line [59]. In stacked technique, one patch is placed above another patch with substrate layer sandwiched between them as shown in Figure 1.11. In stacked antenna technique, parasitic patch of lower permittivity is placed above the radiating patch which reduces the overall effective permittivity and maintains size of such multilayered antenna geometry and increases gain of antenna [60].

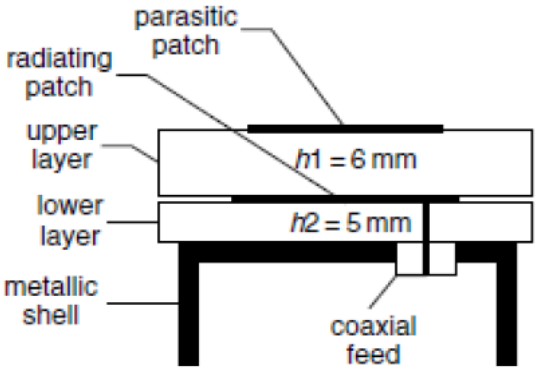

Figure 1.11 Configuration of Stacked Patch Antenna with Parasitic Patch [60]

Out of all the bandwidth enhancement techniques mentioned above to achieve UWB characteristics for microstrip patch antennas, staircase shaped geometry with DGS and use of stubs, slots and notches have been worked upon in this thesis work. Staircase shaped geometry provides good antenna performance as it leads to the significant reduction in size of antenna, provides high gain and larger bandwidth. There is sudden increment in impedance bandwidth when one or more stairs are added to the patch of antenna. The methods such as etching slot, notches and adding tuning stub are used to provide good impedance matching performance and broadband operation. The concept of employing DGS in antenna design provides size reduction and yields best results in terms of bandwidth, return loss and gain without any need additional circuitry for its implementation.

1.5 WIRELESS APPLICATIONS COVERED

Apart from the UWB applications for cancer detection, the presented antennas cover the following wireless applications that are mentioned below in Table 1.1.

Band	Frequency Range	Applications
L-band	1-2 GHz	GPS (1176.45MHz,1227.60MHz,1381.05MHz,1575.42MHz) GSM (Global System for Mobile Communications) mobile phones (800-900MHz, 1800-1900MHz) Aircraft Surveillance (962-1231MHz) Amateur Radio (1249-1300MHz)
S-band	2-4 GHz	WLAN applications (2.4-2.485 GHz) Bluetooth (2.4-2.483 GHz) Microwave ovens (2450MHz) Zig-Bee (2.4-2.485 GHz) IEEE (Institute of Electrical and Electronics Engineers) 802.16/ WiMAX (Worldwide Interoperability for Microwave Access) (3.4-3.69GHz) IMT (International Mobile Telecommunications) band (3.4-3.6GHz) Used in radar Systems such as surface ship radars, weather radars and communication satellites used NASA(National Aeronautics and Space Administration) to communicate with International Space Station and Space Shuttle
C-band	4-8 GHz	WLAN applications (5.15-5.535 GHz, 5.725-5.825GHz) Wi-Fi (Wireless Fidelity) (5.2GHz,5.5GHz and 5.8GHz) HIPERLAN-2 (High Performance Radio Local Area Network) (5.15-5.535 GHz, 5.470-5.725GHz) Downlink X-band Satellite Communication Systems (7.25-7.75 GHz) INSAT (Indian National Satellite Systems) (4.5-4.8 GHz) Radio Astronomy Band (5.01-5.03GHz) STM (Synchronous Transport Module) band (6-6.17GHz) Used for full time satellite television networks especially in areas more prone to tropical rainfall.
X-band	8-12 GHz	Amateur radio operations (10-10.5 GHz) Amateur Satellite operations (10.45-10.5GHz) Used in civil, military and government organizations for the purposes of weather monitoring, defense tracking, vehicle speed detection etc.

Table 1.1 Wireless Applications Covered

1.6 RESEARCH GAPS

An extensive literature survey is undertaken in chapter 2 for the designing of microstrip patch antennas that are capable of achieving both miniaturization and UWB characteristics. Such UWB antennas can be further employed for breast cancer detection using microwave imaging technique. Not much work is reported in literature to detect the presence of cancerous cell in breast phantom based upon reflected power from different breast tissues. In this thesis, mono-static radar based microwave imaging is proposed for the detection of malignant tumor present inside the breast structure with the help of compact microstrip patch antennas that exhibit high gain and satisfies the requirements for UWB operation.

1.7 OBJECTIVES

Rectangular, circular, triangular etc are the most commonly used patch geometries. The innovative task here will be to design new shapes for microstrip patch antennas which are capable of achieving both miniaturization and UWB characteristics. The main objectives of this thesis are summarized below:

- To design compact UWB patch antennas using microstrip feeding technique which meet the standards for microwave imaging applications. Various techniques such as use of DGS, stairs, slots, notches and tuning stubs will be worked upon in this thesis for enhancing gain and bandwidth characteristics. CST MWS'14(Computer Simulation Tool Microwave Studio version 2014) is the simulation tool which will be used for analyzing the effects of various antenna design parameters on performance of the designed antennas.
- To validate the results, the designed antennas will be fabricated, tested and compared with the simulated results in terms of Return Loss (S_{11}) values.
- To design the breast phantom with different values of permittivity and conductivity for tumor, skin layer and fat layer which can be used for microwave imaging system.
- To study the effect of using an UWB MSA (Microstrip Antenna) for detection of tumor in a breast phantom. This will be based upon the comparative study of Return loss values obtained when the same antenna is allowed to transmit and reflect from the affected breast phantom (Mono static Radar based technique).
- Analysis will be done based upon the distance variations between an UWB antenna and breast phantom surface.

1.8 THESIS ORGANISATION

The thesis is organized into six chapters which are listed below:

- Chapter 1: Overview of various technologies available for breast cancer detection and applicability of UWB microstrip patch antenna for early diagnosis of breast cancer based upon radar based active microwave imaging technology.
- Chapter 2: A literature survey related to the designing of UWB microstrip patch antenna that can be employed for microwave imaging system.
- Chapter 3: Designing, simulation and parametric analysis of four UWB antennas namely: staircase shaped slotted MSA with reduced DGS, extended semicircular

MSA with reduced DGS, Rectangular MSA with reduced DGS and fork shaped MSA with reduced DGS for UWB applications is presented.

- Chapter 4: Fabrication and testing of the designed antennas and comparison of the measured results with the simulated results in terms of S_{11} parameter values for validation of results.
- Chapter 5: Modeling of the breast phantom and simulations for the detection of breast cancer based upon Return Loss values obtained with distance variations between the breast phantom surface and UWB patch antenna.
- Chapter 6: Conclusion and the Future research work.

CHAPTER 2

LITERATURE SURVEY

This chapter gives a brief insight on the research work done in the field of designing and usage of UWB microstrip patch antenna for breast cancer detection.

2.1 MICROSTRIP PATCH ANTENNA

Pozar, D.M. *et al.* [29] in 1992 presented a general review on basic characteristics of microstrip patch antenna and various advanced developments in microstrip antenna technology in past few years. Different contacting and non-contacting feeding methods for microstrip patch antenna were discussed. More stress was paid to design new patch antenna geometries including arrays to improve the antenna performance characteristics and manufacturability.

Singh, I. *et al.* [18] in 2011 carried out a survey on microstrip patch antenna and discussed its types, feeding methods, applications, advantages and limitations over conventional microwave antennas. The major limitation of microstrip patch antenna was its narrow bandwidth and low gain which could be overcome by varying the antenna geometry and choosing appropriate feeding technique.

Dheyab, A.A. *et al.* [26] in 2011 investigated a rectangular microstrip patch antenna with different thickness (4mm, 6mm and 8mm) and dielectric constant(ε_r) of 4.4 of the dielectric substrate for bandwidth enhancement. The bandwidth of 155.1MHz, 200MHz and 150MHz and peak return loss of -21.759 dB, -57.8dB and -11.9dB was obtained for 4mm, 6mm and 8mm substrate thickness respectively at 2.4GHz resonant frequency. It could be concluded that if the thickness of substrate was increased too much, it led to large antenna dimensions and loss in accuracy.

Majidzadeh, M. *et al.* [22] in 2012 proposed a compact monopole microstrip fed patch antenna with defected ground structure to achieve UWB characteristics. Three notches were etched from the square radiating patch and rectangular slot along with three steps were etched from the reduced ground plane to excite multiple resonances and to achieve wide bandwidth. By inserting two sleeves at the lower edge of the radiating patch, even wider bandwidth was obtained. The proposed antenna covered the frequency band from 2.34GHz to 21.43GHz and the value of VSWR lies in range from 1 to 2 for entire frequency range which made it beneficial for UWB applications.

Nasr, M.A. *et al.* [21] in 2013 proposed a new technique to achieve UWB characteristics from star shaped microstrip patch antenna by shifting the microstrip line feed from the center to the edge of the patch. In addition, length of the ground plane was also optimized to enhance the bandwidth. The proposed antenna covered extremely wide spectrum from 3.9GHz to 22.5GHz.

Mandal, T. *et al.* [25] in 2013 proposed a spanner shaped regular hexagonal monopole antenna with defected ground plane for UWB communication. It was observed that proposed antenna exhibited bandwidth of 8.6GHz from 2.98GHz to 11.58GHz frequency band and yielded a small sized antenna which made it suitable for WLAN, imaging, radar and medical applications.

Kaur, A. *et al.* [23] in 2015 proposed a stacked sierpinski gasket fractal antenna with an aperture coupled feeding technique and a reduced ground with DGS for UWB and WLAN applications. It covered the operational band from 4.75GHz to 5.28GHz and 6.8GHz to 7.2GHz with gains of 5.85dB and 9dB at the center frequencies of the two bands respectively. The proposed antenna was found to be appropriate for UWB communication systems.

Kumar, A. *et al.* [20] in 2016 discussed various bandwidth enhancement techniques for microstrip patch antenna. The techniques such as feeding methods, parasitic patch, etching slots and notches, air gap, choosing appropriate material for substrate, defected ground structure and many more were introduced to improve the gain and bandwidth of antenna without increasing its height and volume.

2.2 MICROSTRIP PATCH ANTENNA FOR MICROWAVE IMAGING AND DETECTION OF BREAST CANCER

Rufus, E. *et al.* [14] in 2008 designed a compact rounded bow-tie antenna for microwave imaging applications. The proposed antenna provided a good peak return loss of -24dB at 5.8GHz frequency, moderate gain of 5dB and omnidirectional radiation pattern was exhibited by this antenna which made it a suitable candidate for early detection of breast cancer using microwave imaging.

Adnan, S. *et al.* [16] in 2010 proposed an UWB circular patch antenna design for early detection of breast cancer. The affect of variations of a size of ground plane, feed length and diameter of circular patch on the bandwidth and the return loss were studied. The proposed antenna covered a frequency band from 3.5GHz to 8GHz with good directional radiation

pattern and high gain of 8dB over most of the frequency band which was suitable for microwave imaging applications.

Banu, S. *et al.* [9] in 2013 proposed a circular patch antenna fed by microstrip line of 50Ω input impedance with a rectangular slot etched from the ground for microwave imaging system. The proposed antenna provided a peak return loss of -21.26dB and maximum gain of 4.48dB. A breast phantom model was designed with different permittivity and conductivity values from normal and malignant breast tissue. The proposed antenna was placed close to the breast model to determine the current densities on the fatty tissues, skin tissues and cancer. Basically the current density was used to increase the visibility of tumor to antenna. Best results were obtained when the antenna was placed in the direct contact with the breast model.

Sam, A. *et al.* [10] in 2013 compared the performance of both wide slot and stacked patch antenna for breast cancer detection using radar based microwave imaging technique. Specific absorption rate was calculated for both the antennas and it was observed that specific absorption rate for the cancerous tissue was higher as compared to the normal breast tissue for both the antennas. The simulated peak return loss of the stacked patch and wide slot antenna was -27dB and -34.17dB respectively. It was concluded that UWB wide slot antenna is a better choice for breast cancer detection as it was three times smaller in size as compared to the stacked patch and is suitable for high frequency operations.

Karli, R. *et al.* [6] in 2014 presented the design of a miniaturized rectangular microstrip patch antenna to detect malignant tumors present in the breast phantom by using microwave imaging technique. It consisted of a T-slot etched from the center of the radiating patch and an inserted slot in the partial ground plane. The designed antenna provided UWB characteristics in terms of bandwidth (2.85GHz to 13.21GHz) and exhibited a peak gain of 4.33dB. Due to the significant variations in the geometry of the ground plane by inserting a slot, the bandwidth of the proposed antenna design was improved.

Palantei, E. *et al.* [4] in 2015 studied the early breast cancer detection technique based on the reflected power from the breast tissues. A 3D homogeneous breast phantom was modeled and various numerical evaluations are carried out to study effect of various tumor sizes and distance variations between the surface of breast phantom and tumor location. Various return loss values were recorded for different sizes of tumor (10mm, 20mm and 30mm) and it was concluded that with the increase in size of the tumor, the received reflected power decreases. For early breast cancer diagnosis, the effective distance between the breast phantom surface and tumor position was assumed to be less than 2cmm. The antenna covered the frequency

band from 3.5GHz to 7.2GHz and a maximum gain of 4.4 dB was obtained at 3.9GHz resonant frequency.

Caliskan, R. *et al.* [8] in 2015 investigated an inset fed rectangular microstrip antenna structures used for early diagnosis of breast cancer using microwave imaging system. The technique covered was based on the significant contrast in the dielectric properties (permittivity and conductivity) of the cancerous and normal tissue .The proposed antenna structure operated at 2.45GHz frequency. A 3D breast structure was modeled to investigate different electromagnetic field values across the breast tissue with tumor and without tumor. Different antenna designs were studied by varying the dimensions of the ground plane and slotting on radiating patch.

Afyf, A. *et al.* [12] in 2015 proposed a compact UWB monopole antenna with a wide pentagon slot in the radiator and a T-slot etched from the width of reduced ground plane for early breast cancer detection. The proposed antenna covered the frequency band from 2.01 GHz to 4.4GHz with gain of 3.5dB at 3.6 GHz frequency which made it suitable for microwave imaging for early detection of malignant tumors.

Bohra, S. *et al.* [7] in 2016 proposed a wide slot double sided microstrip patch antenna with a fork shaped feed which could be employed for an early diagnosis of breast cancer using radar based active microwave imaging. It covered the frequency from 5.8GHz to 8.8GHz with bandwidth of 3GHz and maximum gain of 4dB at 6.3GHz. Hence the proposed antenna achieved both miniaturization and UWB features which made it a suitable candidate for radar based microwave imaging.

Hassan, N.A. *et al.* [11] in 2016 investigated various microwave imaging techniques and UWB antennas that could be used in microwave imaging for breast cancer detection along with their advantages and limitations. The microwave antennas that could be employed in imaging are dipole and monopole antenna, bow-tie antenna, Vivaldi antenna, Pyramidal Horn antenna, stacked patch antenna, Log periodic and spiral antennas. Out of all these, planar monopole antennas were the most preferred for microwave imaging because the entire imaging region could be illuminated by placing antenna close to the breast whereas in other antennas large distance was required between antenna and breast to provide proper illumination coverage.

Mahmud, M.Z. *et al.* [17] in 2016 proposed an UWB hibiscus petal pattern patch antenna with tapered feed line and a trapezoid shaped reduced ground plane for microwave imaging system. The proposed antenna covered the frequency range from 3.04GHz to 11GHz with

impedance bandwidth of 7.96GHz and provided good impedance matching characteristics. It exhibited stable omnidirectional radiation pattern with average overall gain of 5.1dB. This made the proposed antenna acceptable for UWB microwave imaging applications.

The radar based microwave imaging technique for detection of breast cancer requires small sized antennas with large bandwidth (1GHz to 10GHz), high gain and less mutual coupling. Normally the conventional microstrip patch antenna exhibits narrow bandwidth and low gain. Achieving an UWB from the conventional patch antenna requires some specific techniques which are mentioned in the next section.

2.3 DESIGN OF UWB ANTENNAS FOR MICROWAVE IMAGING APPLICATION

Choi, S.H. *et al.* [45] in 2003 proposed a compact microstrip fed patch antenna with partial ground plane for UWB applications. A slot was etched from the center of the radiating patch which was further combined with two steps on its lower end. It operated in the frequency band from 3.2GHz to 12GHz with bandwidth of 8.8GHz and exhibited a maximum gain of 5dB. There was a good agreement between the simulated and measured results.

Jung, J. *et al.* [30] in 2005 proposed a compact microstrip fed monopole antenna for UWB applications. It consisted of a rectangular radiating patch with two notches etched from its lower end and a reduced ground with DGS. The size of notches was optimized to achieve the required UWB operation. The designed antenna covered a large bandwidth of 7.9GHz from 3.1GHz to 11GHz with maximum gain of 5.26dB which made it acceptable for wireless hand held devices.

Seong, L.H. *et al.* [59] in 2005 designed a compact microstrip antenna fed by coplanar waveguide for UWB applications. For the bandwidth enhancement, curved radiating patch was combined with two steps. It covered the operational band from 3.1GHz to 8.3GHz with bandwidth of 5.2GHz and excited three resonant frequencies at 3.5GHz, 5.5GHz and 7.5GHZ. Experimentally measured results were quite closely matched to the simulated ones.

Vuong, T.P. *et al.* [34] in 2006 proposed a compact U-slotted staircase shaped planar antenna with partial ground plane for Impulse Radio UWB systems. The antenna was fed by a 50Ω microstrip line. The designed antenna covered the frequency band from 3.8GHz to 5.15 GHz and from 5.825GHz to 10.6GHz. This antenna showed good Impulse Radio UWB characteristics and could be employed within compact embedded UWB systems.

Ghassemi, N. *et al.* [36] in 2007 proposed a multilayered probe-fed microstrip patch antenna for UWB operation which was composed of one feed patch along with two parasitic patches

placed on the bottom layer and a parasitic patch placed on the top layer. These two layers were separated by an air gap. The proposed antenna configuration covered an operational bandwidth of 7.6GHz with peak gain of 7dB at 14GHz frequency which satisfied the requirements for UWB communication systems.

Dastranj, A. *et al.* [44] in 2008 designed a compact wide slot patch antenna with DGS for UWB applications. It consisted of an E-shaped radiating patch fed by 50Ω microstrip feed line and an E-shaped wide slot truncated from the ground plane. Various antenna design parameters such as feed line width and slot shapes were modified to achieve the optimized results. It covered a frequency band from 2.8GHz to 11.4GHz with bandwidth of 8.6GHz and exhibited a maximum gain of 7.5dB. There was a close approximation between the simulated and tested results.

Ping, L.C. *et al.* [32] in 2009 proposed an UWB slotted microstrip patch antenna which operated in the frequency range of 1.78 GHz to 11.13 GHz. Various antenna design parameters such as patch shape, feed width and slots were optimized to achieve good return loss characteristics. It was observed that by etching a slot from the patch and modifying the shape of patch with the addition of steps led to better return loss and larger impedance bandwidth results. Best results were obtained when slot was etched near to the feed line.

Koohestani, M. *et al.* [41] in 2009 proposed a compact U-shaped square patch antenna combined with two tuning stubs for UWB applications. The proposed antenna was fed by a CPW (Coplanar Waveguide). It covered the frequency band from 2.76GHz to 12.8GHz with bandwidth of 10.04GHz and a maximum gain of 5.3dB which showed that the antenna exhibited good UWB characteristics.

Moghadasi, M.N. *et al.* [53] in 2009 proposed a diamond shaped UWB microstrip patch antenna with a square slot truncated from the ground plane for microwave imaging applications. It covered a broad frequency spectrum from 2.9GHz to 13GHz at -10dB return loss and exhibited a maximum gain of 4dB. There was a good agreement between the simulated and fabricated antenna results. Due to compact size, low cost, simple geometry and good directional properties, the proposed antenna served as an excellent candidate for early diagnosis of breast cancer using microwave imaging system.

Zhang, H. *et al.* [47] in 2010 proposed an UWB elliptical monopole antenna with a reduced ground plane. Two slots were etched along the edges of the elliptical radiating patch to enhance the bandwidth of the proposed antenna. The effects of various design parameters such as patch shape, feed line width and dimensions of slots on return loss response were

studied. It covered a frequency band from 3GHz to 11GHz with impedance bandwidth of 7GHz. It exhibited a maximum gain of 4.5dB. The proposed antenna was fabricated and experimentally measured. There was a close approximation between experimentally measured results and the predicted UWB behavior.

Ping, L.C. *et al.* [48] in 2010 proposed a staircase shaped slotted rectangular patch with reduced ground for UWB applications. A slot was truncated from the reduced ground plane just behind the feed line. The proposed antenna exhibited both miniaturization and good UWB characteristics. It operated in the frequency range from 3.34GHz to 20GHz with impedance bandwidth of 16.66GHz and the value of VSWR lied below 2 for the entire frequency band of operation which made it applicable for wireless communication systems.

Azim, R. *et al.* [33] in 2011 presented a compact square patch antenna with multiple slots engraved on the top edge of the reduced ground plane to achieve UWB characteristics. The slots were etched to improve the impedance matching performance of antenna as the gap between the radiating patch and ground plane was increased. The proposed antenna covered a frequency band from 2.57GHz to 16.72GHz with a maximum gain of 6.28dB which made it suitable for UWB communication systems.

Kasi, B. *et al.* [37] in 2011 proposed a compact microstrip fed patch antenna with a rectangular slot etched from the radiating patch and a reduced ground plane with DGS for cost effective UWB application. A small rectangular stub was loaded on the top of the radiating patch for improving the peak return loss and shifting the frequency band towards left. The antenna covered a frequency band from 3.8GHz to 12GHz and exhibited a maximum gain of 4.5dB at 9GHz frequency which satisfied the requirement for UWB system.

Liu, L. *et al.* [40] in 2011 proposed a compact circular ring monopole antenna with reduced ground plane for UWB applications. A small rectangular slot was etched from the reduced ground plane to achieve UWB range. By optimizing the dimensions of ground plane and circular ring patch, a large bandwidth of 17.9GHz from 3.7 GHz to 14.3GHz with average overall gain of 3.97dB was obtained which made it acceptable for UWB wireless applications.

Lee, C.P. *et al.* [52] in 2011 proposed a diamond slotted microstrip patch antenna with DGS and it exhibited good UWB characteristics. Simulation of various antenna parameters were carried out in CST Microwave Studio and the design was fabricated for measurements. Simulated results showed that the antenna covered a frequency band from 3.28 GHz to 19.64

GHz whereas the measured result displayed a frequency band from 2.01 GHz to 18.67 GHz. The antenna achieved a peak return loss of -29.74dB at 10.48GHz resonant frequency and VSWR less than 2 throughout the frequency band which made it acceptable for the practical UWB applications.

Djalal, Z.K. *et al.* [43] in 2012 proposed a compact diamond shaped microstrip patch antenna where the radiating patch was combined with five steps at its lower edge and partial ground plane for UWB applications. Various antenna design parameters such as patch shape, feed line width and length of the ground plane were optimized to achieve the desired antenna performance. The proposed antenna covered a frequency range from 3.38GHz to 14GHz with bandwidth of 10.62GHz and exhibited omnidirectional radiation pattern over the entire frequency range which made it appropriate for wireless communication systems.

Wu, C.M. *et al.* [50] in 2012 proposed a miniaturized planar microstrip fed UWB antenna suitable for wireless USB (Universal Serial Bus) dongle application. By simply notching and slotting the rectangular patch, multiple resonances were excited which added to provide a continuous frequency band from 2.86GHz to 13.38GHz with overall bandwidth of 10.42GHz. The proposed antenna provided a gain larger than 3dB and VSWR lied in between 1 and 2 from the entire frequency band which made it suitable enough for proposed wireless communication applications.

Yaccoub, M.H. *et al.* [39] in 2013 proposed low cost and compact ring shaped patch antenna with reduced ground plane that was fed by 50Ω microstrip feed line for UWB applications. The proposed antenna covered the wireless band from 2.5GHz to 9.4GHz with a maximum gain of 5dB at 7GHz frequency which made it suitable for Bluetooth, WLAN and WiMAX applications.

Kaur, S. *et al.* [31] in 2014 proposed a compact staircase shaped patch antenna with double strip notch and DGS printed on FR4 (Flame Retardant) substrate to achieve UWB response. The proposed antenna was tested for different materials of substrate and the best results in terms of bandwidth and mechanical characteristics were obtained for Duroid 5880.The proposed antenna covered the dual frequency from 3.19 GHz to 4.60 GHz and 4.66 GHz to 10.02 GHz which satisfied the requirement for UWB characteristics and was thus preferred for WPAN (Wireless Personal Area Networks).

Telsang, T.M. *et al.* [46] in 2014 proposed a compact UWB microstrip patch antenna with reduced ground plane fed by microstrip line and CPW. The parametric analysis of various antenna design parameters such as semicircular patch radius and dimensions of slots were

studied which affected the antenna performance. The rectangular and semicircular slots were etched from the edge of the semicircular patch. The CPW fed and microstrip line fed patch antenna covered a frequency band from 1GHz to 28GHz and from 2GHz to 13GHz respectively. The CPW fed patch antenna exhibited a higher gain as compared to microstrip fed patch antenna at higher frequencies.

Hanapi, K.M. *et al.* [54] in 2014 proposed an elliptical UWB planar antenna fed by 50Ω microstrip feed line. Eleven step slots were truncated from the ground plane to form a DGS which resulted in bandwidth enhancement. The proposed antenna operates in the frequency range from 3.125GHz to 10.625GHz with impedance bandwidth of 7.5GHz. Tested results of the proposed antenna were in good agreement with simulated ones. The antenna was suitable for UWB communication systems due to its ease of fabrication and compact size.

Elkorany, A.S. *et al.* [38] in 2015 presented an UWB microstrip patch antenna with two unsymmetrical slots that was fed by a 50Ω coaxial probe. The parametric study of various antenna parameters such as dielectric material type, slot dimensions and substrate thickness was carried out to achieve an optimum UWB operation. It covered a frequency range from 3.9GHz to 10.3GHz with bandwidth of 6.4GHz and the gain varied from 4.5dB to 7.5dB.

George, N. *et al.* [42] in 2015 proposed a compact microstrip patch antenna with hexagonal shaped patch and a reduced ground with a rectangular slot for UWB applications. The proposed antenna operated over the frequency band from 5.73GHz to 10.8GHz with impedance bandwidth of 5.07GHz and a peak return loss of -40dB. The antenna efficiently resonated at 8.2GHz and 9.76GHz and provided a peak gain of 6dB. The proposed antenna was fabricated and tested which showed that the experimentally measured results were closely matched with the simulated results in terms of return loss.

Beigi, P. *et al.* [49] in 2015 proposed a compact wideband square monopole antenna with dual band notch characteristics for UWB applications. It consisted of a stepped radiating patch and a reduced ground plane with two rectangular slots which resulted in bandwidth enhancement and covered a frequency band from 2.35GHz to 13GHz. To achieve dual band notch characteristics, a U-shaped slot was etched from the stepped radiating patch and a butterfly shaped parasitic element was inserted in the ground plane. The designed antenna offered two rejection bands from 3.25GHz to 3.85GHz and 4.9GHz to 6.2GHz. There was good agreement between the measured and simulated results.

Kaur, A. *et al.* [35] in 2017 proposed a small staircase shaped slotted microstrip patch antenna with DGS for UWB applications. The effect of varying the patch shape and ground

plane was investigated to achieve both miniaturization and UWB characteristics. The proposed design achieved an UWB ranging from 3.11 GHz to 12.93 GHz with bandwidth (S_{11}<-10dB) of 9.82 GHz which covered S-band (3-4GHz), C-band (4-8GHz) and X-band (8-12GHz). The antenna showed a peak gain of 7.16dB at 12.6GHz frequency and had an average overall gain of 4.15dB for the entire frequency band.

Kaur, A. *et al.* [51] in 2017 proposed a half circular patch antenna with an extended length and a reduced ground with DGS for UWB applications. Various antenna design parameters such as the tuning stub, patch shape and slots were studied and compared with the main focus to achieve the best results in terms of return loss and impedance bandwidth. The designed antenna covered an ultra wideband from 3.09 GHz to 9.7 GHz with bandwidth of 6.61 GHz and a peak return loss of -26.05 dB was obtained at 4.4GHz resonant frequency. The maximum achievable gain for the proposed antenna was 4.58dB at 7.6GHz frequency.

The main objective of this research work is to design small sized UWB microstrip patch antennas using microstrip feeding by employing bandwidth enhancement techniques such as use of DGS, staircase geometry, slots, tuning stubs and notches which have been covered in chapter 3. Further in chapter 5, analysis of UWB MSA for detection of tumor inside the breast structure is carried out based upon the comparative study of return loss values obtained.

CHAPTER 3

DESIGN AND SIMULATION OF UWB MICROSTRIP PATCH ANTENNAS FOR BREAST CANCER DETECTION

This chapter presents the design and simulation of four UWB microstrip patch antennas which can be employed for microwave imaging applications. The antennas are designed using transmission line equations. The parametric analysis of various antenna design parameters such as patch shape, feed line dimensions and width of ground plane are carried out in CST MWS'14 to design an optimized antenna geometry which is capable of achieving both miniaturization and UWB characteristics.

3.1 WORKING MODEL OF MICROSTRIP PATCH ANTENNA

The proposed UWB antennas are designed using transmission line equations presented in next subsection.

3.1.1 Rectangular Microstrip Patch Antenna using Transmission line model

The design procedure for rectangular microstrip patch antenna is given below where it is assumed that dielectric constant of the substrate (ε_r), thickness of the substrate (h) and resonant frequency (f_r) are already known [19].

- Width (W_p) of the patch is calculated using Equation (3.1) as given below:

$$W_p = \frac{c}{2f_r\sqrt{\frac{\varepsilon_r+1}{2}}} \tag{3.1}$$

  where f_r is resonant frequency , ε_r is dielectric constant of substrate and c is speed of light.

- Due to fringing effect, effective dielectric constant (ε_{eff}) for $\frac{W_p}{h} > 1$ is calculated using Equation (3.2) as given below:

$$\varepsilon_{eff} = \frac{\varepsilon_r+1}{2} + \frac{\varepsilon_r-1}{2}\left[1 + 12\frac{h}{W_p}\right] \tag{3.2}$$

  where h is the thickness of substrate.

- The dimensions of patch are extended by ΔL due to fringing effect which is calculated using Equation (3.3) which is given below:

$$\Delta L = 0.412h\frac{(\varepsilon_{eff}+0.3)\left(\frac{W_p}{h}+0.264\right)}{(\varepsilon_{eff}-0.258)\left(\frac{W_p}{h}+0.8\right)} \quad (3.3)$$

- The actual length of patch (L_p) is calculated by using Equation (3.4) as given below:

$$L_p = \frac{c}{2f_r\sqrt{\varepsilon_{eff}}} - 2\Delta L \quad (3.4)$$

- The length ($L^{"}$) and width ($W^{"}$) of the substrate is calculated using Equations (3.5) and (3.6) given below:

$$L" = 6h + L_p \quad (3.5)$$

$$W" = 6h + W_p \quad (3.6)$$

Since this chapter presents the design of circular patches also. Next subsection presents the design equations of a circular MSA using cavity model.

3.1.2 Circular Microstrip Patch Antenna using Cavity model

The circular microstrip patch antenna exhibits only one degree of freedom (radius of patch). The cavity model is used for analysis of circular microstrip patch antenna. The design equations are listed below where it is assumed that dielectric constant of the substrate (ε_r), thickness of the substrate (h) and resonant frequency (f_r) are already known [19].

- Under the effect of fringing, the circular patch appears to look electrically larger. The effective radius (a_e) is determined using Equation (3.7) given below:

$$a_e = \sqrt{\left\{1 + \frac{2h}{\pi a\varepsilon_r}\left[\ln\left(\frac{\pi a}{2h}\right) + 1.7726\right]\right\}} \quad (3.7)$$

  where a is actual radius of patch, h is thickness of substrate and ε_r is dielectric constant of substrate.

- The actual radius (a) of the circular patch is evaluated using Equation (3.8) given below:

$$a = \frac{F}{\sqrt{\left\{1+\frac{2h}{\pi F\varepsilon_r}\left[\ln\left(\frac{\pi F}{2h}\right)+1.7726\right]\right\}}} \quad (3.8)$$

  where F is given as

$$F = \frac{8.791\times10^9}{f_r\sqrt{\varepsilon_r}} \quad (3.9)$$

  where f_r is the resonant frequency which is calculated using Equation (3.10) given as:

$$f_r = \frac{1.8412c}{2\pi a_e \sqrt{\varepsilon_r}} \quad (3.10)$$

where c is the speed of light.

Since the triangular notches are truncated from the ground plane of microstrip patch antenna in this chapter, design equations for right angled isosceles and equilateral triangular notches are presented in next subsections.

3.1.3 Design Equation for Right Angled Isosceles Triangular Notch

The side of right angled isosceles triangular notch for dominant TE_{10} is evaluated using Equation (3.11) given below [61]:

$$A = \frac{c}{2f_r\sqrt{\varepsilon_r}} \quad (3.11)$$

where A is side of triangle, f_r is resonant frequency , ε_r is dielectric constant of substrate and c is speed of light.

3.1.4 Design Equation for Equilateral Triangular Notch

The side of equilateral triangular notch for dominant TE_{10} is evaluated using Equation (3.12) given below [62]:

$$A = \frac{2c}{3f_r\sqrt{\varepsilon_r}} \quad (3.12)$$

where A is side of triangle, f_r is resonant frequency , ε_r is dielectric constant of substrate and c is speed of light.

3.2 DESIGN OF A COMPACT STAIRCASE SHAPED SLOTTED MICROSTRIP PATCH ANTENNA WITH DGS FOR UWB APPLICATIONS

This section presents the designing and simulation of a compact microstrip patch antenna with a staircase shaped slotted radiating patch and a reduced DGS for UWB applications. All the simulations are carried out using CST MWS'14. The simulation results are analyzed in terms of return loss, bandwidth, gain and current distribution. The parametric study of various antenna design parameters are carried out to achieve optimum UWB operation.

3.2.1 Antenna design and Specifications

Figure 3.1(a) presents the top view of the proposed antenna which is composed of a staircase shaped patch with multiple slots and is fed by 50Ω microstrip feeding line. The proposed

antenna is printed on FR4 substrate with dielectric constant of 4.4, dielectric loss tangent value of 0.0024 and thickness of 1.57mm. The dimensions of various antenna design parameters such as patch, ground and substrate are calculated using transmission line model with Equations from (3.1) to (3.6). Five stairs are added to the radiating patch, two at the lower edge and three at upper edge whose lengths and widths are optimized to achieve the desired results. There is an enhancement in bandwidth of antenna when one or more stairs are introduced in the radiating patch. A rectangular ring and two plus shaped slots are truncated from the radiating patch. In addition, patch antenna is combined with two stubs at left and right corners for shifting the frequency towards left. A tuning stub is added to lower end of feed line which improves impedance matching characteristics of proposed antenna.

Figure 3.1(b) shows the back view of proposed antenna with a reduced DGS. Dual right angled isosceles triangular notches are cut out from the reduced ground plane to achieve UWB characteristics and to improve the peak return loss. The side of right angled isosceles triangular notch is calculated using Equation (3.11). Table 3.1 presents the optimized dimensions of all the antenna parameters that are labeled in Figure 3.1(a) and (b).

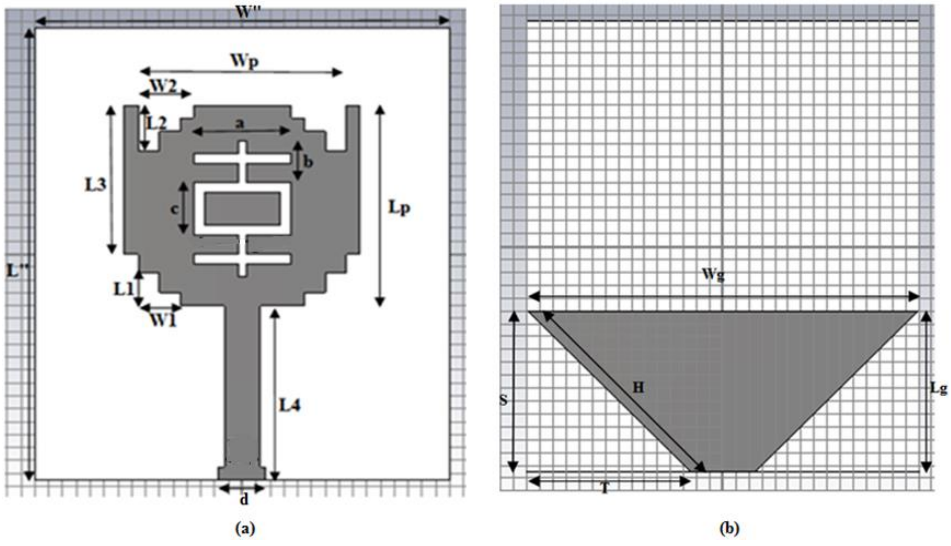

Figure 3.1 Proposed antenna design (a) Top view (b) Bottom view with DGS

Parameter	Description	Value
L”	Length of substrate	35mm
W”	Width of substrate	30mm
Lp	Length of patch	15.5mm
Wp	Width of patch	15mm
Lg	Length of ground	12.5mm
Wg	Width of ground	30mm
L1	Length of lower staircase	2.5mm
W1	Width of lower staircase	3mm
L2	Length of upper staircase	3.5mm

W2	Width of upper staircase	4mm
L3	Length of Patch stub	11.5mm
L4	Length of feed line	13.5mm
A	Width of plus shaped slot arm	7mm
B	Length of plus shaped slot arm	3.25mm
C	Length of rectangular ring	4mm
D	Width of feed line stub	3.4mm
S	Height of right angled isosceles triangle	12.5mm
T	Base of right angled isosceles triangle	12.5mm
H	Slant height of right angled isosceles triangle	17.67mm

Table 3.1 Optimized Dimensions of the proposed antenna design

3.2.2 Simulation Results and Discussions

CST MWS (Computer Simulation Technology Microwave Studio) 2014 is used for designing and simulating the results of antenna parameters such as Return Loss, Smith Chart, Gain and Current Distribution which are discussed below.

3.2.2.1 Return Loss and Antenna Bandwidth

Figure 3.2 shows the simulated return loss as the function of frequency .The return loss should be as less as possible in the negative range (below -10dB) for maximum power transfer to the antenna. The proposed antenna covers the frequency range from 3.11 GHz to 12.93 GHz with bandwidth of 9.82 GHz. A peak return loss of -30.72dB is obtained at resonant frequency of 8.47GHz which makes the antenna suitable for the UWB operation (3.1-10.6GHz), WiMAX (3.4-3.69GHz), IMT (3.4-3.6GHz), INSAT (4.5-4.8GHz), Radio Astronomy Band (5.01-5.03GHz), WLAN (5.15-5.535GHz, 5.725-5.825GHz) and Amateur Satellite operations (10.45-10.5GHz).

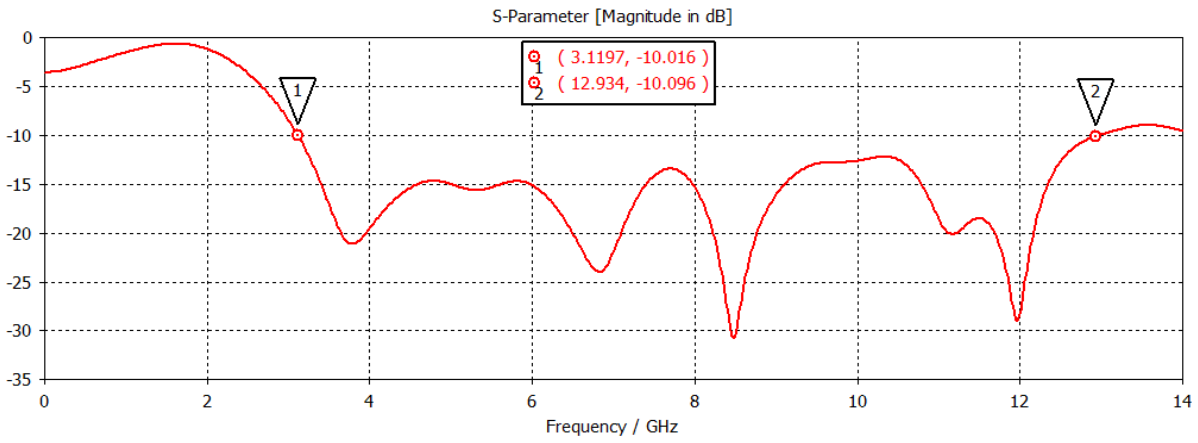

Figure 3.2 Simulated Return Loss (S_{11}) versus frequency plot of proposed antenna

3.2.2.2 Smith Chart

The smith chart for the proposed antenna is shown in Figure 3.3. It is the polar plot of complex refection coefficient which is used for visualizing the antenna impedance as the function of frequency. For proper impedance matching, the locus of the smith chart must pass through its center. It provides an impedance of 50 ohm which is makes the proposed antenna suitable for practical applications. Markers 1 and 2 represent the impedance bandwidth of antenna which is 9.82GHz from 3.11GHz to 12.93GHz.

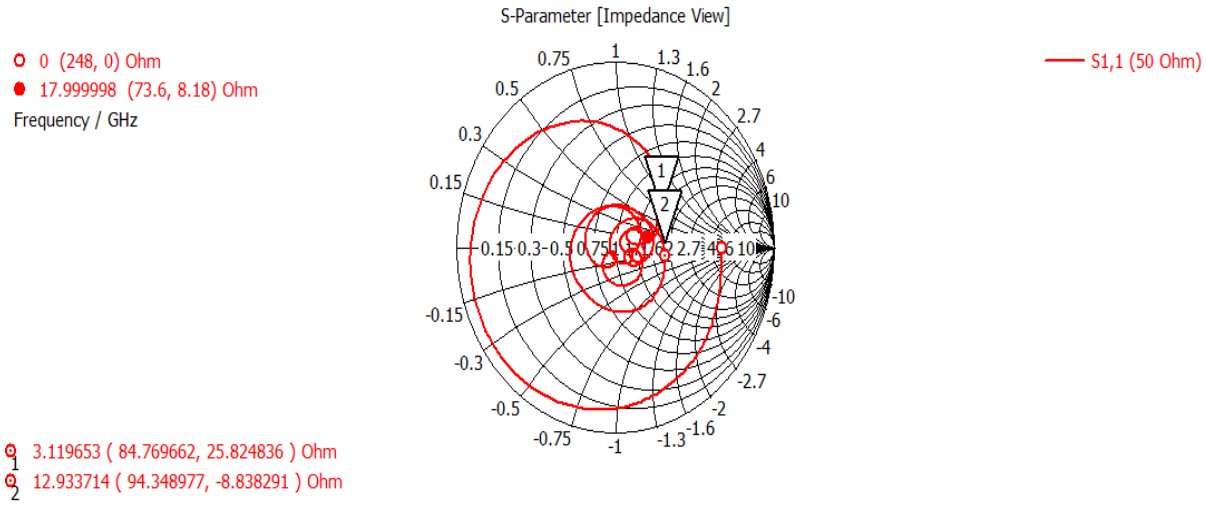

Figure 3.3 Smith Chart of proposed antenna

3.2.2.3 Gain

Figure 3.4 shows the broadband gain plot of the proposed antenna which varies as a function of frequency. The antenna shows the peak gain of 7.15dB at 12.6GHz frequency and has an average overall gain of 4.15dB for the entire frequency band of operation. Figure 3.5(a) demonstrates the 3D plot of peak gain at a frequency of 12.6GHz of the proposed UWB antenna. Figures 3.5(b) and 3.5(c) show the Elevation and Azimuth view of this gain plot. Antenna gain at transmitter determines the how well the antenna converts the input power into the radio waves moving in a particular direction and vice versa at the receiver. It should be greater than 3dB for practical UWB applications. As shown in Figure 3.5(b), the main lobe is directed at an angle of 22 degrees with angular beam width of 93.4 degrees at 12.6GHz frequency. As shown in Figure 3.5(c), the major lobe is directed at an angle of 56.0 degrees with magnitude of 0.485dB and half power beam width of 44.1degrees at 12.6GHz frequency.

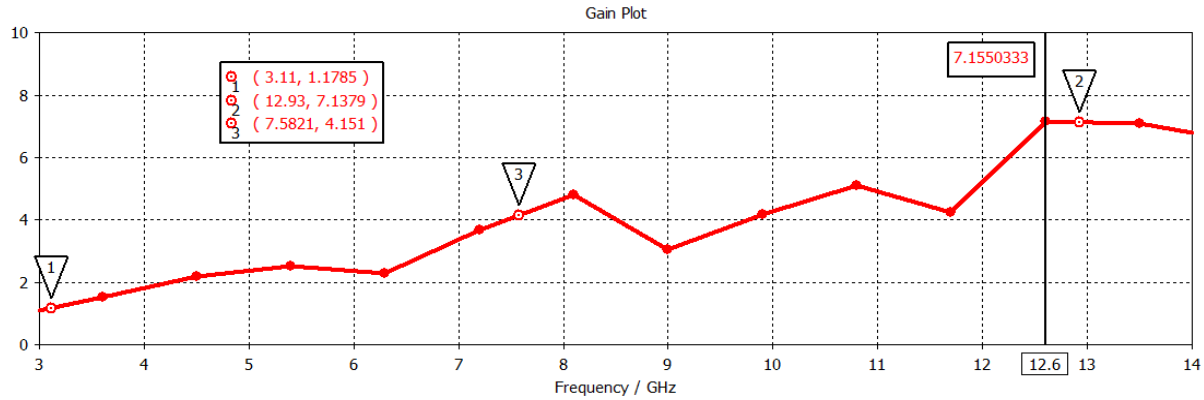

Figure 3.4 Simulated broadband gain plot against frequency

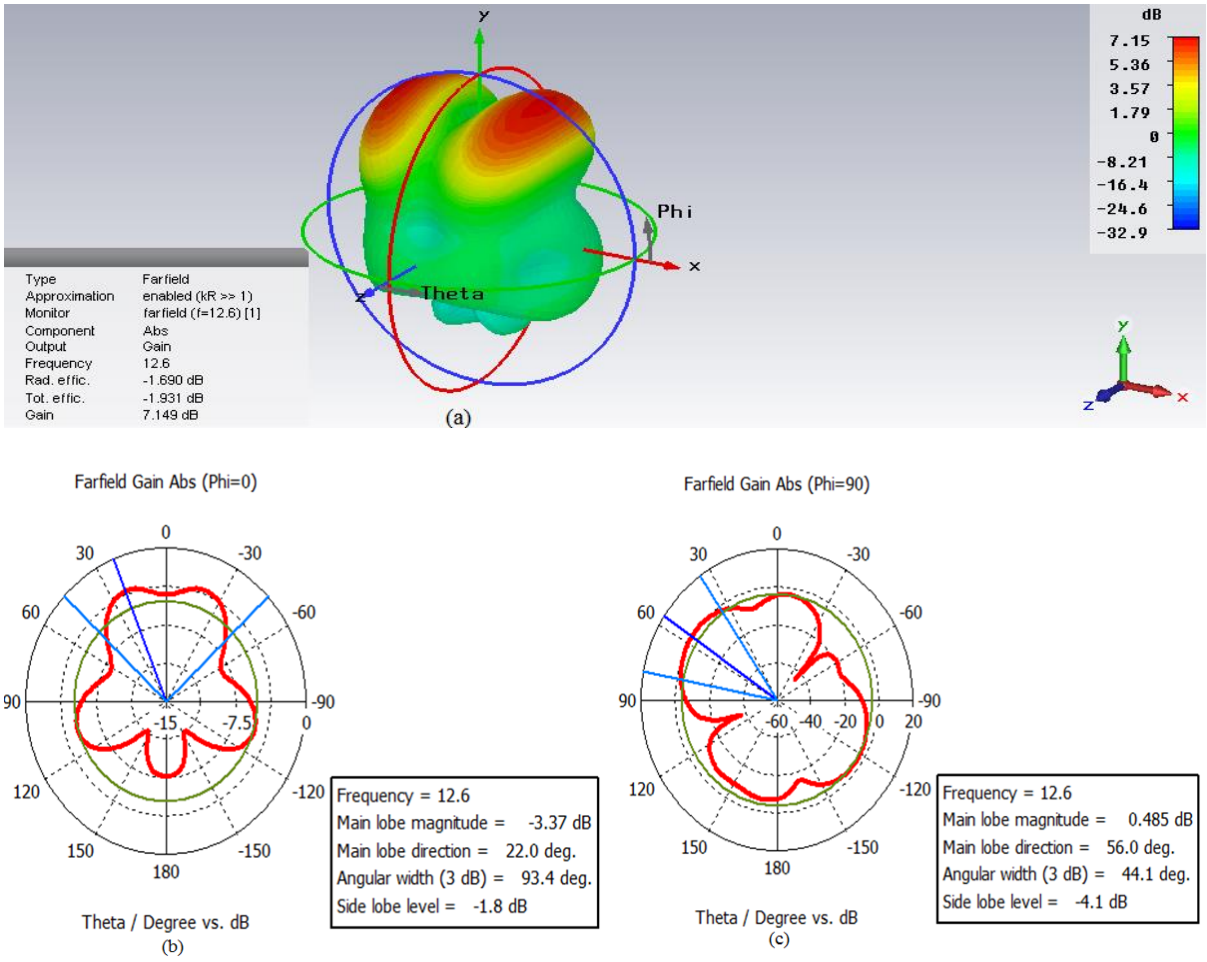

Figure 3.5 Proposed antenna (a) 3D plot of peak gain at 12.6GHz frequency (b) Polar plot for Elevation plane at 12.6GHz frequency (c) Polar plot for Azimuth plane at 12.6GHz frequency

3.2.2.4 Surface Currents

As shown in Figures 3.6(a) to 3.6(h), the proposed UWB antenna is excited at the feed point with 1W power using CST MWS'14 software to observe surface current distribution on the radiating patch and the reduced ground with DGS at four resonant frequencies of 3.77GHz,

6.82GHz, 8.47GHz and 11.97GHz. Figure 3.6 (a) and 3.6(b) show that the maximum current of 66.2A/m present along the lower boundary of the radiating patch joined to the feed line which responsible for exciting a resonance at 3.77GHz frequency. Figures 3.6(c) and 3.6(d) show that the current flows through almost the entire patch and ground plane but maximum amount of current (65.2A/m) is present at the points where the lower edge of the radiating patch is attached to the feed line which produces a resonance at 6.82GHz frequency. Figures 3.6(e) and 3.6(f) reveal that the surface current of the proposed UWB antenna is highest (96.4A/m) near the lower boundaries of the upper staircase and tuning stubs of the radiating patch which excites a resonance at 8.47GHz frequency. As shown in Figures 3.6(g) and 3.6(h), maximum magnitude of the surface current (149A/m) is present near the edges of the lower plus shaped slot of the radiating patch which is responsible for exciting a resonance at 11.97GHz frequency.

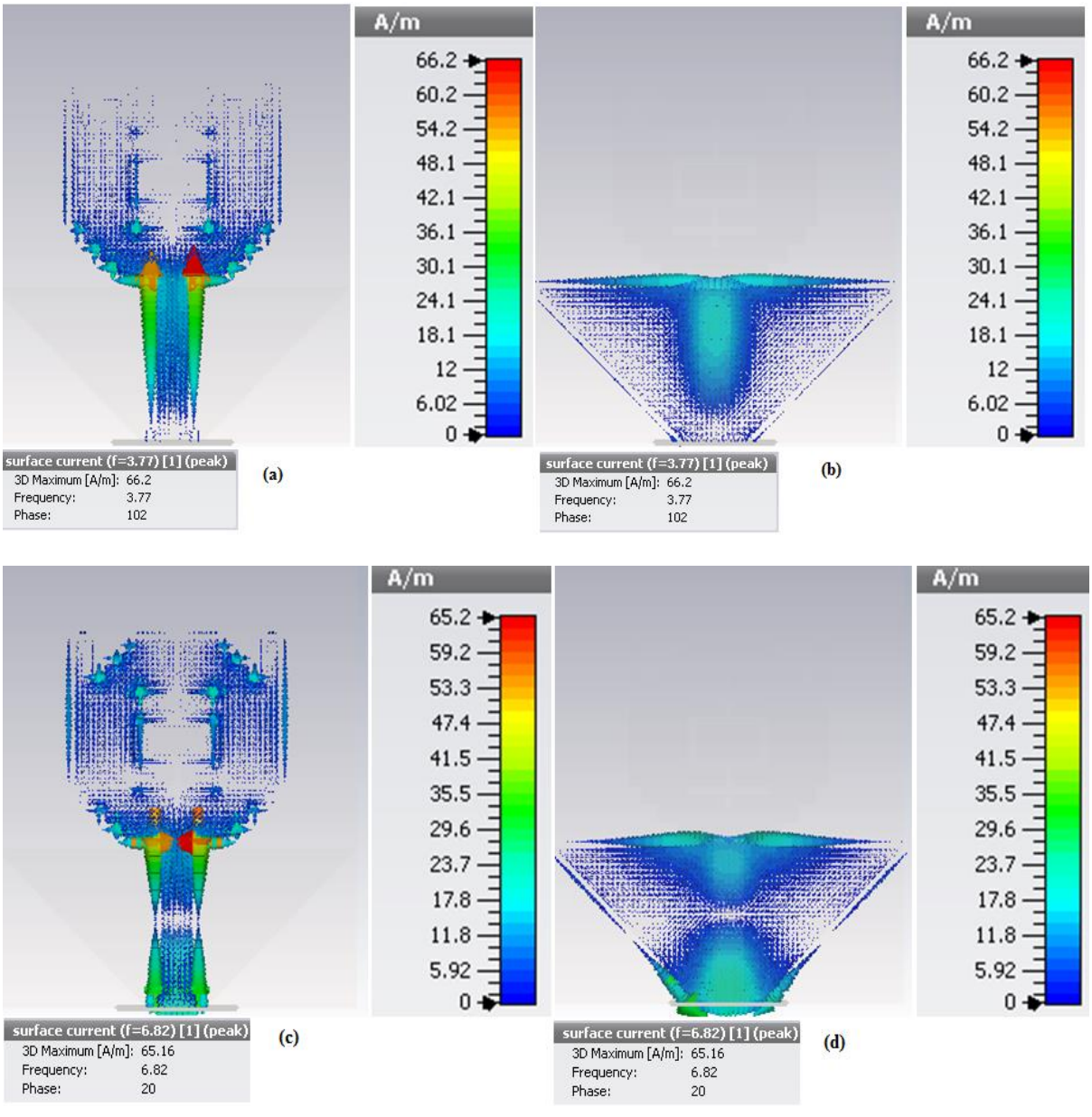

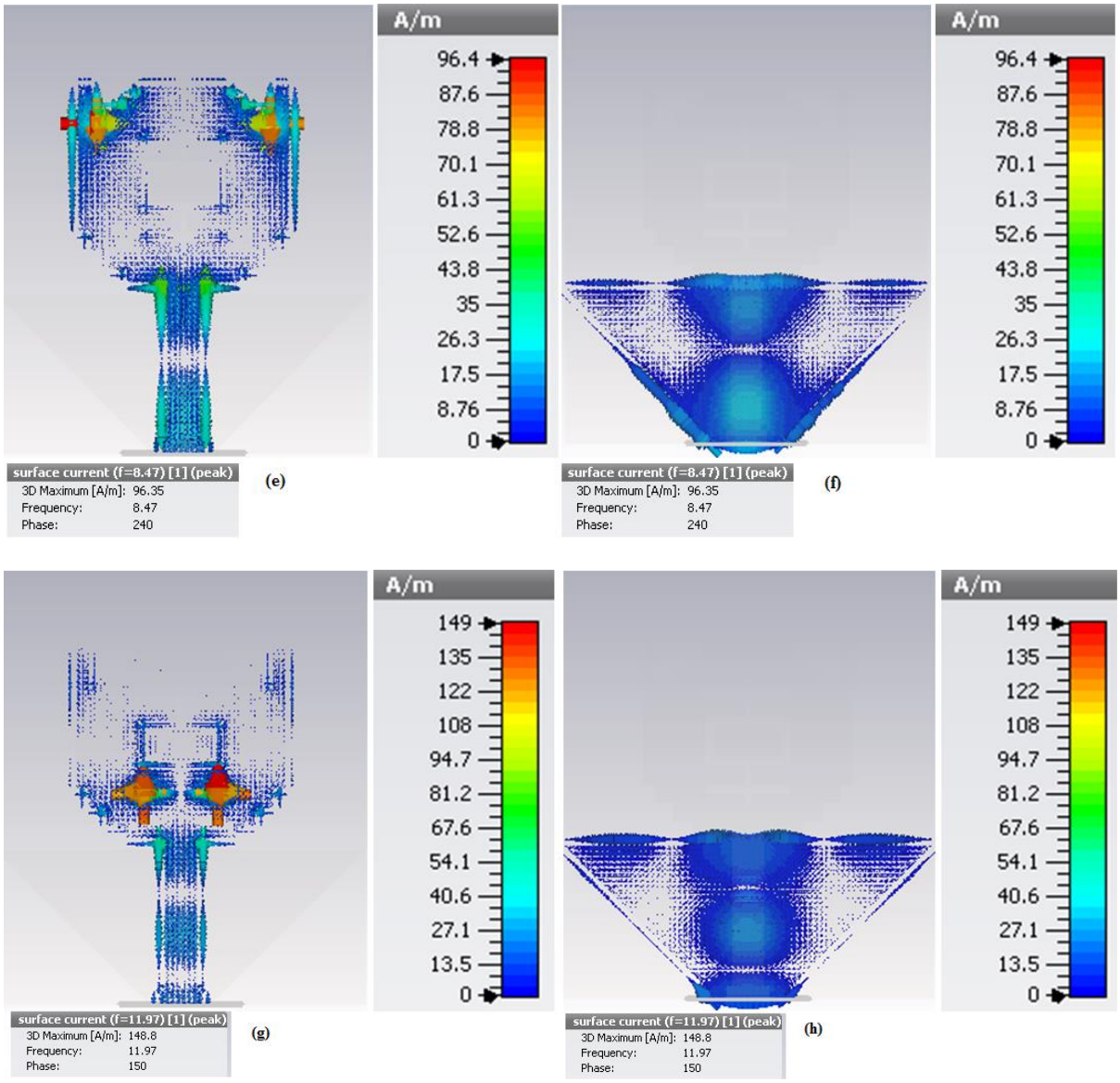

Figure 3.6 Surface current distributions at resonant frequencies of (a-b) 3.77GHz (c-d) 6.82GHz (e-f) 8.47GHz (g-h) 11.97GHz

3.2.3 Parametric variations and Antenna Optimization

The major goal of the proposed antenna design is to achieve miniaturization and ultra wideband characteristics with good impedance matching performance. In this section, various antenna design parameters such as slots, notches and tuning stubs are investigated to enhance the bandwidth of antenna. The best optimized dimensions for the antenna parameters are chosen to achieve the desired performance from the proposed antenna.

3.2.3.1 Effects of DGS

Figure 3.7 shows the design procedure of reduced DGS whose dimensions are specified in Table 3.1. Figure 3.8 represents the comparison of simulated return loss curves versus

frequency for three different geometries of the ground plane. It is observed that bandwidth of the proposed antenna with DGS is greater as compared to without DGS. The partial ground plane with length 12.5mm as shown in Figure 3.7(b) covers wide frequency band from 3.07GHz to 13.4GHz with bandwidth of 10.33GHz as compared to ground plane geometry with length 35mm as shown in Figure 3.7(a) which exhibits a multiband behavior. To improve the impedance matching performance of the designed antenna, two right angled isosceles triangular notches are truncated from the left and right corners of the reduced ground plane as shown in Figure 3.7(c). As shown in Figure 3.8, it covers an operational frequency band from 3.11GHz to 12.93GHz with impedance bandwidth of 9.82GHz which is acceptable for practical UWB applications.

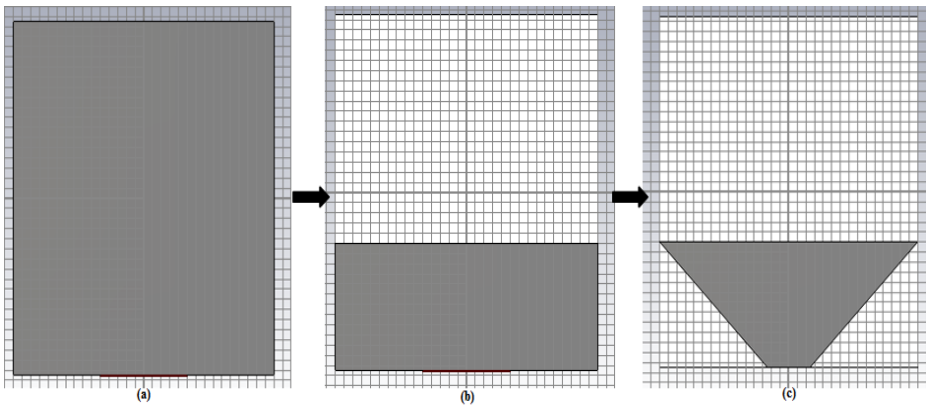

Figure 3.7 Proposed antenna designs with (a) Full ground with length 35mm (b) Reduced ground plane with length 12.5mm(c) Defective ground plane with length 12.5mm (dual isosceles triangular notches)

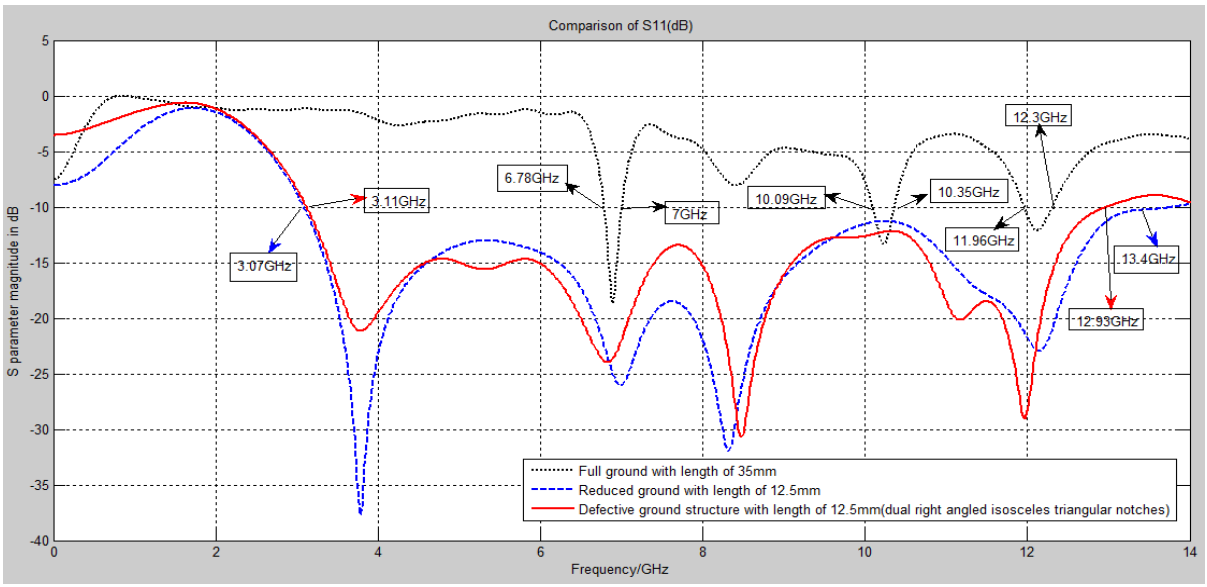

Figure 3.8 Comparisons of Simulated Return Loss (S_{11}) curve as the function of frequency for different geometries of the ground plane

3.2.3.2 Effect of the variations in patch shape

By modifying the shape of the radiating patch, bandwidth of proposed antenna can be enhanced. Figure 3.9 shows the different patch geometries of proposed antenna while keeping the other design parameters constant. Figure 3.10 shows the comparison of the simulated return loss curves against frequency for different patch geometries. As shown in the Figure 3.9(b), five stairs are added to the radiating patch, two at the lower end and three at the upper end of the patch which allows the antenna to operate in the frequency range from 3.38GHz to 12.19GHz with bandwidth of 8.81GHz and also excite additional resonant frequencies as compared to simple patch geometry. One rectangular ring and two plus shaped slots are truncated from the radiating patch as shown in Figure 3.9 (c) which slightly shifts the frequency band towards left and covers more wide frequency band as shown in Figure 3.10 as compared to the previous geometry. Further to improve peak return, the slotted staircase patch geometry is combined with two stubs added at the left and right corners of patch as shown in Figure 3.9 (d). The lengths of the tuning stubs are optimized to achieve the desired antenna performance. It provides an improved peak return loss of -48.19dB but results in bandwidth reduction. To improve the impedance matching performance and enhance the bandwidth of the proposed antenna, a tuning stub is added to the lower end of the feeding network as shown in Figure 3.9 (e). It can be observed from Figure 3.10 for the patch design presented in Figure 3.9 (e) covers frequency band from 3.11GHz to 12.93GHz with bandwidth of 9.82GHz which makes it acceptable for desired UWB operation.

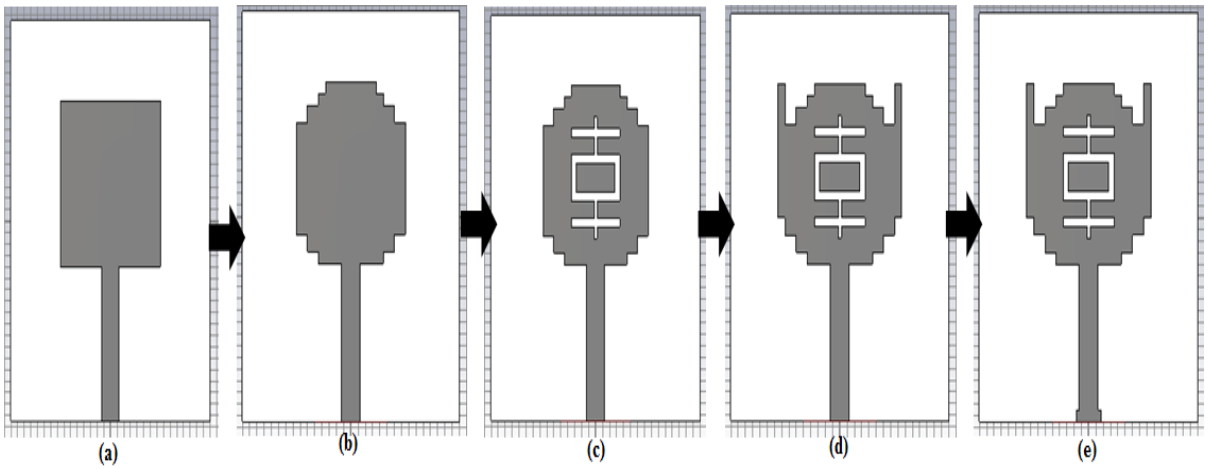

Figure 3.9 Proposed antenna design with (a) Simple patch (b) Staircase Patch(c) Staircase and slotted patch with one rectangular ring slot and two plus shaped slots (d) Staircase and slotted patch with two stubs at left and right corners of the patch (e) tuning stub added to feed line of modified patch geometry

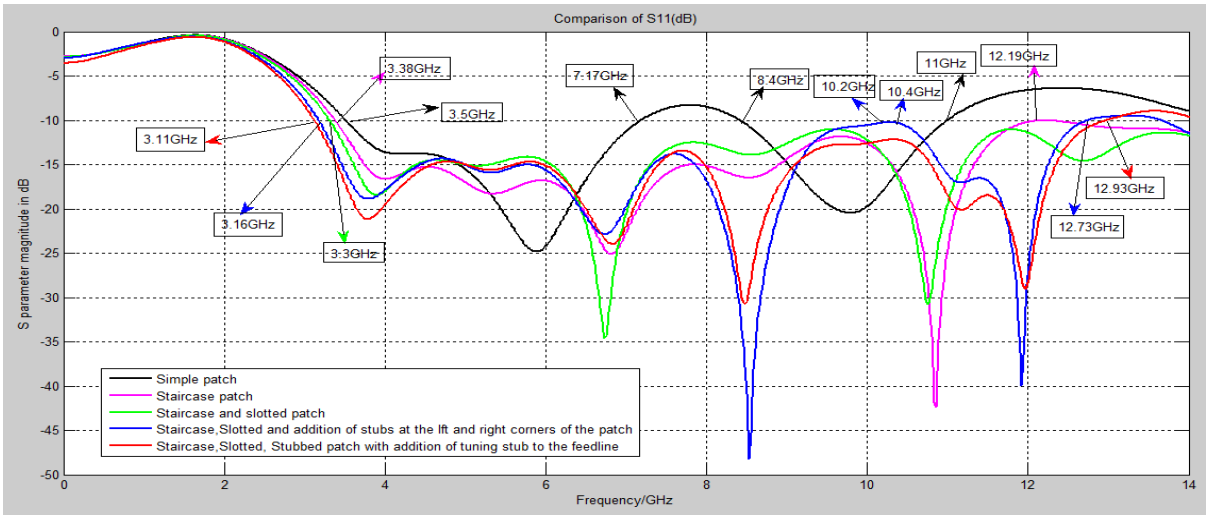

Figure 3.10 Comparisons of Simulated Return Loss (S_{11}) curve which varies as the function of frequency for different patch shapes

3.2.3.3 Effects of varying the feed width

The proposed antenna is energized by a fixed feed line positioned at the centerline of symmetry. The parameter optimized in this section is feed width which is varied to achieve good impedance matching performance for the proposed antenna. Figure 3.11 shows the comparison graph of return loss characteristics plotted against the frequency for feed width varying from 1.4mm to 3.8mm. It is observed that initially the bandwidth increases with increase in feed width from 1.4mm to 2.6mm but later it decreases with increase in feed width from 3.2mm to 3.8mm. The feed width of 2.6mm covers the largest bandwidth of 10.77GHz and efficiently resonates at 3.87GHz, 6.93GHz and 10.91GHz frequencies. Therefore, it is considered as the optimized one for the desired applications.

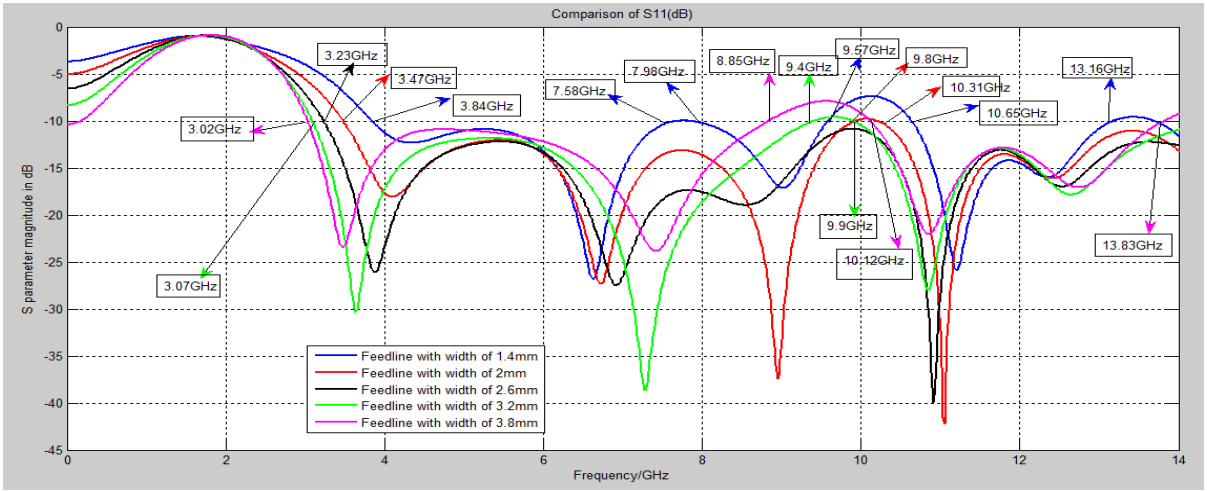

Figure 3.11 Comparisons of Simulated Return Loss (S_{11}) curve vs. frequency for different values of feed width

3.2.4 Applications Covered

The proposed antenna operates in the frequency range from 3.11GHz to 12.93GHz with bandwidth of 9.82GHz and peak return loss of-30.72dB at 8.47GHz resonant frequency. This frequency band makes the antenna appropriate for the UWB operation (3.1-10.6 GHz), WiMAX applications (3.4-3.69GHz), IMT band (3.4-3.6GHz), INSAT (4.5-4.8GHz), Radio Astronomy Band (5.01-5.03GHz), WLAN applications (5.15-5.535 GHz, 5.725-5.825GHz), Amateur radio operations (10-10.5GHz) and Amateur Satellite operations (10.45-10.5GHz).

3.3 DESIGN OF AN EXTENDED SEMICIRCULAR MICROSTRIP PATCH ANTENNA WITH REDUCED DGS FOR UWB APPLICATIONS

In this section, a half circular patch antenna with an extended length and a partial ground structure with an inverted T-shaped slot and dual right angled isosceles triangular notches is designed and simulated using CST MWS'14 for UWB applications. Various antenna design parameters such as tuning stub, patch shape and slots are optimized to achieve desired antenna performance.

3.3.1 Antenna design and Parameters

Figure 3.12(a) shows the front view of the proposed antenna which consists of a semicircular patch whose overall size is extended by combining it with a rectangular patch. The proposed antenna is fabricated on FR4 substrate with relative permittivity of 4.4, dielectric loss tangent value of 0.0024 and thickness of 1.57mm. The antenna is energized by 50 Ω microstrip feeding line. The radius of the circular patch is calculated using cavity model Equations from (3.7) to (3.10). A tuning stub is added to the lower end of the feeding network to extend the bandwidth of the proposed antenna.

Figure 3.12(b) presents the back view of the proposed antenna which consists of a reduced ground plane with a DGS. An inverted T-shaped slot is truncated from upper edge of the reduced ground plane just behind the feed line which results in improvement in return loss curve below -10dB. In addition, dual right angled isosceles triangular notches are etched from the left and right corners of the reduced ground plane to improve the peak return loss. The side of right angled isosceles triangular notch is calculated using Equation (3.11). Such antenna geometry helps to achieve both miniaturization and ultra wideband characteristics. The various antenna design parameters with their values are specified in Table 3.2.

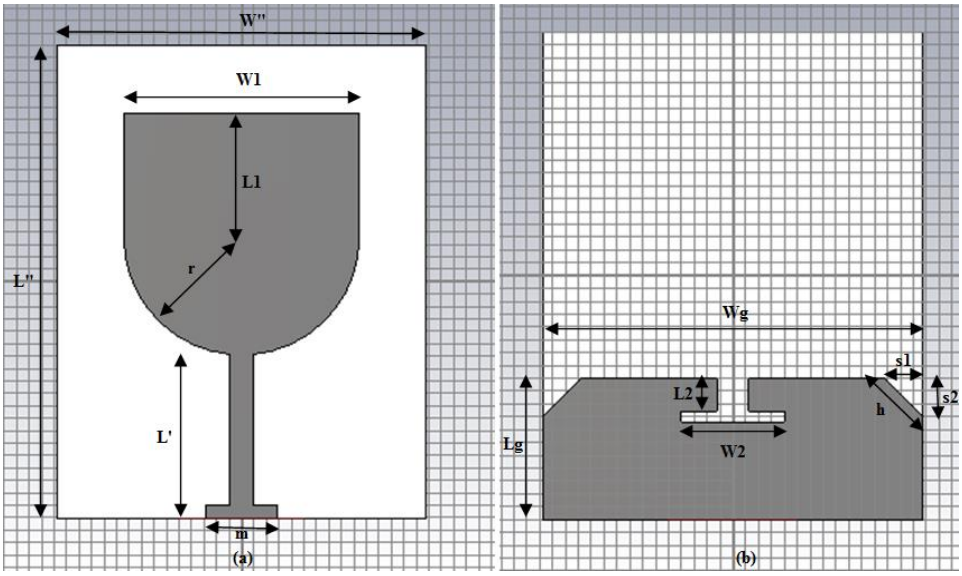

Figure 3.12 Proposed antenna design (a) Top view with an extended semicircular patch and feed line with tuning stub (b) Bottom view with a reduced DGS

Parameter	Description	Value
L”	Length of substrate	38mm
W”	Width of substrate	29.5mm
L1	Length of rectangular patch	10mm
W1	Width of rectangular patch	18.8mm
Lg	Length of ground	11mm
Wg	Width of ground	29.5mm
L’	Length of feed line	13.16mm
L2	Length of T-shaped slot	2.6mm
W2	Width of T-shaped slot	8mm
s1	Base of right angled isosceles triangular notch	3mm
s2	Height of right angled isosceles triangular notch	3mm
h	Slant height of right angled isosceles triangular notch	4.36mm
m	Width of feed line stub	3.4mm
r	Radius of semicircular patch	9.4mm

Table 3.2 Optimized Design Parameters of the proposed antenna

3.3.2 Simulation Results and Discussions

This section presents the simulation results of the proposed antenna for Return Loss, Smith Chart, Gain and Surface Current distribution using CST MWS’14.

3.3.2.1 Return Loss and Antenna Bandwidth

Figure 3.13 shows the S_{11}(dB) plot of the proposed antenna with respect to the frequency. The antenna resonates efficiently at 4.4GHz, 6.6GHz and 8.8GHz frequencies. A peak return loss of -26.05 dB is obtained at 4.4GHz resonant frequency which reveals that the proposed

antenna exhibits good impedance matching characteristics and power loss is minimal. It covers the frequency band from 3.09GHz to 9.7GHz with impedance bandwidth of 6.61GHz which makes the antenna suitable for UWB operation (3.1-9.7GHz), IMT band (3.4-3.6 GHz), WiMAX applications (3.4-3.69GHz), INSAT (4.5-4.8 GHz), Radio Astronomy Band (5.01-5.03GHz), WLAN applications (5.15-5.825GHz) and Downlink X-band satellite communication (7.25-7.75GHz).

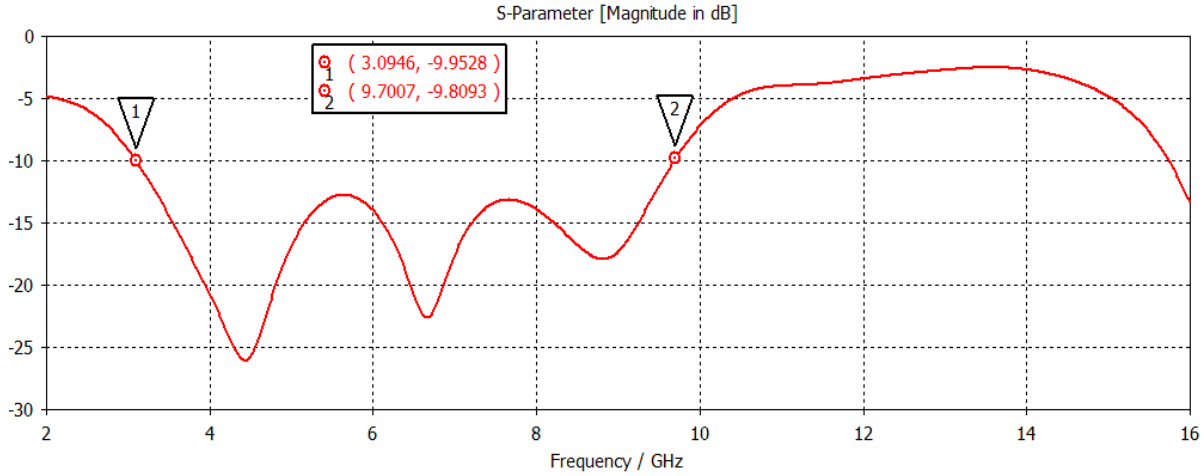

Figure 3.13 Simulated Return Loss (S_{11}) versus frequency plot

3.3.2.2 Smith Chart

Figure 3.14 shows the smith chart of the proposed antenna which depicts the variations of antenna impedance with frequency. It provides an impedance of 50 ohm. Markers 1 and 2 demonstrate the bandwidth of 6.61GHz for the frequency range from 3.09GHz to 9.7GHz. Hence the proposed antenna exhibits good impedance matching characteristics.

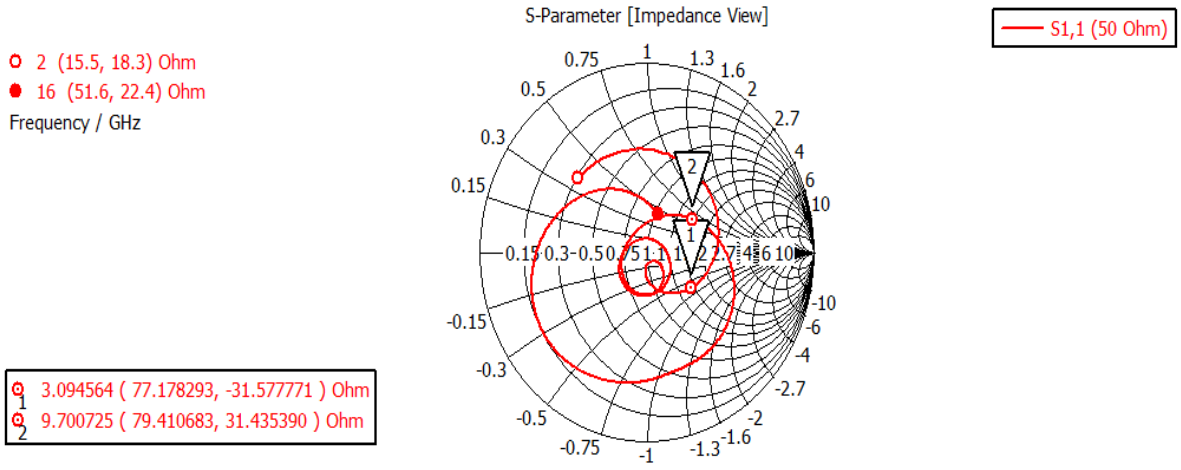

Figure 3.14 Smith Chart of proposed antenna

3.3.2.3 Gain

The antenna with high gain is preferred for long distance applications. Figure 3.15 shows the simulated broadband gain plot versus frequency of the proposed antenna. The maximum achievable gain for the proposed antenna is 4.58dB at a frequency of 7.6GHz. Figure 3.16 (a) demonstrate the 3D view of peak gain and Figure 3.16 (b) and (c) show the Elevation and Azimuth view of gain for the proposed UWB antenna at 7.6GHz frequency. As shown in Figure 3.16 (b), the main lobe is directed at an angle of 15degrees with angular beam width of 114degrees along the Elevation plane. As shown in Figure 3.16 (c), the major lobe is directed at an angle of 24 degrees with magnitude of 1.47dB and half power beam width of 49.8degrees along the Azimuth plane.

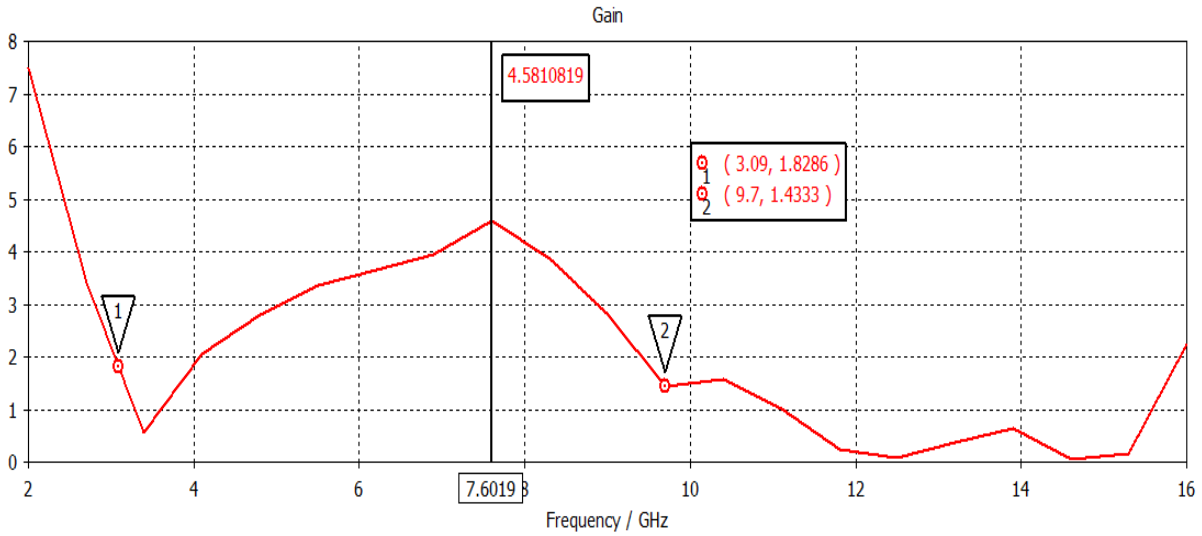

Figure 3.15 Simulated broadband gain plot against frequency of proposed antenna

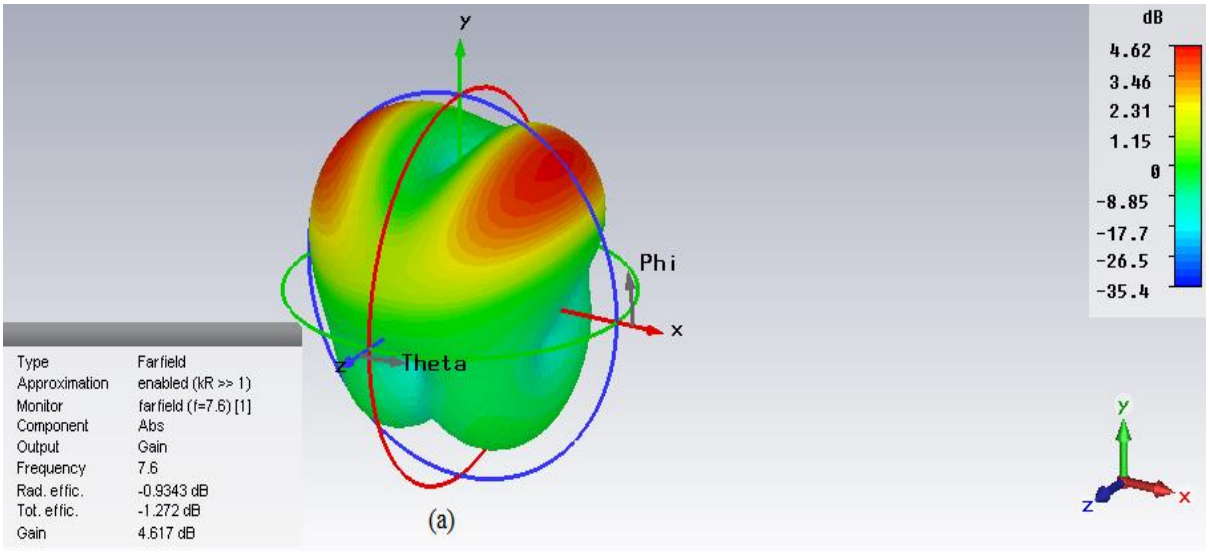

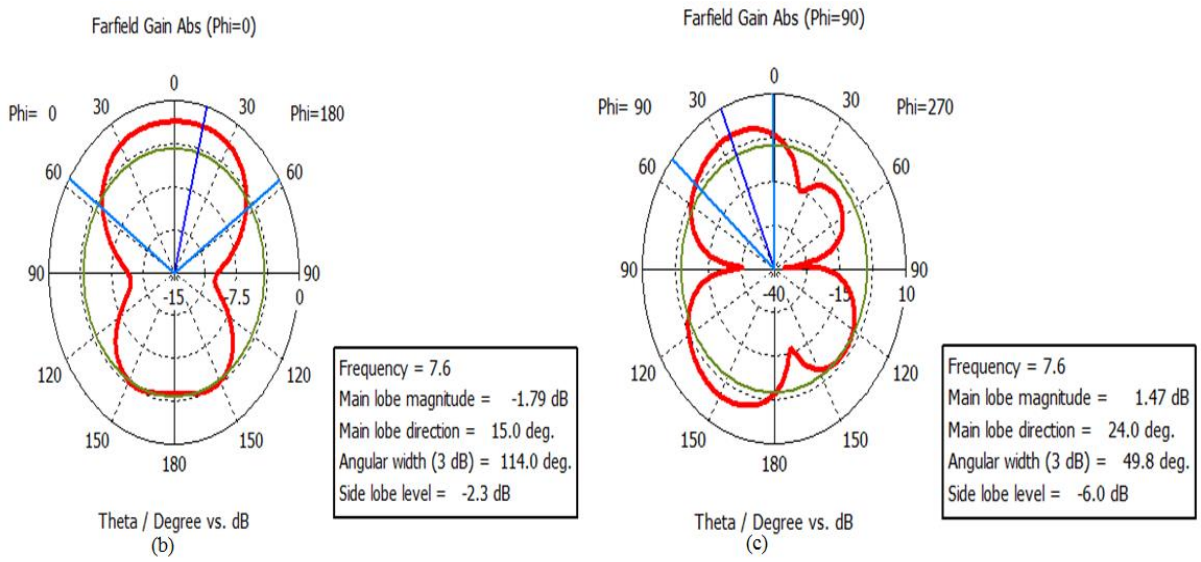

Figure 3.16 Proposed antenna (a) 3D gain view at 7.6 GHz frequency (b) Elevation view of gain plot at 7.6 GHz frequency (c) Azimuth view of gain plot at 7.6 GHz frequency

3.3.2.4 Surface Currents

As shown in Figure 3.17(a-f), the proposed antenna is energized with 1W power at the feed point to see the surface current distribution on the extended semicircular patch and the reduced ground with DGS at 4.4GHz, 6.6GHz and 8.8GHz resonant frequencies. It can be observed from the Figure 3.17(a) that the current is flowing through almost the entire patch but highest magnitude of current (57.4A/m) is present at the point where feeding network is joined to the semicircular patch which excites the resonance at 4.4GHz frequency. As shown in Figure 3.17(b), the magnitude of the current is more around the boundaries of T-shaped slot in the ground plane at 4.4GHz frequency. Figure 3.17(c) shows that maximum surface current (74.5A/m) is present along the upper boundaries of the tuning stub which is attached to the feed line and at the upper edge of the feeding network which is joined to radiating patch which is responsible for exciting the resonance at 6.6GHz frequency. Figure 3.17(d) reveals the magnitude of the current is more at the center just below T-shaped slot in the ground plane and around the upper edges of the ground plane. Figure 3.17(e) depicts that the current is flowing through the entire patch but more in magnitude around the upper boundaries of the tuning stub attached to the feed line at 8.8GHz frequency. Figure 3.17(f) shows the maximum magnitude of the current (117A/m) is flowing around the boundaries of the T-shaped slot in the ground plane which is responsible for exciting the resonance at 8.8GHz frequency.

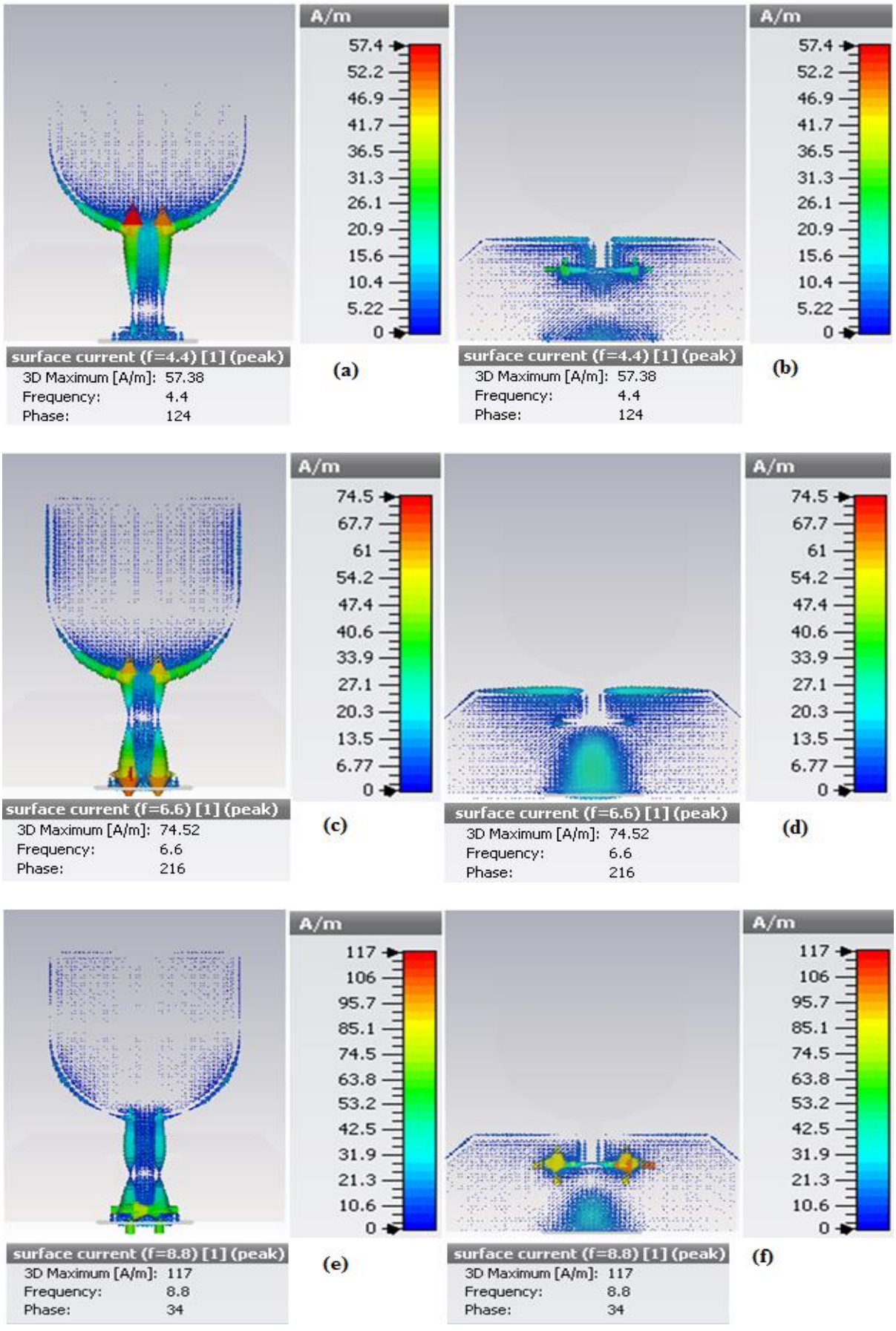

Figure 3.17 Surface current distributions at resonant frequencies of (a-b) 4.4GHz (c-d) 6.6GHz (e-f) 8.8GHz

3.3.3 Antenna Optimization

In this section, various antenna design parameters such as the tuning stub, patch shape and slots are studied and compared with the main focus to achieve the best results in terms of return loss and impedance bandwidth. The designing and simulation results are carried out using CST MWS'14 software.

3.3.3.1 Effects of varying the patch shape and addition of a tuning stub

Different patch geometries affect the proposed antenna performance in terms of bandwidth. Figure 3.18 shows design procedure for different patch geometries and addition of tuning stub to the feed line while keeping the other antenna design parameters constant. Figure 3.19 shows the comparison plots of the simulated return loss (S_{11}) curves against frequency for different patch geometries. The circular patch with radius of 9.4mm is shown in Figure 3.18 (a) which covers the frequency band from 3.1GHz to 8.8GHz with bandwidth of 5.7GHz. To shift the frequency band towards left, a rectangular patch is combined with the circular patch as shown in Figure 3.18(b). It operates in the frequency range from 3.1GHz to 9GHz with impedance bandwidth of 5.9GHz. Further to enhance the bandwidth characteristics of the proposed antenna design, a rectangular tuning stub is added to the lower end of the feeding network which covers a wide frequency band from 3.09GHz to 9.7GHz with impedance bandwidth of 6.61GHz.

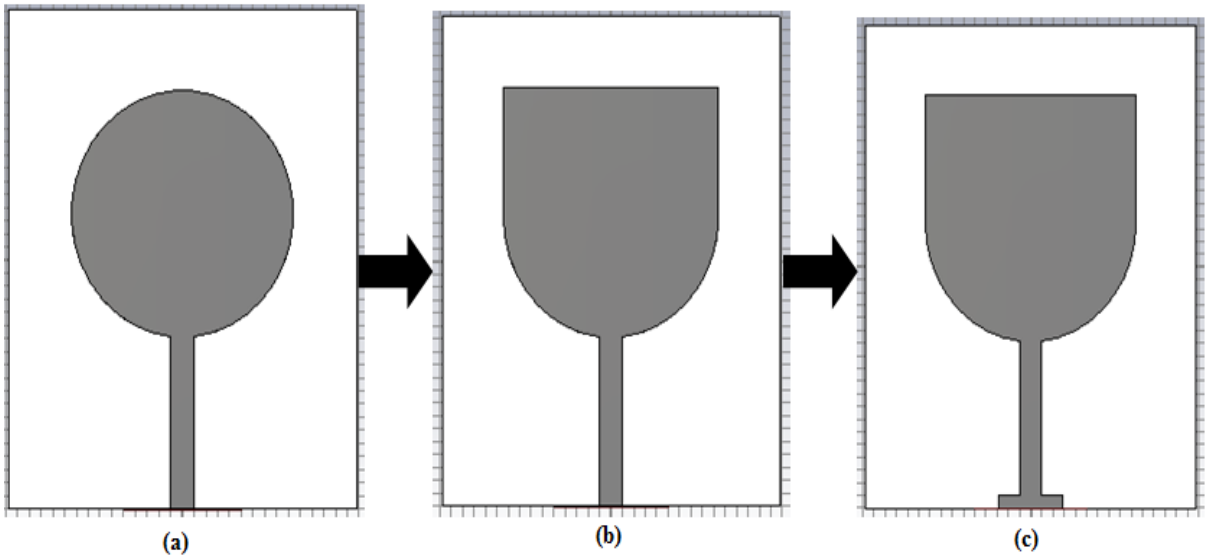

Figure 3.18 Proposed antenna design with (a) Circular patch of radius 9.4mm (b) Extended semicircular patch with a rectangular patch (c) Modified patch with addition of tuning stub to the feed line

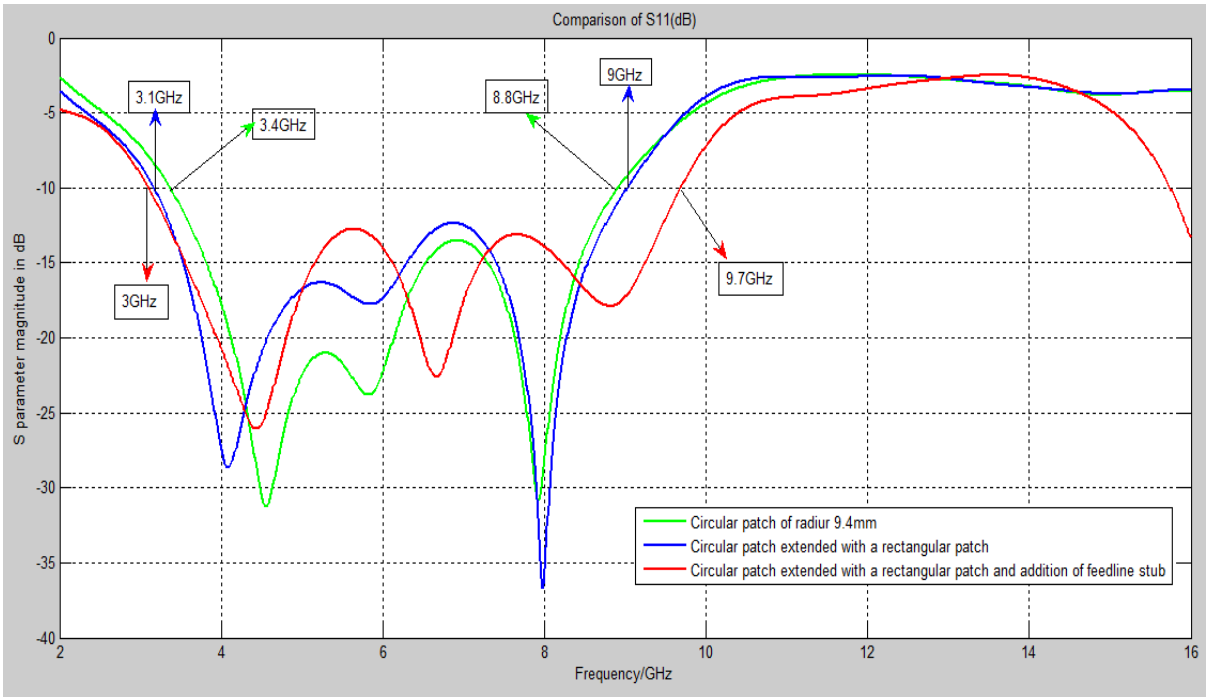

Figure 3.19 Comparisons of Simulated Return Loss (S_{11}) curve which varies as the function of frequency for modified patch shapes and addition of tuning stub to the feed line

3.3.3.2 Effects of DGS

Figure 3.20 illustrates the design procedure of reduced ground plane with DGS which helps the antenna to cover an UWB range. Figure 3.21 shows the comparison of simulated return loss curves versus frequency for five different geometries of the ground plane. The reduced ground plane with length of 8mm as shown in Figure 3.20 (c) exhibits triple band behavior with impedance bandwidths of 3.5GHz, 1.2GHz and 1.4GHz as compared to ground plane geometries with length of 38mm and 19mm as shown in Figure 3.20(a) and 3.20(b) which exhibits dual band behavior. To enhance the impedance bandwidth of the semicircular antenna, an inverted T-shaped slot is etched from the upper edge of the reduced ground plane just below the feed line as shown in Figure 3.20(d). It provides an impedance bandwidth of 6.3GHz with the frequency range from 3.1GHz to 9.4GHz. As shown in Figure 3.20(e), two right angled isosceles triangular notches are truncated from the left and right corners of the reduced ground plane to achieve good impedance matching characteristics and bandwidth enhancement. It covers an ultra wideband from 3.09GHz to 9.7GHz with impedance bandwidth of 6.61GHz which makes the antenna acceptable for wireless communication systems. It can be concluded that impedance bandwidth of the proposed semicircular antenna with DGS is greater as compared to without DGS.

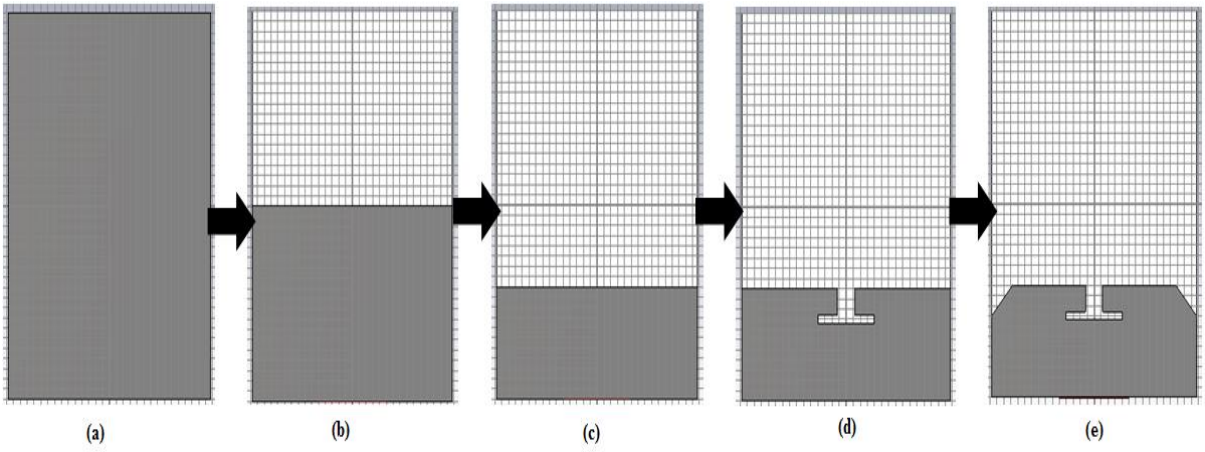

Figure 3.20 Proposed antenna designs with (a) Full ground with length 38mm (b) Reduced ground plane with length 19mm(c) Reduced ground plane with length 8mm (d) Reduced ground plane with DGS (inverted T-shaped slot) (e) Reduced ground plane with DGS (inverted T-shaped slot and dual isosceles triangular notches)

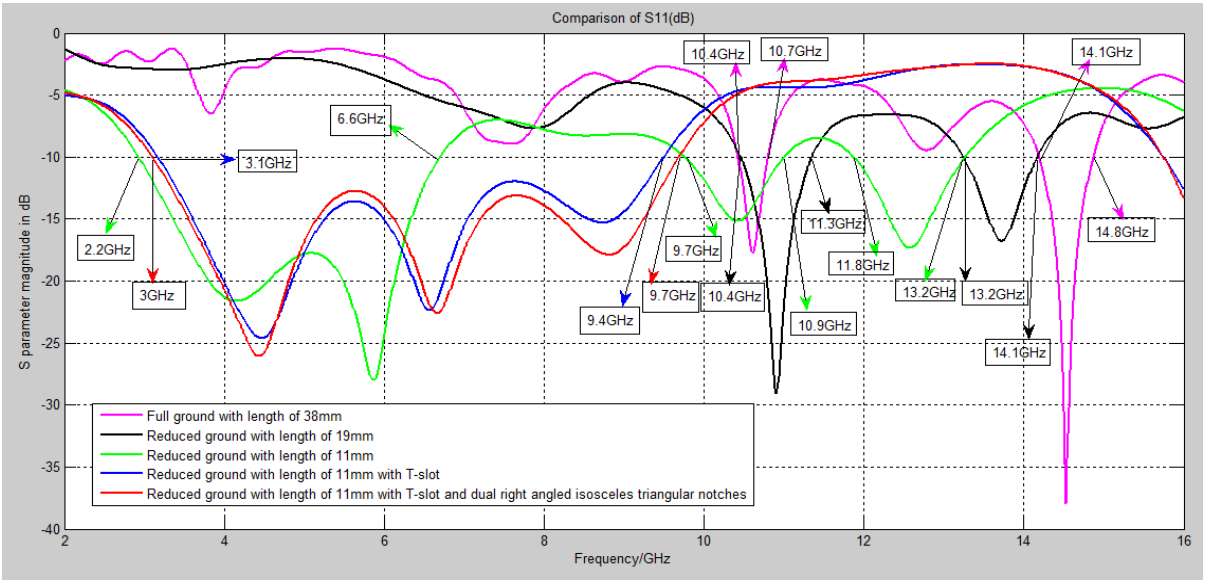

Figure 3.21 Comparisons of Simulated Return Loss (S_{11}) curve which varies as the function of frequency for different ground plane geometries

3.3.4 Applications Covered

The proposed antenna exhibits the peak gain of 4.58dB is obtained at 7.6GHz frequency which makes the antenna acceptable for practical applications. It operates in the frequency band from 3.09GHz to 9.7GHz with bandwidth of 6.61GHz makes the antenna suitable for the UWB operation (3.1-9.7GHz), IMT band (3.4-3.6GHz), WiMAX applications (3.4-3.69GHz), INSAT (4.5-4.8GHz), Radio Astronomy Band (5.01-5.03GHz), IEEE 802.11a WLAN applications (5.15-5.825GHz) and Downlink X-band satellite communication (7.25-7.75GHz).

3.4 DESIGN OF A MINIATURE FORK SHAPED MICROSTRIP PATCH ANTENNA WITH L-SHAPED TUNING STUBS AND A REDUCED GROUND WITH DGS FOR UWB APPLICATIONS

An UWB antenna that was designed as a miniature fork shaped structure with a reduced DGS is presented in this section.

3.4.1 Antenna design and Specifications

Figure 3.22(a) shows the top view of the proposed fork shaped microstrip patch antenna fabricated on FR4 substrate with dielectric constant of 4.4, dielectric loss tangent value of 0.0024 and thickness of 1.57mm. The radiating patch is fed by 50 Ω microstrip feed line along the centerline of symmetry. The dimensions of various antenna parameters like patch, ground and substrate are calculated using transmission line model with Equations (3.1) to (3.6). The design procedure starts with choosing appropriate dimensions for the rectangular patch to achieve the desired antenna operation. Based on the current distributions, an inverted U-shaped slot is etched from the top edge of the radiating patch. Two L-shaped tuning stubs are joined to the right and left corners of the patch to achieve an optimum UWB operation.

Figure 3.22(b) show a reduced ground with DGS of the proposed antenna. The length of the ground is optimized and a slot is etched from the upper edge of the reduced ground to achieve the desired results. In addition, two right angled isosceles triangular notches are truncated from the left and right corners of the reduced ground to improve the peak return loss and achieve the desired UWB operation. The side of the right angled isosceles triangular notch is evaluated using Equation (3.11). The optimized dimensions of the various antenna parameters are specified in Table 3.3.

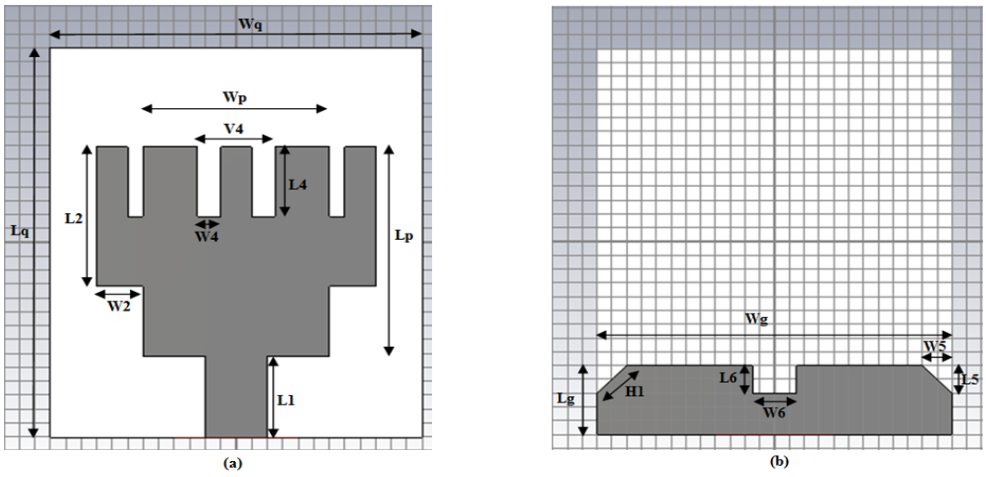

Figure 3.22 Proposed antenna (a) Top view (b) Bottom view

Parameter	Description	Value
Lq	Length of substrate	28mm
Wq	Width of substrate	24mm
Lp	Length of rectangular patch	15mm
Wp	Width of rectangular patch	12mm
Lg	Length of ground	5mm
Wg	Width of ground	24mm
L1	Length of feed line	5.85mm
L2	Length of the L-shaped stub	10mm
W2	Width of the L-shaped stub	3mm
L4	Length of U-shaped slot	8.7mm
V4	Total width of U-shaped slot	5mm
W4	Width of the arm of U-shaped slot	1.5mm
W5	Base of right angled isosceles triangular notch	2mm
L5	Height of right angled isosceles triangular notch	2mm
H1	Slant height of right angled isosceles triangular notch	2.82mm
L6	Length of slot in ground	2mm
W6	Width of slot in ground	3mm

Table 3.3 Optimized Dimensions of the proposed antenna

3.4.2 Simulation Results and Discussions

The designing and simulation of the proposed fork shaped microstrip antenna is carried out in CST MWS'14 software for determining the antenna performance in terms of Return Loss, Smith Chart, Gain and Surface Current Distribution which are discussed in the next subsections.

3.4.2.1 Return Loss and Antenna Bandwidth

Figure 3.23 show that the proposed antenna exhibits UWB behavior when simulated return loss S_{11}(dB) is plotted on Y-axis with respect to the frequency on X-axis. The proposed antenna provides a peak return loss of -57.71 dB at a resonant frequency of 4.55GHz which show that proposed antenna exhibits good impedance matching performance with minimum power loss. The frequency range for which the return loss is less than -10dB is from 3.71GHz to 11.48GHz with impedance bandwidth of 7.77GHz. This makes the proposed antenna suitable for wireless applications such as UWB operation (3.71-10.6GHz), INSAT (4.5GHz-4.8GHz), WLAN applications (5.15-5.825GHz), Radio Astronomy applications (5.01-5.03GHz), STM band applications (6–6.17GHz), Downlink X-band satellite communication (7.25-7.75GHz), Amateur radio operations (10-10.5GHz) and Amateur satellite operations (10.45-10.5GHz).

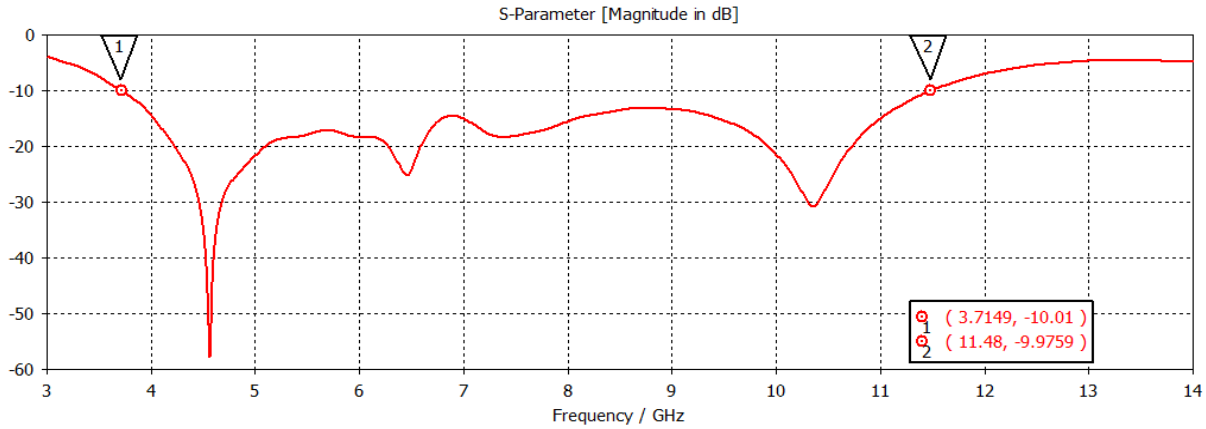

Figure 3.23 Simulated Return Loss (S_{11}) versus frequency plot of proposed antenna

3.4.2.2 Smith Chart

The smith chart of the proposed antenna which shows the variation of antenna impedance with respect to the frequency is illustrated in Figure 3.24. The proposed antenna provides the characteristic impedance of 50 ohms which shows that the antenna is perfectly matched and is appropriate for practical applications. The markers 1 and 2 show the bandwidth of 7.77GHz in frequency range of 3.71GHz to 11.48GHz.

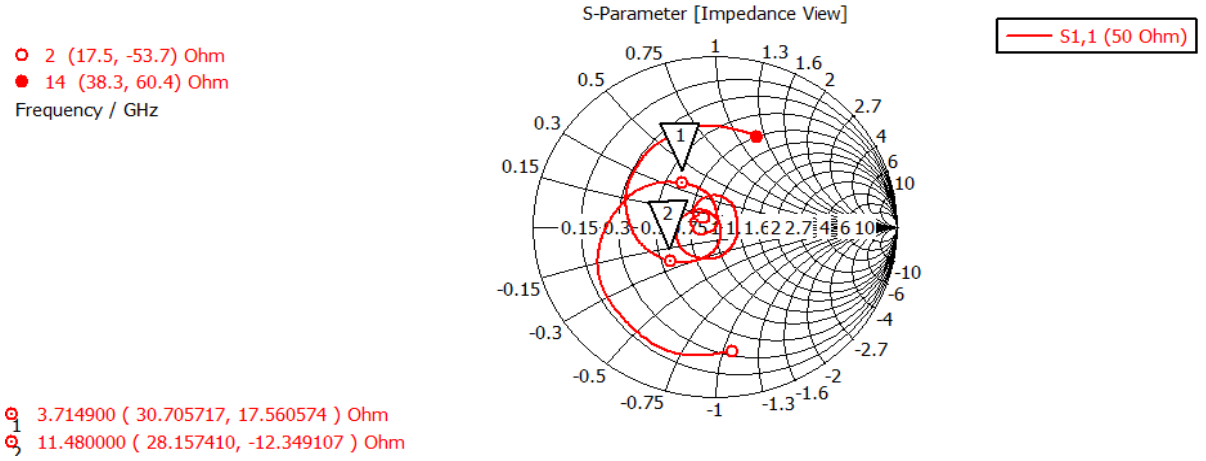

Figure 3.24 Smith Chart of proposed antenna

3.4.2.3 Gain

Figure 3.25 shows the broadband gain of the proposed antenna which varies with respect to the frequency. The proposed antenna shows the peak gain of 5.82dB at 11GHz frequency and has an average overall gain of 4.03dB for the entire band of its operation which makes the antenna suitable for indoor wireless applications. Figure 3.26(a) show a 3D gain view of the proposed antenna at 11GHz frequency. As shown in Figure 3.26(b), the main lobe is directed

at an angle of -85degrees with angular beam width of 63.4degrees along the Elevation plane. As shown in Figure 3.26(c), the major lobe is directed at an angle of 37degrees with magnitude of 2.55dB and angular beam width of 48.6degrees.

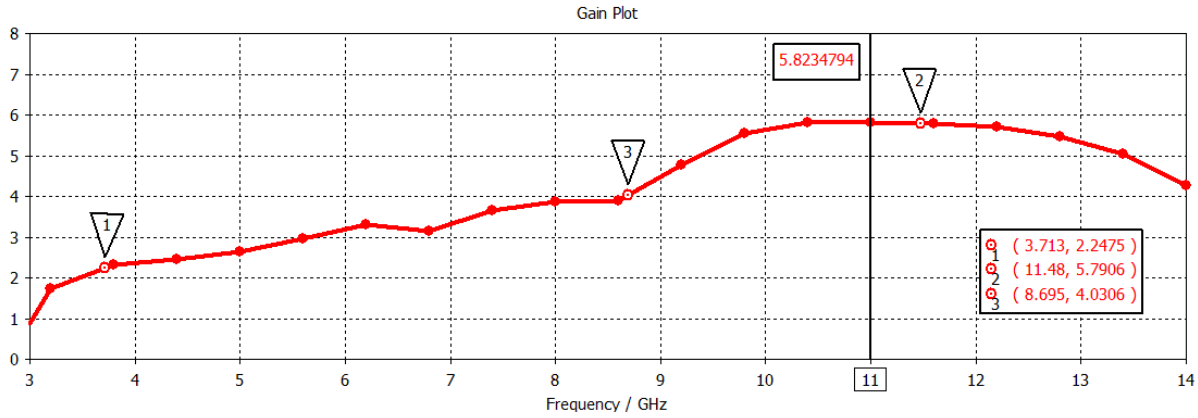

Figure 3.25 Simulated broadband gain plot against frequency

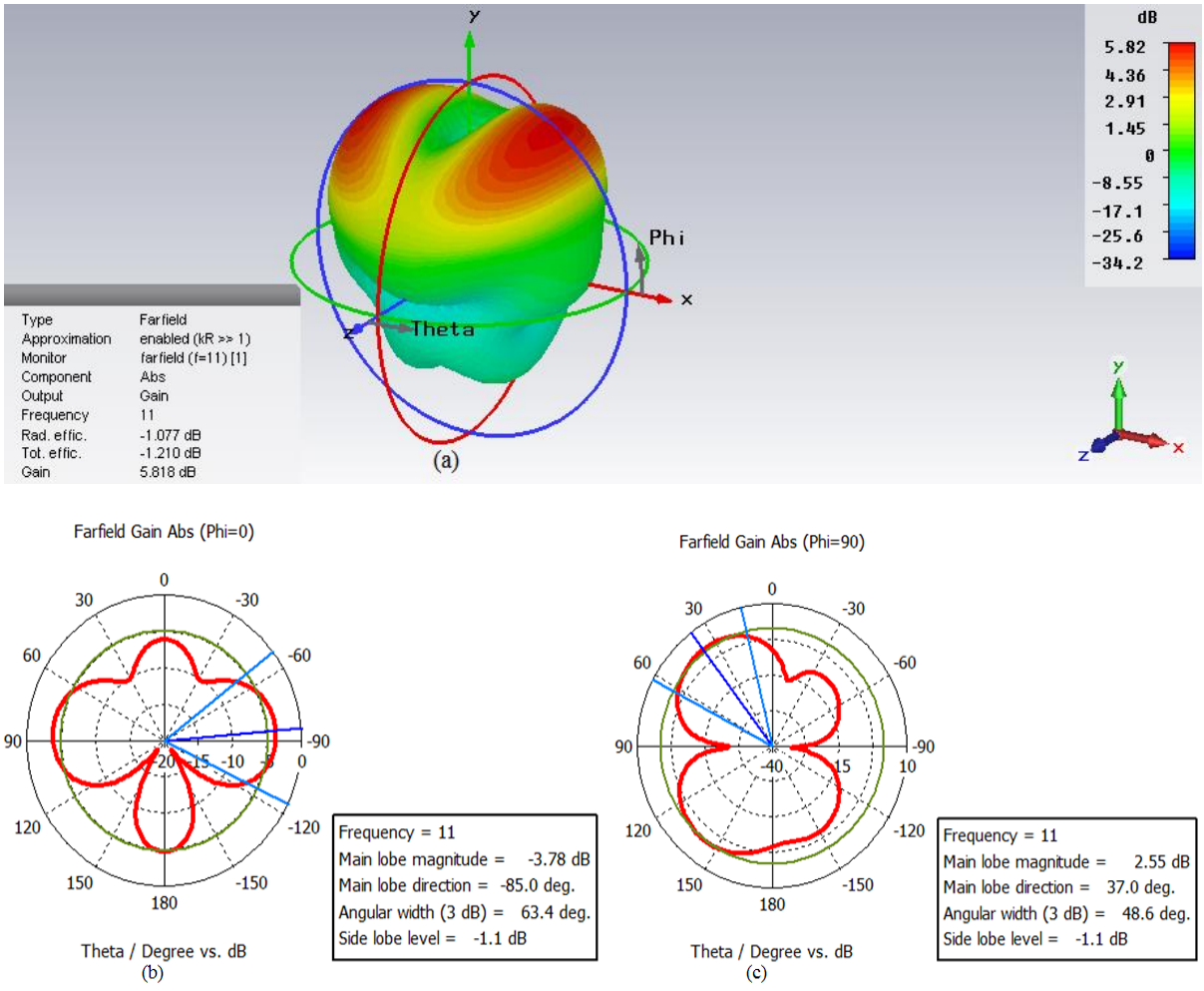

Figure 3.26 Proposed antenna (a) 3D plot of peak gain at 11GHz frequency (b) Polar gain plot for Elevation plane at 11GHz frequency (c) Polar gain plot for Azimuth plane at 11GHz frequency

3.4.2.4 Surface Currents

The proposed antenna is excited with 1W power in the software at the feed point in CST MWS'14 software to see the surface current distribution on the fork shaped radiating patch and reduced ground plane with DGS at resonant frequencies of 4.55GHz, 6.45GHz and 10.35GHz. As shown in Figure 3.27(a) and (b), maximum magnitude of surface current (59.2A/m) flows at the point where the feed line is attached to the radiating patch which excites a resonance at a frequency of 4.55GHz. Figure 3.27(c) and (d) show that the current flows through almost the entire patch and the ground plane but highest magnitude of current (68.8A/m) is distributed along arms of L-shaped stubs which are joined on each side of the radiating patch which excite resonant frequency of 6.45GHz. Figure 3.27(e) and (f) show the maximum surface current of 68.1A/m is present near the lower edge of the rectangular patch attached to the feed line which excites a resonance at 10.35GHz frequency.

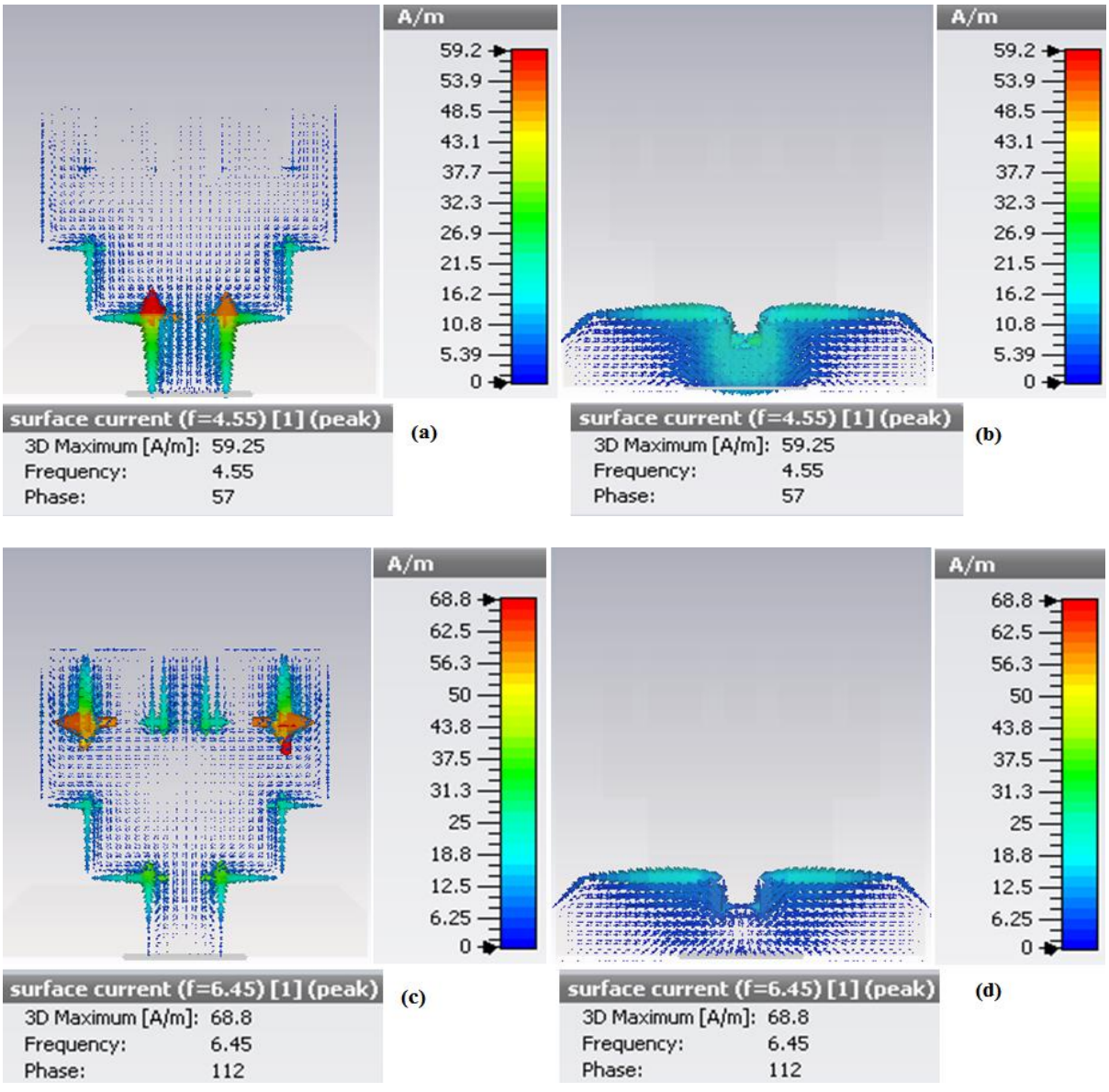

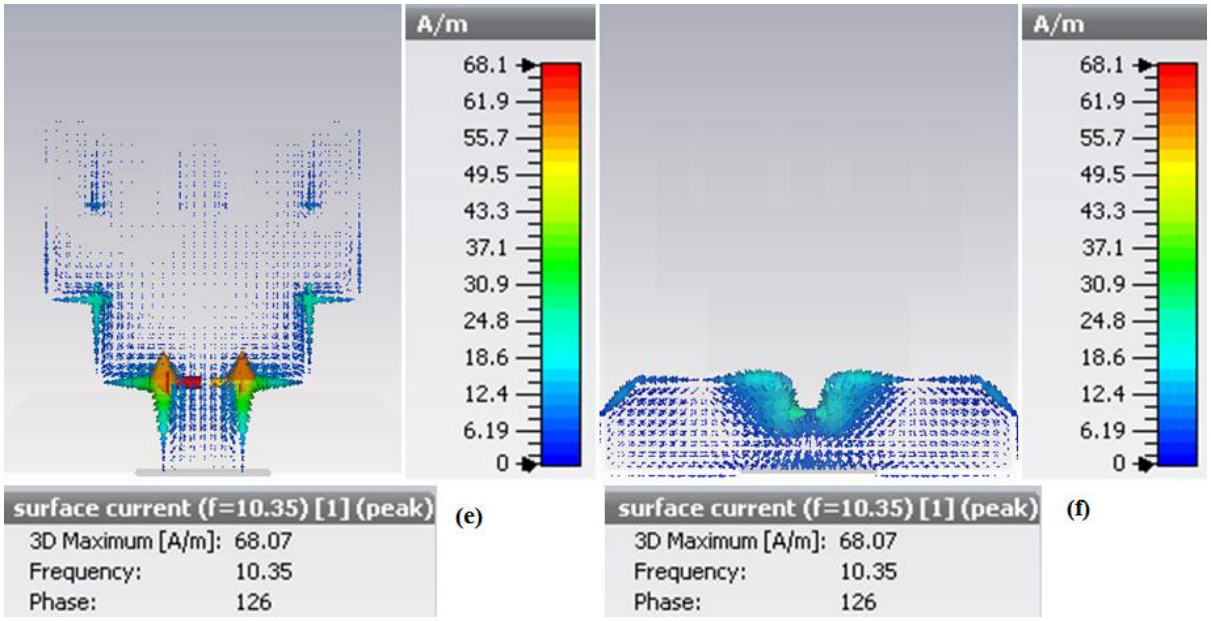

Figure 3.27 Surface current distributions on the radiating patch and ground plane at resonant frequencies of (a-b) 4.55GHz (c-d) 6.6GHz (e-f) 10.35GHz

3.4.3 Antenna Optimization

The study on parametric variations of the proposed antenna is carried out in CST MWS'14. The effect of varying the antenna design parameters such as slots, notches, stubs and feed width are discussed in this section. The antenna is designed with best optimized dimensions to achieve the desired UWB behavior.

3.4.3.1 Effects of Reduced DGS

Figure 3.28 shows the design procedure of reduced ground with DGS. Figure 3.29 depicts the comparison of simulated return loss curves against frequency for different ground geometries while keeping the other design parameters constant. The reduced ground plane with length 5mm as shown in Figure 3.28(c) covers wide frequency band from 3.73GHz to 12GHz with bandwidth of 8.27GHz as compared to ground plane with length of 28mm and 14mm as shown in Figure 3.28(a) and 3.28(b) respectively. To improve the impedance matching antenna performance, a slot is truncated from the upper edge of the reduced ground plane as shown in Figure 3.28(d). To improve the peak return loss, one right angled isosceles triangular notch is etched from the left corner of the reduced ground plane as shown in Figure 3.28(e). The clearest change is seen in the first resonance frequency with an improvement in peak return loss from -36.52dB to -42.32dB. Another right angled isosceles triangular notch is etched from right corner of the reduced ground plane as shown in Figure 3.28(f). It leads to further increment in peak return loss from -42.32dB to -57.71 dB and covers an ultra

wideband from 3.71GHz to 11.48GHz with bandwidth of 7.77GHz. The optimized parameters of a reduced DGS are mentioned in Table 3.3.

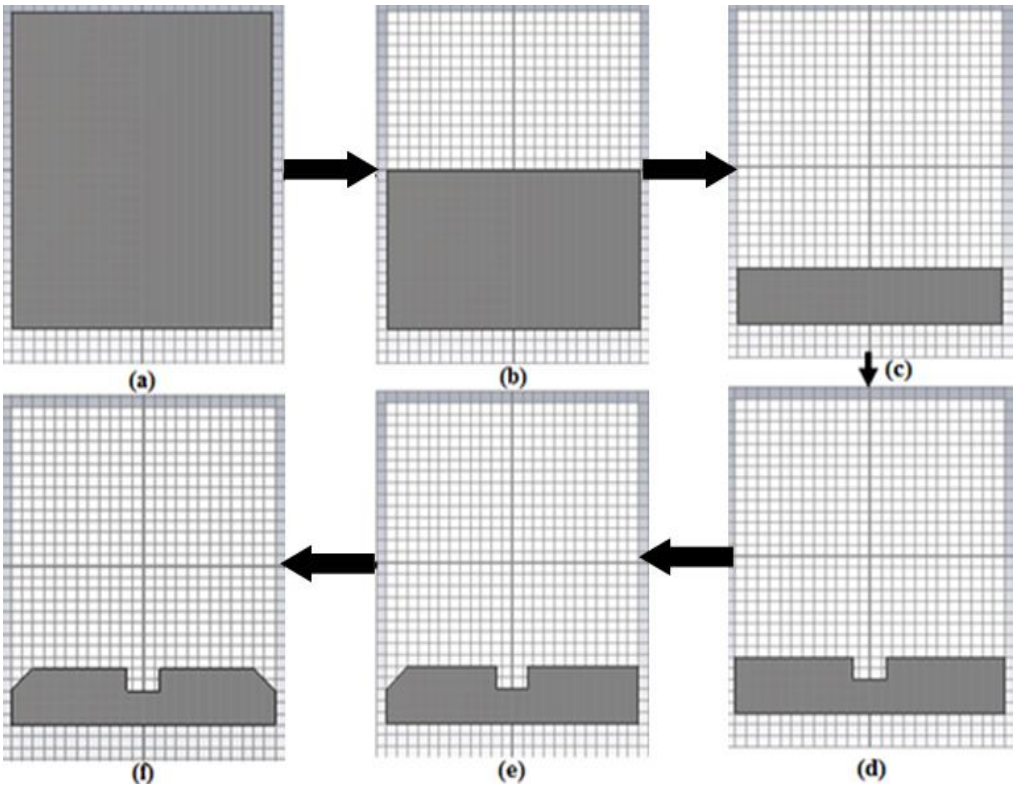

Figure 3.28 Proposed antenna design with (a) Full ground plane with length 28mm (b) Half ground plane with length 14mm(c) Reduced ground with length 5mm (d) Reduced DGS with length 5mm (with slot) (e) Reduced DGS with length 5mm (with slot and one notch) (f) Reduced DGS with length 5mm (with slot and dual notches)

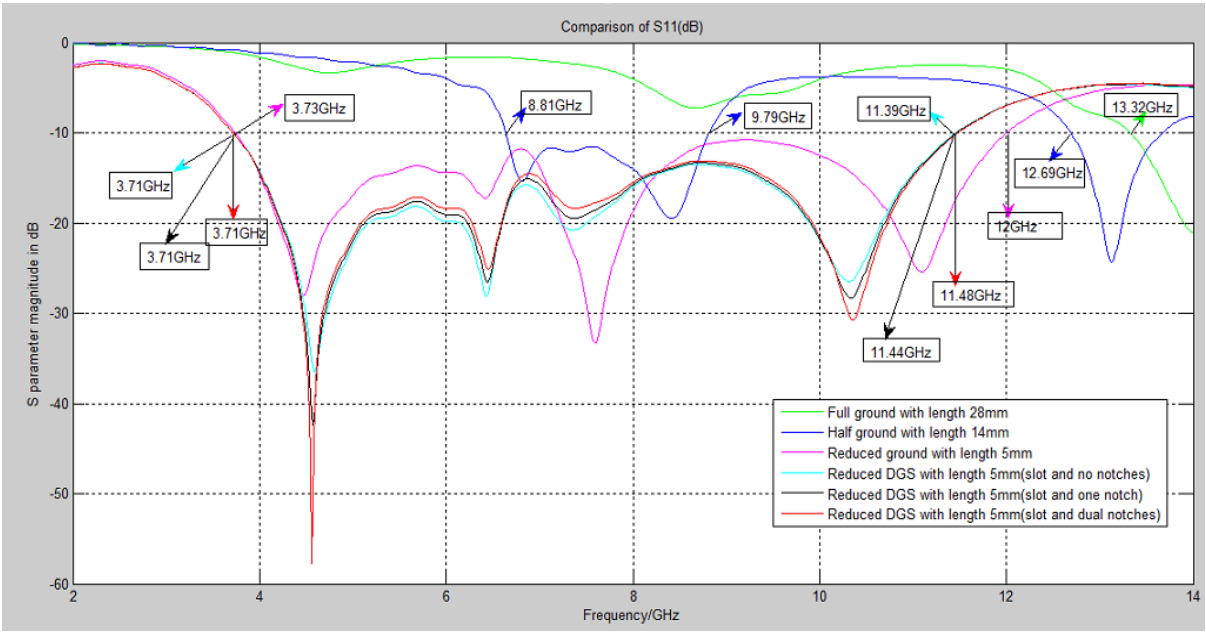

Figure 3.29 Comparisons of Simulated Return Loss (S_{11}) curve against frequency for different ground geometries

3.4.3.2 Effect of varying the feed width

Figure 3.30 shows the variation of S_{11}(dB) parameter values plotted as the function of the frequency when the width of the microstrip feed line is varied from 2mm to 8mm. It is observed that initially bandwidth of the proposed antenna increases with increase in width of feed line from 2mm to 4mm but later on it decreases with increase in feed width from 6mm to 8mm. The desired antenna performance is obtained for the feed line with width of 4mm. It exhibits an UWB behavior as it operates in the frequency range from 3.74GHz to 12GHz with impedance bandwidth of 8.26GHz. The proposed antenna resonates efficiently at frequencies of 4.48GHz, 6.45GHz, 7.6GHz and 11.12GHz with return loss S_{11}(dB) values of -28.2dB, -16.98dB, -33.25dB and -25.41dB respectively.

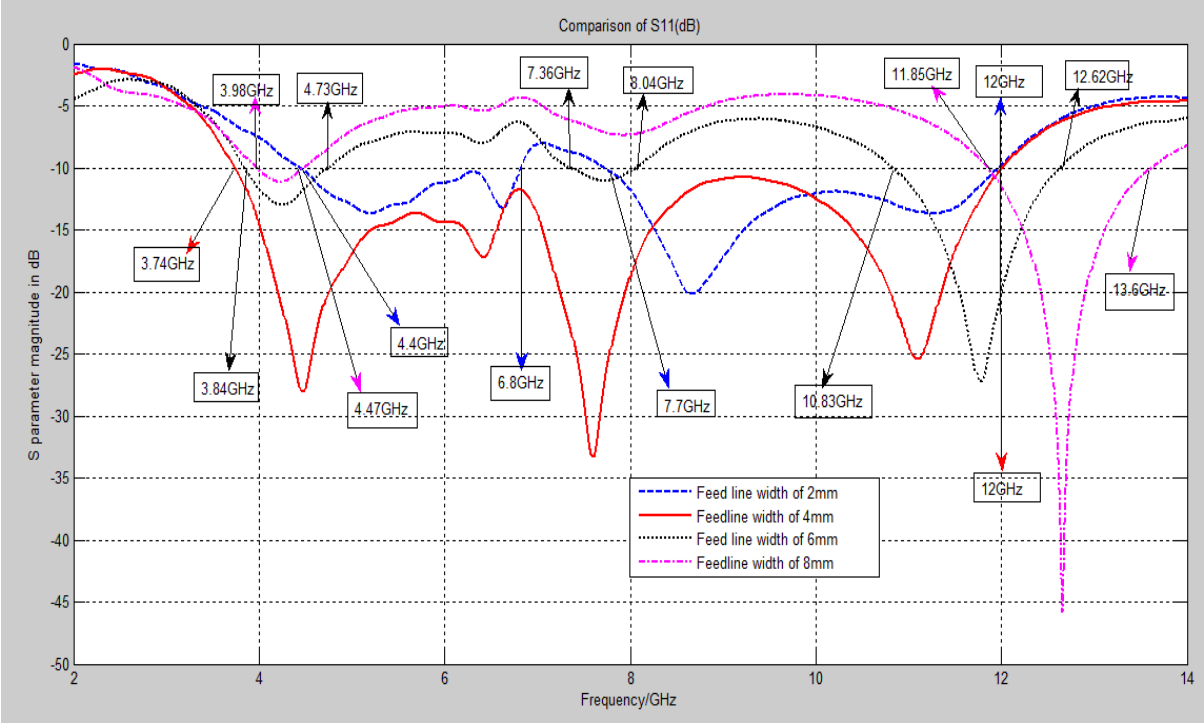

Figure 3.30 Comparisons of Simulated Return Loss (S_{11}) curves against frequency by varying the feed width

3.4.3.3 Effects of slots and stubs to the patch shape

Figure 3.31 illustrates the various designs of radiating patch while keeping the other design parameters constant. The comparison of the simulated return loss curves against frequency for different patch shapes is shown in Figure 3.32.Though there is less significant variations in bandwidth for the slotted and unslotted patch antenna as shown in Figure 3.31(b) and Figure 3.31(a) but an inverted U-shaped slotted patch antenna excites an additional resonant frequency at 7.31GHz.

Further one L-shaped stub (L2=14mm) is joined to left side of the U-slotted rectangular patch as shown in Figure 3.31(c) which results an improvement in impedance bandwidth of the proposed antenna. To improve the impedance matching performance of the proposed antenna, another L-Shaped stubs (L2=14mm) is added to right corner of the slotted radiating patch such that these stubs form the mirror images of each other as shown in Figure 3.31(d). It offers a dual band behavior. The length of the L-shaped stubs is optimized to achieve the desired UWB behavior. The L-shaped stubs with L2=10mm as shown in Figure 3.31(f) provides desired antenna performance which covers the frequency band from 3.71GHz to 11.48GHz with bandwidth of 7.77GHz and improved peak return loss of -57.71dB. Hence the proposed antenna exhibits good impedance matching performance and UWB characteristics which makes the antenna suitable for wireless communication systems.

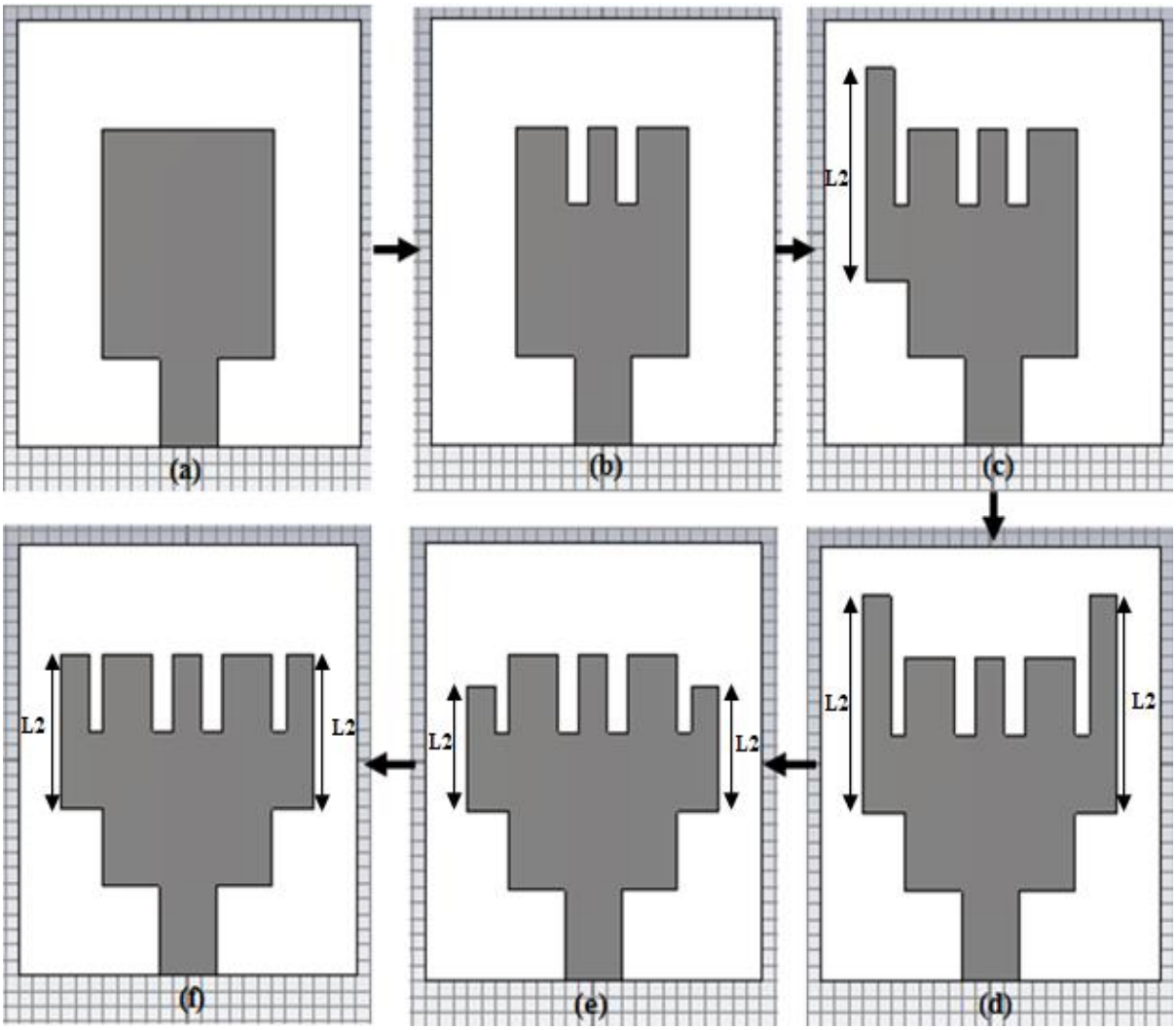

Figure 3.31 Proposed antenna with (a) rectangular patch (b) with inverted U-shaped slot(c) with inverted U-shaped slot and one L-Shaped stub (L2=14mm) (d) with inverted U-shaped slot and two L-Shaped stubs (L2=14mm) (e) with inverted U-shaped slot and two L-Shaped stubs (L2=8mm) (f) with inverted U-shaped slot and two L-Shaped stubs (L2=10mm)

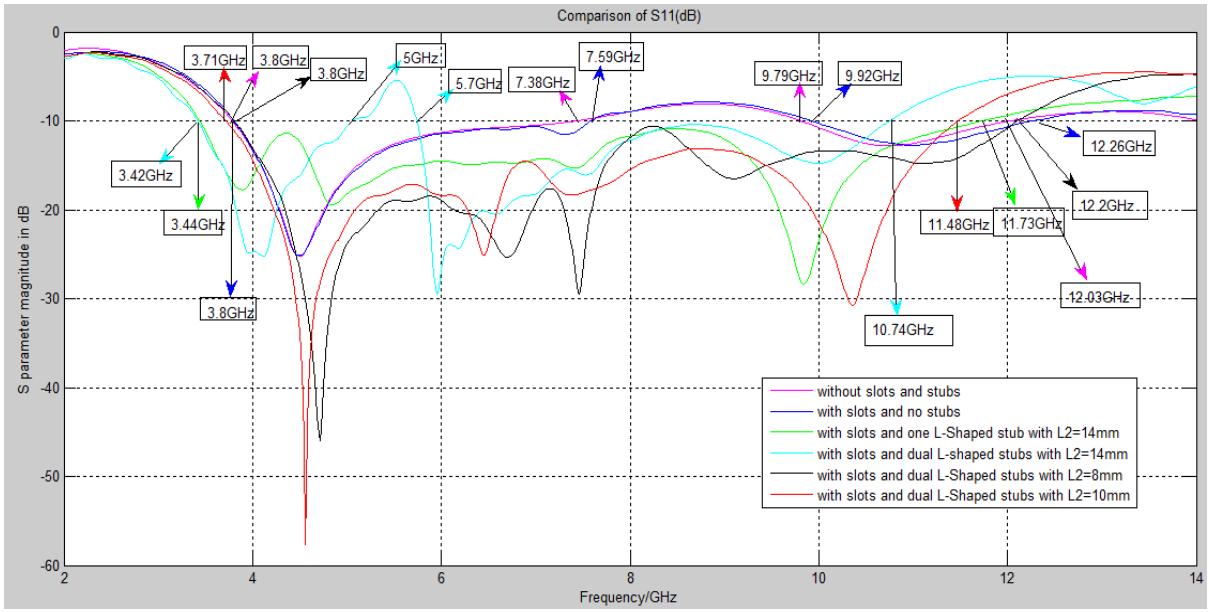

Figure 3.32 Comparisons of Simulated Return Loss (S_{11}) curve against frequency for different patch shapes

3.4.4 Wireless Applications Covered by the proposed antenna

The proposed antenna covers the frequency range from 3.71GHz to 11.48GHz with bandwidth of 7.77 GHz which allows the antenna to operate in C-band (4-8GHz) and X-band (8-12GHz). This helps to make the proposed antenna to be acceptable for UWB operation (3.71-10.6GHz), INSAT (4.5-4.8 GHz), WLAN applications (5.15-5.825 GHz), Radio Astronomy applications (5.01-5.03 GHz), STM band applications (6–6.17 GHz), Downlink X-band satellite communication (7.25-7.75 GHz), Amateur radio operations (10-10.5GHz) and Amateur satellite operations (10.45-10.5GHz).

3.5 DESIGN OF A COMPACT RECTANGULAR MICROSTRIP PATCH ANTENNA LOADED WITH STUBS AND DEFECTED PARTIAL GROUND STRUCTURE FOR UWB APPLICATIONS

This section is aimed at describing the design and realization of a compact microstrip patch antenna with a stubbed rectangular patch and a reduced ground with a defected structure for UWB applications. The effect of cutting notches, adding stubs and reducing the feed line length on resonances is studied.

3.5.1 Antenna design and Specifications

The top view of the antenna structure is shown in Figure 3.33(a). It is a compact structure printed on a rectangular patch. The design process begins with selecting a compact

rectangular patch with optimized dimensions to achieve the desired antenna performance. Further two rectangular stubs are joined to the upper and lower edges of the patch to achieve the final optimized antenna geometry with UWB characteristics. The proposed antenna is fabricated on FR4 substrate with relative permittivity of 4.4, dielectric loss tangent value of 0.0024 and thickness of 1.57mm. The dimensions of rectangular patch, substrate and the ground plane are evaluated using transmission line equations mentioned as Equations (3.1) to (3.6). As shown in Figure 3.33(b), an equilateral triangular notch is truncated from the reduced ground plane for shifting the frequency towards left and to improve return loss characteristics of the proposed antenna. The side of an equilateral triangular notch is calculated using Equation (3.12). The dimensions of the various antenna parameters to achieve optimal UWB operation are listed in Table 3.4.

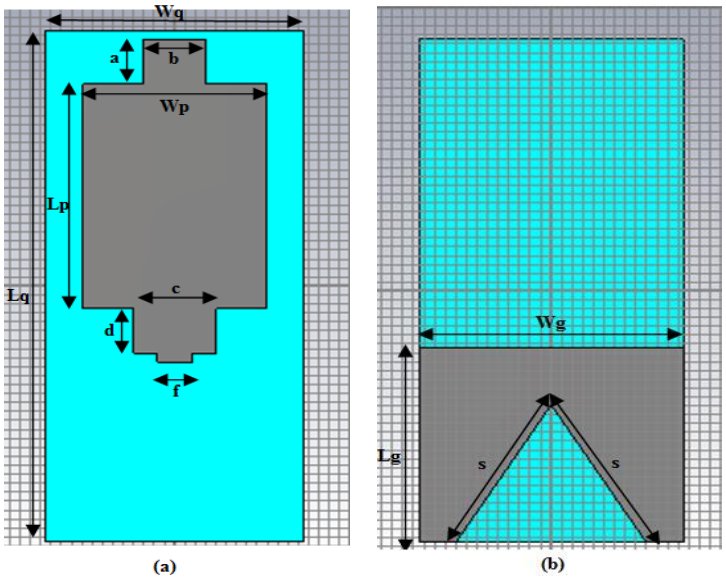

Figure 3.33 Proposed antenna (a) Top view (b) Bottom view of reduced ground with DGS

Parameter	Description	Value
Lq	Length of substrate	57mm
Wq	Width of substrate	25mm
Lp	Length of rectangular patch	25mm
Wp	Width of rectangular patch	17.8mm
Lg	Length of ground	22mm
Wg	Width of ground	25mm
f	Width of feed line	3.4mm
a	Length of upper stub	5mm
b	Width of upper stub	6mm
c	Width of lower stub	8mm
d	Length of lower stub	5mm
s	Side of equilateral triangular notch	18mm

Table 3.4 Optimal Geometrical Parameters of the proposed antenna

3.5.2 Simulation Results and Discussions

The proposed antenna was designed and simulated using the software CST MWS'14. The simulation results in terms of return loss, smith chart, gain and surface current distribution are presented in the next subsection.

3.5.2.1 Return Loss and Antenna Bandwidth

Figure 3.34 shows the return loss versus frequency plot of the proposed antenna. It can be observed that the proposed antenna shows a peak return loss of -29.74dB at a resonant frequency of 1.5GHz. It covers the operational band from 0.17GHz to 7.25GHz with bandwidth of 7.08GHz which makes it appropriate for UWB operation (3.1-7.25GHz), GSM mobile phones (800-900MHz, 1800-1900MHz), WLAN applications (2.4-2.485GHz, 5.15-5.535GHz, 5.725-5.825GHz), Bluetooth (2.4-2.483 GHz), Microwave ovens (2450MHz), Zig-Bee (2.4-2.485GHz), WiMAX (3.4-3.69GHz), IMT band (3.4-3.6GHz), INSAT (4.5-4.8GHz), Radio Astronomy Band (5.01-5.03GHz) and STM band applications (6-6.17GHz).

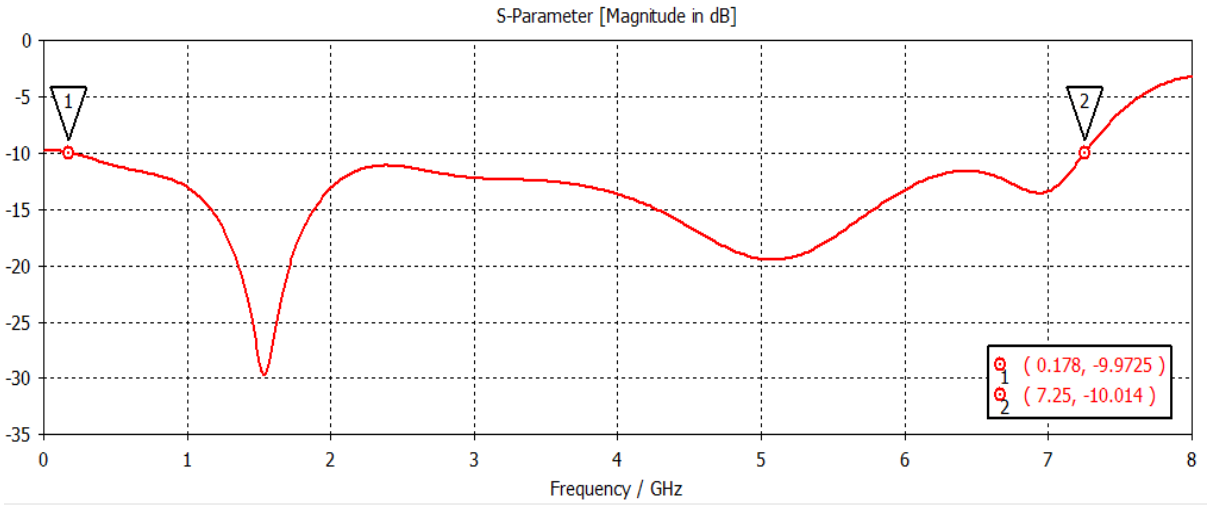

Figure 3.34 Simulated Return Loss (S_{11}) versus frequency plot of proposed antenna

3.5.2.2 Smith Chart

Figure 3.35 shows the smith chart of the proposed antenna in which antenna impedance varies as the function of the frequency. It is the plot of complex impedance of S-parameter (S_{11}) within a unit circle for the given operational band. The proposed antenna is perfectly matched for the frequency band from 0.17GHz to 7.25GHz as it provides the characteristic impedance of 50 ohms. The markers 1 and 2 show the bandwidth of 7.08GHz in frequency range of 0.17GHz to 7.25GHz.

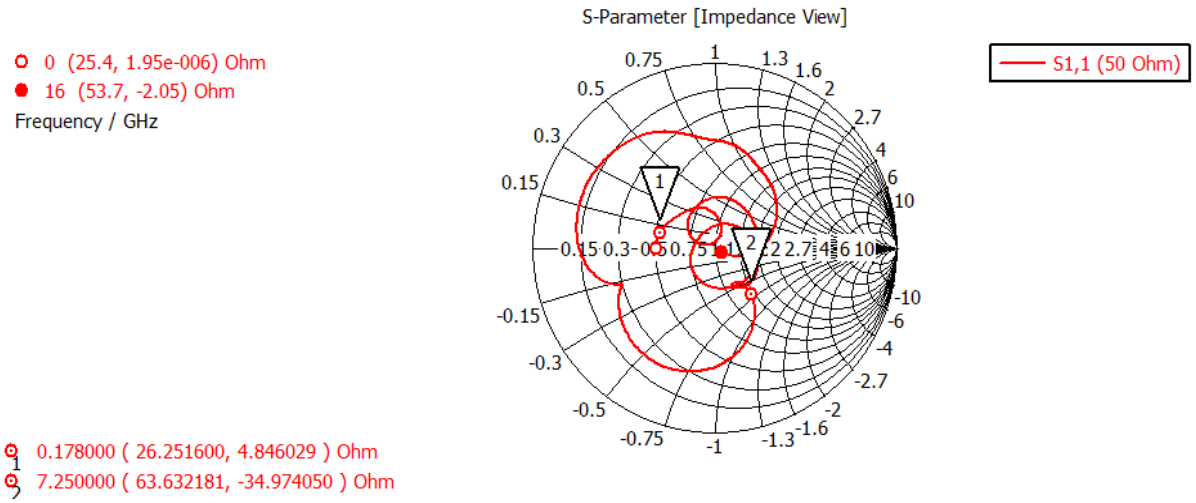

Figure 3.35 Smith Chart of proposed antenna

3.5.2.3 Gain

Figure 3.36 shows the broadband gain plot versus frequency of the proposed antenna. The antenna gain determines the antenna's ability to concentrate more energy in a particular direction. The proposed antenna shows the peak gain of 5.007dB at 7.25GHz frequency which makes the antenna suitable for practical applications of interest. Figure 3.37 (a) show the 3D radiation pattern plot of the proposed antenna at 7.25GHz frequency. Figure 3.37(a) and (b) show the Elevation and Azimuth pattern of this gain plot. As shown in Figure 3.37 (b), the major lobe is directed at an angle of -94degrees with angular width of 74.4degrees along the elevation plane. As shown in Figure 3.37(c), the main lobe is directed at an angle of 47degrees with magnitude of 3.34dB and half power beam width of 47.5degrees along the azimuth plane.

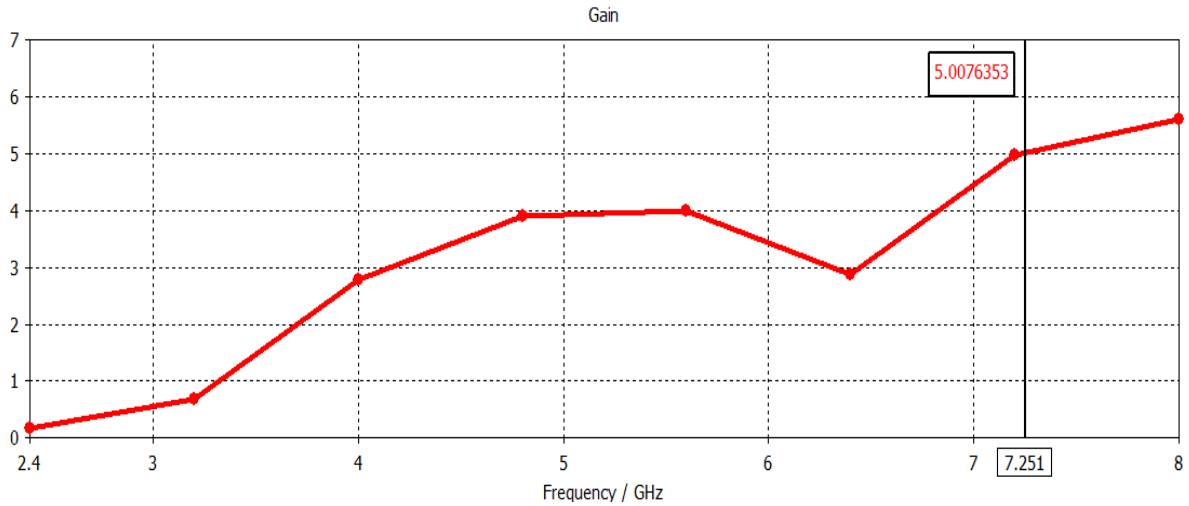

Figure 3.36 Simulated broadband gain versus frequency of the proposed antenna

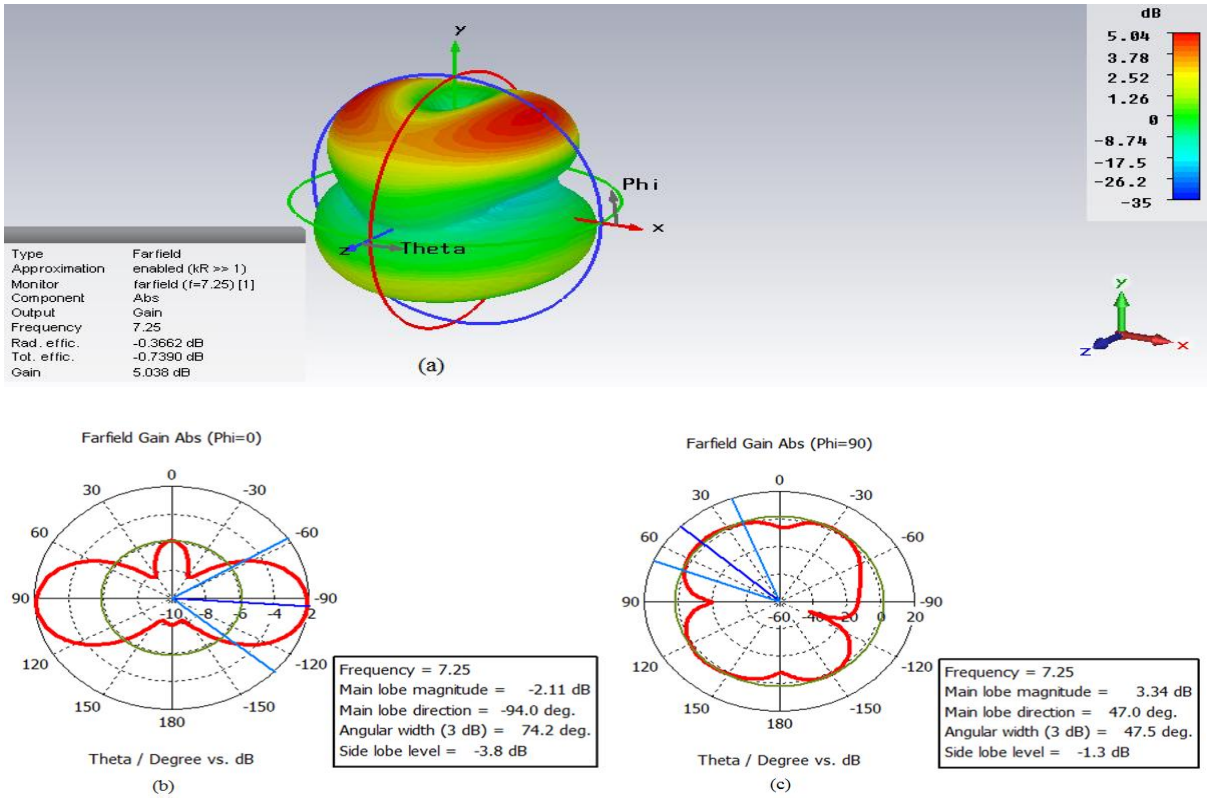

Figure 3.37 Proposed antenna (a) 3D plot of peak gain at 7.25GHz frequency (b) Polar gain plot for Elevation plane at 7.25GHz frequency (c) Polar gain plot for Azimuth plane at 7.25GHz frequency

3.5.2.4 Surface Currents

As shown in Figures 3.38(a) to 3.38(f), the proposed antenna is energized with peak 1W power at the feed point to observe the surface current distribution on the rectangular radiating patch and the reduced ground with DGS at the frequencies of 1.5GHz, 5.07GHz and 6.9GHz. Figure 3.38(a) show that more magnitude of current is distributed along the lower boundaries of the lower stub of the rectangular patch joined to the feed line at a frequency of 1.5GHz. Figure 3.38(b) shows that highest magnitude of the current (157A/m) is present in the region just behind the feed line in the reduced ground which excites resonance at a frequency of 1.5GHz frequency. Figure 3.38(c) show that maximum current (69.6A/m) is flowing along the lower boundaries of the lower stub of the rectangular patch attached to the feed line which excites at a frequency of 5.07GHz. Figure 3.38(d) the show that more magnitude of current is in the region just behind the feed line in the ground at a frequency of 5.07GHz. Figure 3.38(e) shows that the highest current (59.6 A/m) is flowing along the boundaries of the lower stub which is attached to the feed line which excites at a frequency of 6.9GHz. Figure 3.38(f) shows that more current is flowing in the region just behind the feed line in the reduced ground plane at a frequency of 6.9GHz.

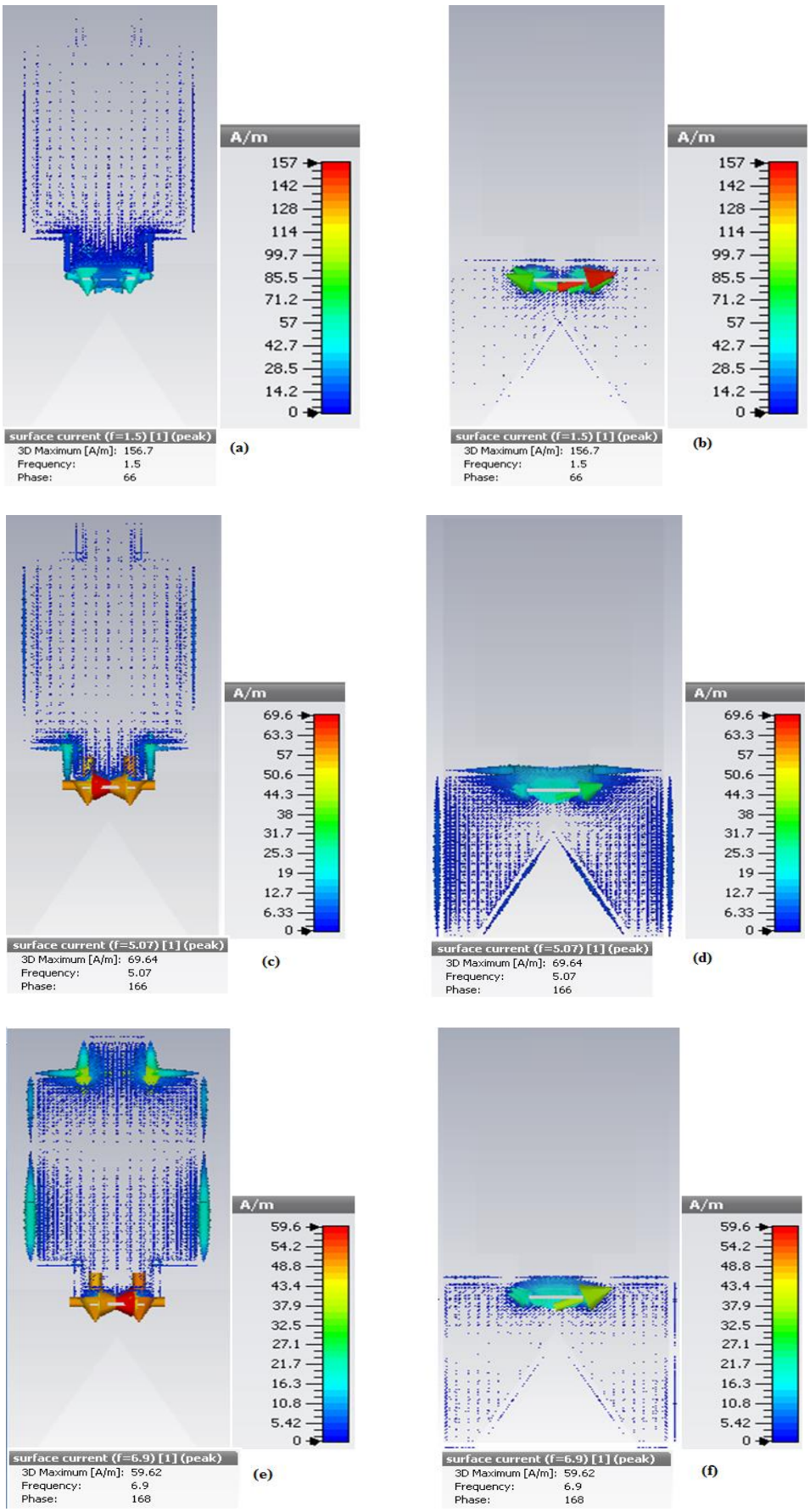

Figure 3.38 Surface current distributions on the radiating patch and reduced ground plane at resonant frequencies of (a-b) 1.5GHz (c-d) 5.07GHz (e-f) 6.9GHz

3.5.3 Antenna Optimization

The antenna parameters like notches, stubs and feed line width were optimized to obtain the desired impedance bandwidth results. The next subsection presents the parametric variations carried out for antenna optimization.

3.5.3.1 Effects of reduced ground with DGS

Figure 3.39 illustrates the design procedure of a reduced ground plane with DGS. Figure 3.40 shows the comparison plots of simulated return loss (S_{11}) values versus frequency for different ground geometries while keeping other design parameters constant. The reduced ground with length 22mm as shown in Figure 3.39 (b) covers a large operational band from 0.47GHz to 7.27GHz with bandwidth of 6.8GHz as compared to ground plane with length of 57mm as shown in Figure 3.39 (a) which covers the frequency range from 14.03GHz to 14.38GHz. For improving the impedance matching performance of the proposed antenna, an equilateral triangular notch is etched from the reduced ground plane as shown in Figure 3.39 (c). It improves the peak return loss from -23.52dB to -29.74dB and covers an ultra wideband from 0.17GHz to 7.25GHz with bandwidth of 7.08GHz. It can be concluded that the proposed antenna with DGS offers wider bandwidth and good impedance matching performance as compared to without DGS. Therefore, the optimized length and width for the reduced ground plane is 22mm and 25mm respectively with optimized side of equilateral triangular notch of 18mm.

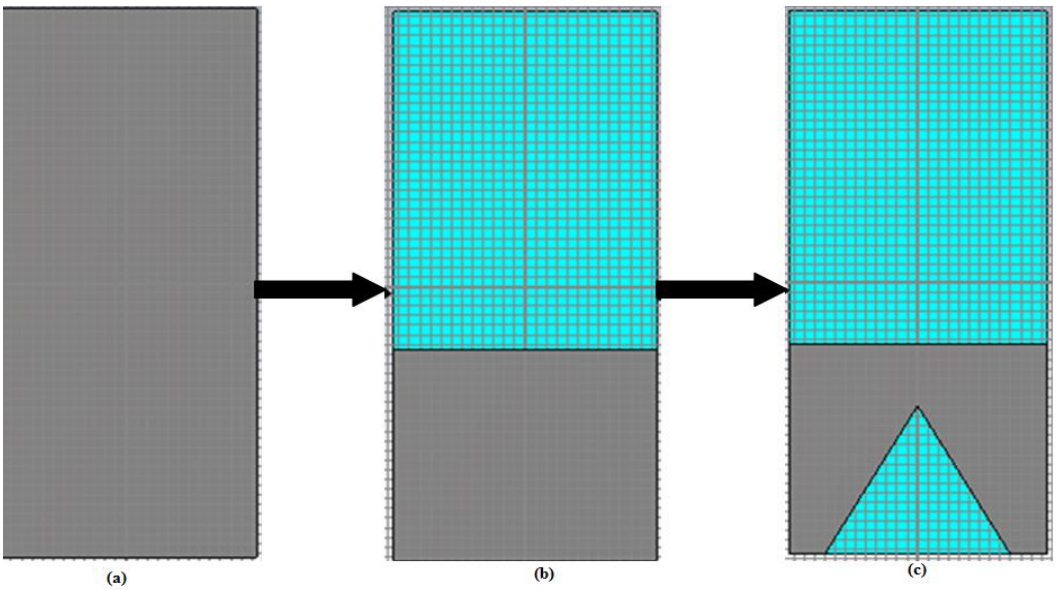

Figure 3.39 Proposed antenna design (a) Full ground plane with length 57mm (b)Reduced ground with length 22mm(c) Reduced ground with length 22mm and an equilateral triangular notch of side 18mm

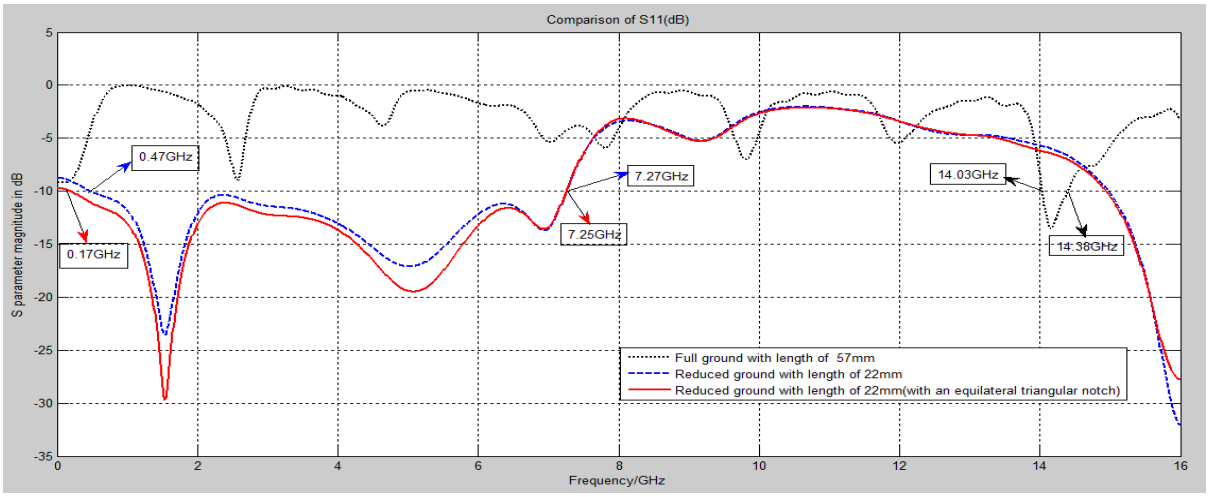

Figure 3.40 Comparisons of Simulated Return Loss (S_{11}) curve against frequency for different ground geometries

3.5.3.2 Effect of varying the feed length

Figure 3.41 shows the design procedure carried out for the designed antenna with optimized length of feed line while keeping other design parameters constant. Figure 3.42 shows the comparison plots of S_{11}(dB) parameter versus frequency for different lengths of feed line when it is varied from 21mm to 1mm. The impedance bandwidth is measured at -10dB which shows that the feed lengths of 21mm and 16mm are not appropriate for the proposed antenna. The major aim of the proposed antenna is to achieve UWB characteristics. The feed line with lengths of 11mm and 6mm offers dual band and multiband behavior respectively. The feed line with length of 1mm provides best optimized results and covers a wide frequency range from 0.17GHz to 7.25GHz with bandwidth of 7.08GHz and provides three resonant peaks of -29.74dB, -19.6dB and -14.04dB at frequencies of 1.5GHz, 5.07GHz and 6.9GHz respectively.

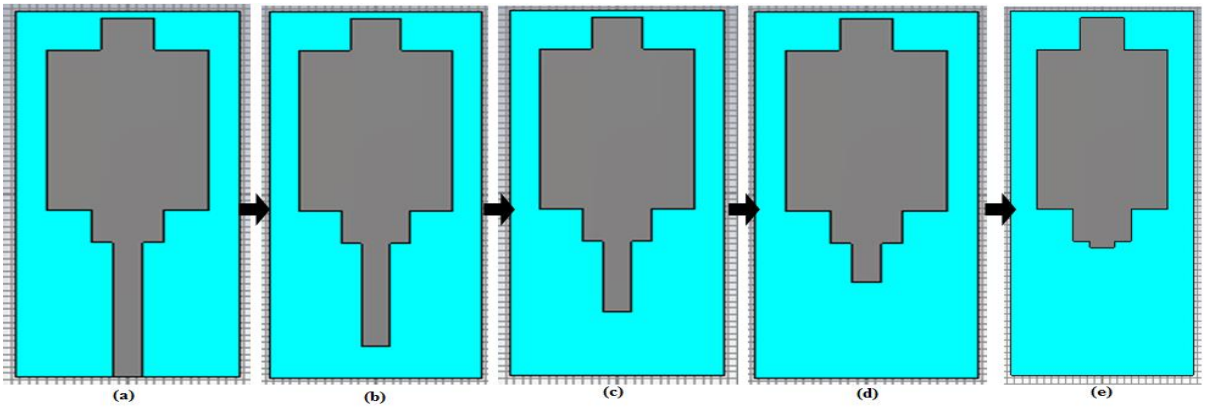

Figure 3.41 Proposed antenna designs with feed length of (a) 21mm (b) 16mm (c) 11mm (d) 6mm (e) 1mm

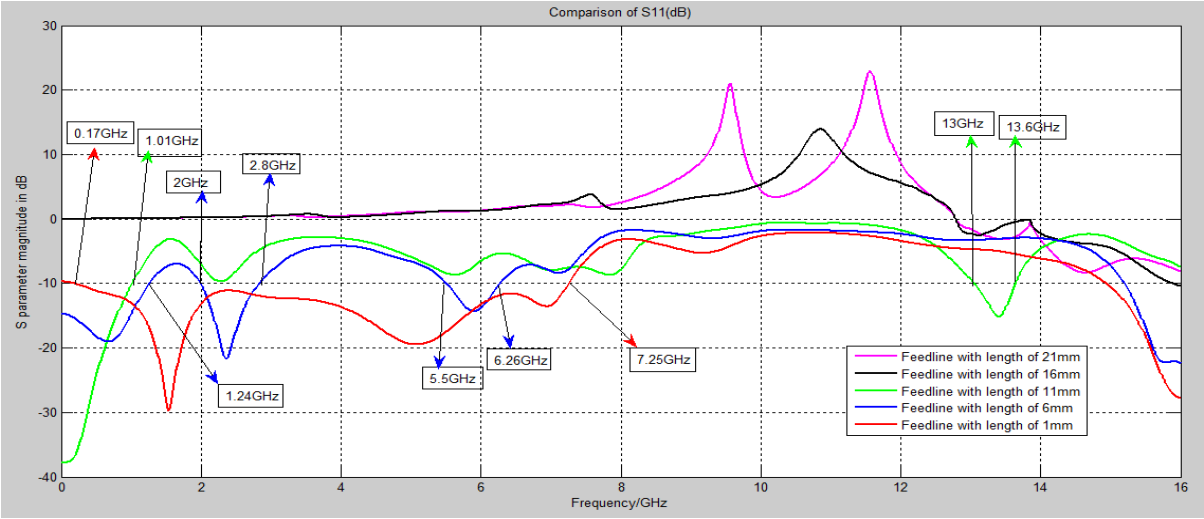

Figure 3.42 Comparisons of Simulated Return Loss (S_{11}) curves against frequency by varying the feed length

3.5.3.3 Effects of adding stubs to the patch shape

Figures 3.43(a) to 3.43(c) illustrate the different geometries of radiating patch with addition of stubs. The parametric variations carried out to obtain the desired impedance bandwidth results are listed in Table 3.4. Figure 3.44 show the comparison of the simulated return loss curves against frequency for different patch geometries. Figure 3.43(a) shows a rectangular radiating patch which exhibits dual band behavior. To achieve an UWB behavior, a rectangular stub is added to the lower end of the radiating patch which offers the bandwidth of 6.08GHz. For improving the impedance matching performance and bandwidth of the proposed antenna, one more rectangular stub is joined to the radiating patch at its upper end as shown in Figure 3.43 (c). It covers the wide frequency range from 0.17GHz to 7.25GHz with bandwidth of 7.08GHz which makes the antenna appropriate for large number of wireless applications.

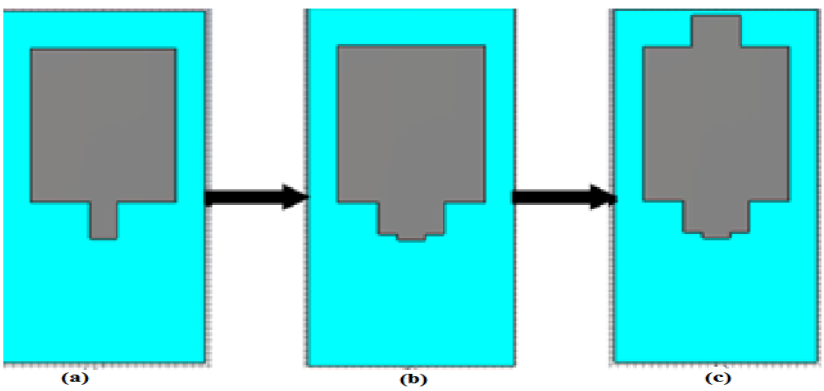

Figure 3.43 Proposed antenna design for (a) Simple rectangular patch (b) Rectangular patch joined with a stub (c) Rectangular patch joined with two stubs

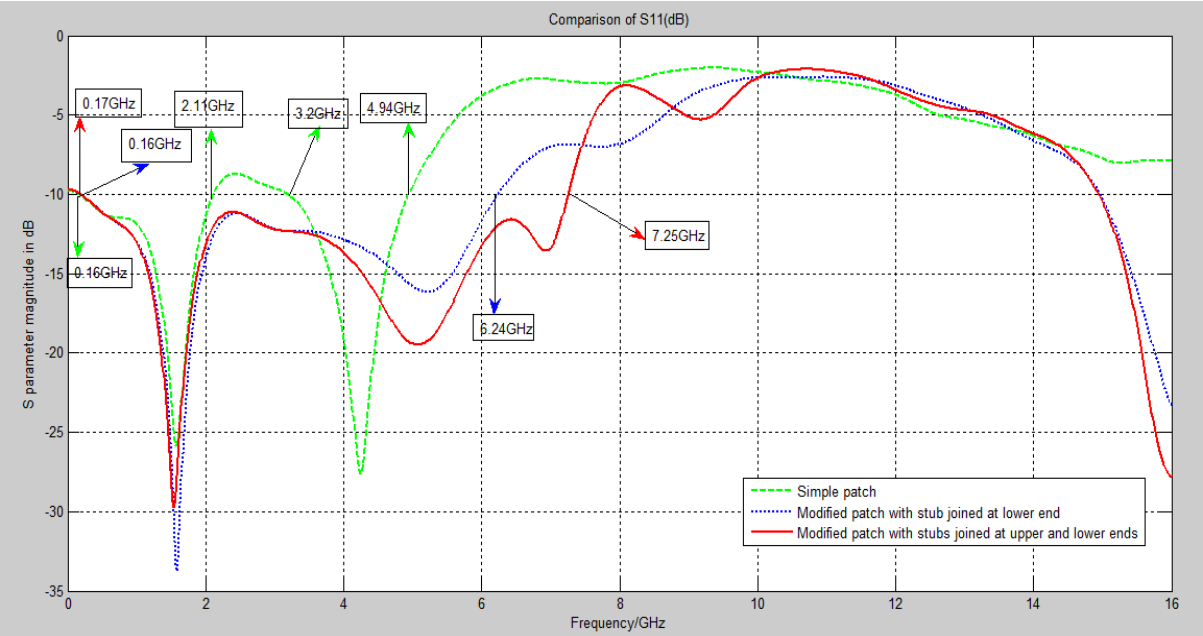

Figure 3.44 Comparisons of Simulated Return Loss (S_{11}) curves against frequency for different patch geometries

3.5.4 Applications Covered

The proposed antenna shows an impedance bandwidth of 7.08GHz and covers a frequency band from 0.17GHz to 7.25GHz which allows it to operate in L-band (1-2GHz), S-band (2-4GHz) and C-band (4-7.25GHz). This frequency range makes the proposed antenna suitable for UWB operation (3.1-7.25GHz), GSM mobile phones (800-900MHz, 1800-1900MHz), WLAN applications (2.4-2.485GHz, 5.15-5.535 GHz, 5.725-5.825GHz), Bluetooth (2.4-2.483 GHz), Microwave ovens (2450MHz), Zig-Bee (2.4-2.485GHz), WiMAX (3.4-3.69GHz), IMT band (3.4-3.6GHz), INSAT (4.5-4.8GHz), Radio Astronomy Band (5.01-5.03GHz) and STM band applications (6-6.17GHz).

CHAPTER 4

FABRICATION AND TESTING OF MICROSTRIP PATCH ANTENNAS

To validate the results of antennas for proposed practical wireless applications, the fabrication and testing of antennas is carried out. This chapter describes the fabrication procedure of the antennas whose designing and simulation results are presented in chapter3. Comparison between simulated and experimentally measured results is also demonstrated.

4.1 FABRICATION PROCEDURE

The various steps followed for the fabrication process of the antenna are shown in Figure 4.1.

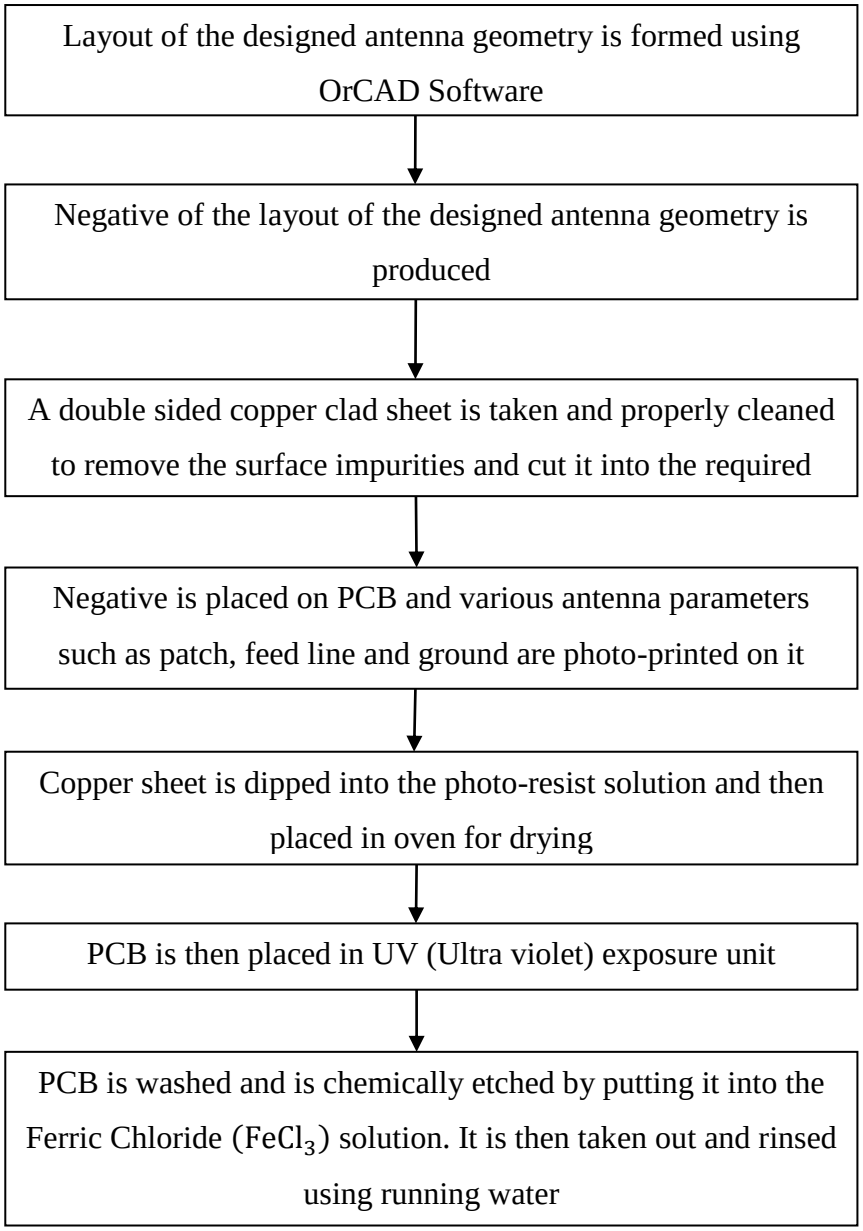

Figure 4.1 Flowchart of Antenna Fabrication Procedure

4.2 FABRICATION OF STAIRCASE SHAPED SLOTTED MSA WITH REDUCED DGS

The negative of layout of the proposed antenna is produced using OrCAD software and PCB of antenna is prepared according to fabrication process given in the flowchart. Figure 4.2 shows the fabricated design of the proposed antenna with SMA (Sub Miniature version A) connector.

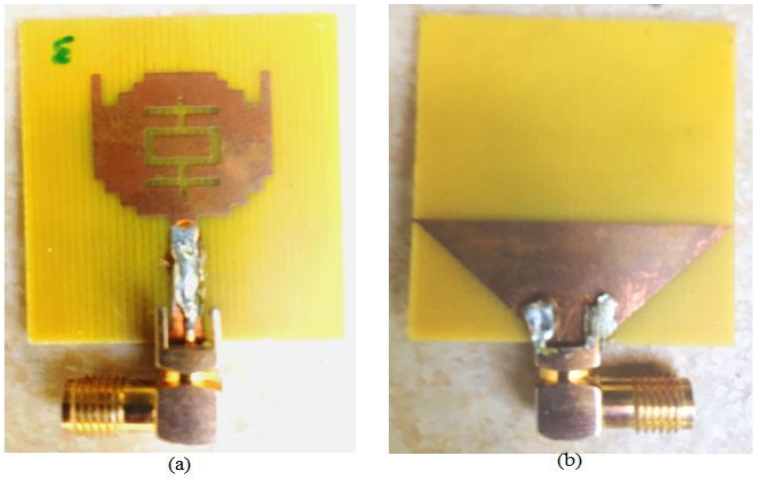

Figure 4.2 (a) Top view of the fabricated antenna (b) Reduced DGS view of the fabricated antenna

4.2.1 Equipment used for testing

The fabricated antenna has been tested for measuring S_{11}(dB) values by using Vector Network Analyzer (VNA) model no. E5063A of Agilent Technologies with an operating frequency range of 100 KHz to 18 GHz and is shown in Figure 4.3 below.

Figure 4.3 Network analyzer used for Testing

4.2.2 Comparison of Simulated and Fabricated Results of the proposed MSA

Figure 4.4 shows the comparison plot of simulated and tested results of the proposed antenna with S_{11}(dB) values plotted on Y-axis and frequency on X-axis. Table 4.1 shows the comparison of the results which shows that there is a close approximation between the tested and simulated results. The simulated results show an impedance bandwidth of 9.82GHz from 3.11GHz to 12.93GHz and the measured results show impedance bandwidth of 7.315GHz and 4.16GHz with the frequency bands from 0.135GHz to 7.45GHz and 8.86GHz to 13.02GHz respectively. For experimentally measured results, there is a shift in frequency band towards left as compared to the simulated results. This may be due to the misalignment of SMA connector and the errors introduced during antenna fabrication.

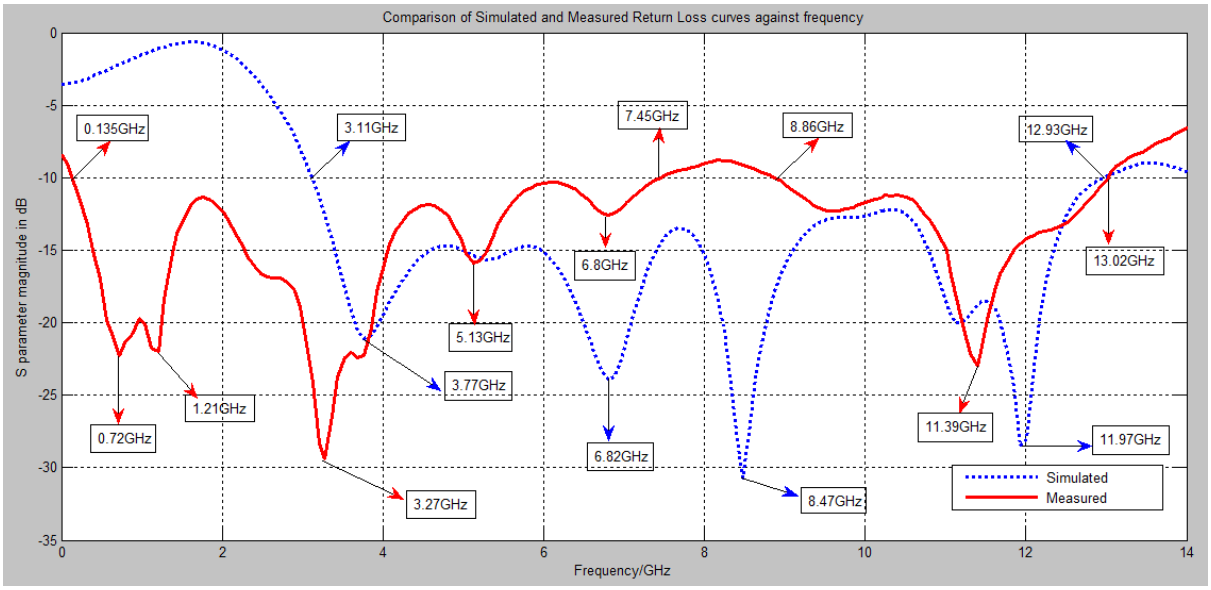

Figure 4.4 Comparison of Simulated and Measured Return loss curves of the proposed antenna

Parameter	Simulated Results	Measured Results
Frequency Range	3.11GHz to 12.93GHz	0.135GHz to 7.45GHz, 8.86GHz to 13.02GHz
Resonant Frequencies	3.77GHz,6.82GHz,8.47GHz,11.97GHz	0.72GHz,1.21GHz,3.27GHz, 5.13GHz, 6.8GHz,11.39GHz
Bandwidth	9.82 GHz	7.315GHz,4.16GHz
Return Loss	-21.1dB,-23.9dB,-30.7dB,-29.1dB	-22.28dB, -21.96dB,-29.35dB, -15.96dB,-12.58dB,-22.99dB
Applications Covered	UWB operation (3.1-10.6GHz) which makes the proposed antenna appropriate for breast cancer detection, WiMAX (3.4-3.69GHz), IMT band (3.4-3.6GHz) , INSAT (4.5-4.8 GHz), Radio Astronomy Band (5.01-5.03GHz), WLAN applications (5.15-5.535GHz, 5.725-5.825GHz), STM band	UWB operation (3.1-7.45GHz) which makes the proposed antenna suitable for breast cancer detection, GSM mobile phones (800-900MHz, 1800-1900MHz), WLAN applications (2.4-2.485GHz, 5.15-5.535GHz, 5.725-5.825GHz), Bluetooth (2.4-2.483GHz), Microwave ovens (2450MHz), Zig-Bee

	applications (6-6.17GHz), Downlink X-band satellite communication (7.25-7.75GHz), Amateur radio operations (10-10.5GHz), Amateur Satellite operations (10.45-10.5GHz)	(2.4-2.485GHz), IMT band (3.4-3.6GHz), WiMAX applications (3.4-3.6GHz), INSAT (4.5-4.8GHz), Radio Astronomy Band (5.01-5.03GHz), STM band (6-6.17GHz) applications, Amateur radio operations (10-10.5GHz), Amateur Satellite operations (10.45-10.5GHz)

Table 4.1 Comparison of Simulated and Measured Results for Staircase Shaped Slotted MSA

4.3 FABRICATION OF AN EXTENDED SEMI-CIRCULAR MSA WITH REDUCED DGS

Figure 4.5 shows the front and back view of the fabricated antenna design which consists of an extended semicircular radiating patch soldered with a SMA connector and a reduced ground plane with DGS.

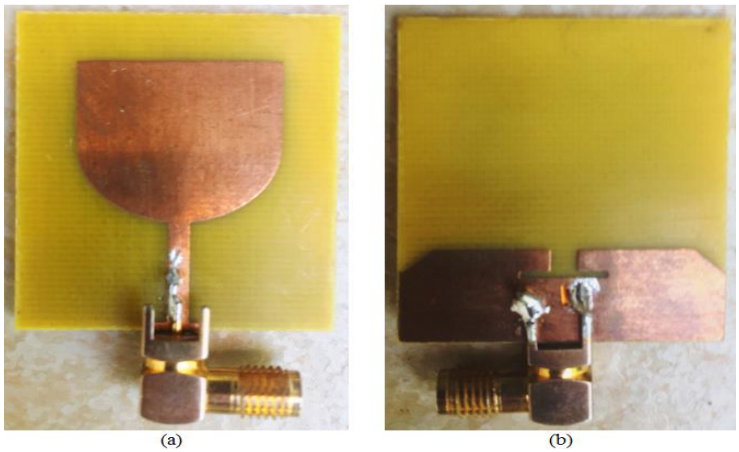

Figure 4.5 Fabricated antenna (a) Top view (b) Back view with Reduced DGS

4.3.1 Comparison of Simulated and Measured Results of the proposed MSA

Figure 4.6 shows the comparison plot of simulated and measured results of the proposed semicircular antenna for return loss (S_{11}) values which varies as the function of frequency. The simulated results show an impedance bandwidth of 6.61GHz with frequency range from 3.09GHz to 9.7GHz whereas the tested results cover four operational bands from 3.17GHz to 7.83GHz, 8.75GHz to 9.36GHz, 11.04GHz to 11.96GHz and 13.07GHz to 13.42GHz with impedance bandwidth of 4.66GHz, 0.61GHz, 0.92GHz and 0.35GHz respectively. Table 4.2 illustrates the comparison results which show that the experimentally measured and simulated result shows good agreement and the proposed UWB antenna is good candidate for microwave imaging applications.

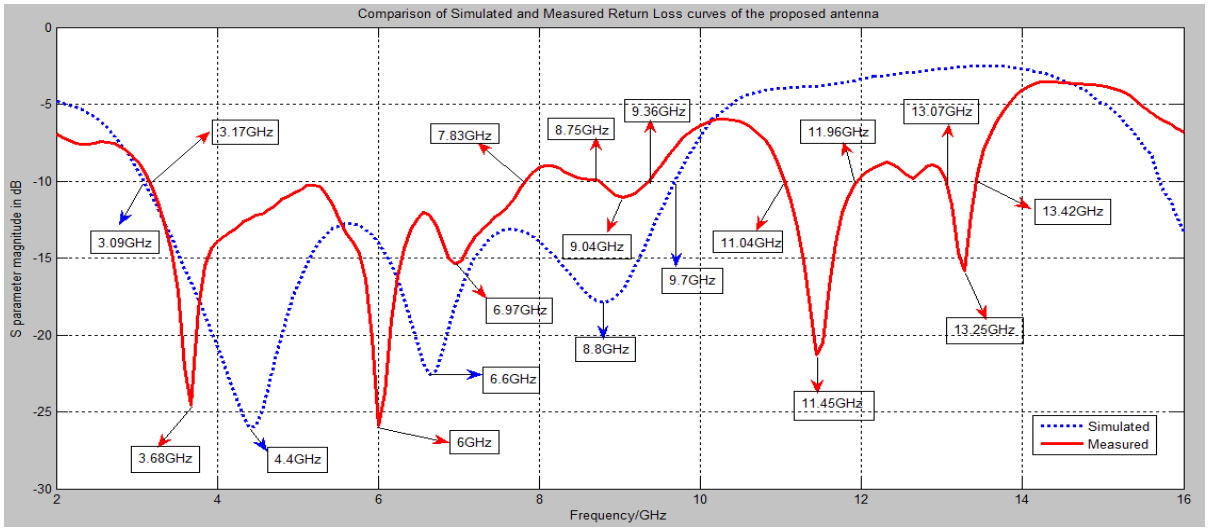

Figure 4.6 Comparison of Simulated and Tested Return loss curves

Parameters	Simulated Results	Measured Results
Frequency Range	3.09GHz to 9.7GHz	3.17GHz to 7.83GHz, 8.75 GHz to 9.36GHz,11.04GHz to 11.96 GHz, 13.07 GHz to 13.42 GHz
Resonant Frequencies	4.4 GHz, 6.6 GHz, 8.8GHz	3.68GHz, 6GHz, 6.97GHz, 9.04GHz, 11.45GHz, 13.25GHz
Bandwidth	6.61GHz	4.66GHz,0.61GHz,0.92GHz,0.35GHz
Return Loss	-26.05dB, -22.6dB, -17.9dB	-24.6 dB,-26 dB,-15.35 dB,-11.07dB, -21.3 dB,-15.84 dB
Applications Covered	UWB operation (3.1-9.7GHz) which makes the proposed antenna suitable for breast cancer detection, IMT band (3.4-3.6GHz), WiMAX (3.4-3.69GHz), INSAT (4.5-4.8GHz), Radio Astronomy Band (5.01-5.03GHz), WLAN (5.15-5.825GHz), STM band (6-6.17GHz) applications, Downlink X-band satellite communication (7.257.75GHz)	UWB operation (3.17-7.83 GHz) which makes the proposed antenna appropriate for breast cancer detection, IMT Band (3.4-3.6GHz), WiMAX (3.4-3.6GHz), INSAT (4.5-4.8GHz), Radio Astronomy Band (5.01-5.03GHz), WLAN applications (5.15-5.825GHz), STM band (6-6.17GHz) applications, Downlink X-band satellite communication (7.25-7.75GHz)

Table 4.2 Comparison of Simulated and Measured Results for an Extended Semicircular MSA

4.4 FABRICATION OF FORK SHAPED MSA WITH REDUCED DGS

Figure 4.7 shows the front and back view of the fabricated antenna which consists of a fork shaped radiating patch soldered with a SMA connector and a reduced ground plane with DGS. PEC (copper) is the material used for antenna fabrication. The thickness of copper coating deposited on each side of FR4 substrate is 0.035mm. The height of FR4 substrate is 1.6mm with overall antenna height of 1.67mm.

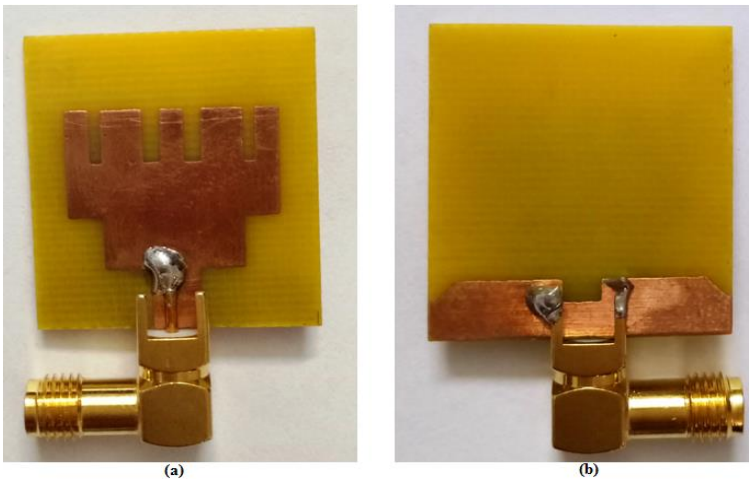

Figure 4.7 (a) Top view of the fabricated antenna with a fork shaped radiating patch (b) Back view of the reduced ground plane with DGS of the fabricated antenna

4.4.1 Comparison of Simulated and Measured Results of the proposed MSA

Figure 4.8 shows the comparison of simulated and tested S_{11}(dB) values of the proposed antenna which shows that the measurement results are closely matched with simulated ones. The simulated results show an impedance bandwidth of 7.77GHz with frequency range from 3.71GHz to 11.48GHz whereas the tested results cover two frequency bands from 2.8GHz to 9.36GHz and 10.4GHz to 12.88GHz with impedance bandwidth of 6.56GHz and 2.48GHz respectively. This slight deviation may be due to the inaccuracies introduced during antenna fabrication and testing. Table 4.3 demonstrates the comparison of simulated and measured results. Hence the proposed fork shaped antenna exhibit UWB characteristics which make it appropriate for breast cancer detection using microwave imaging technique.

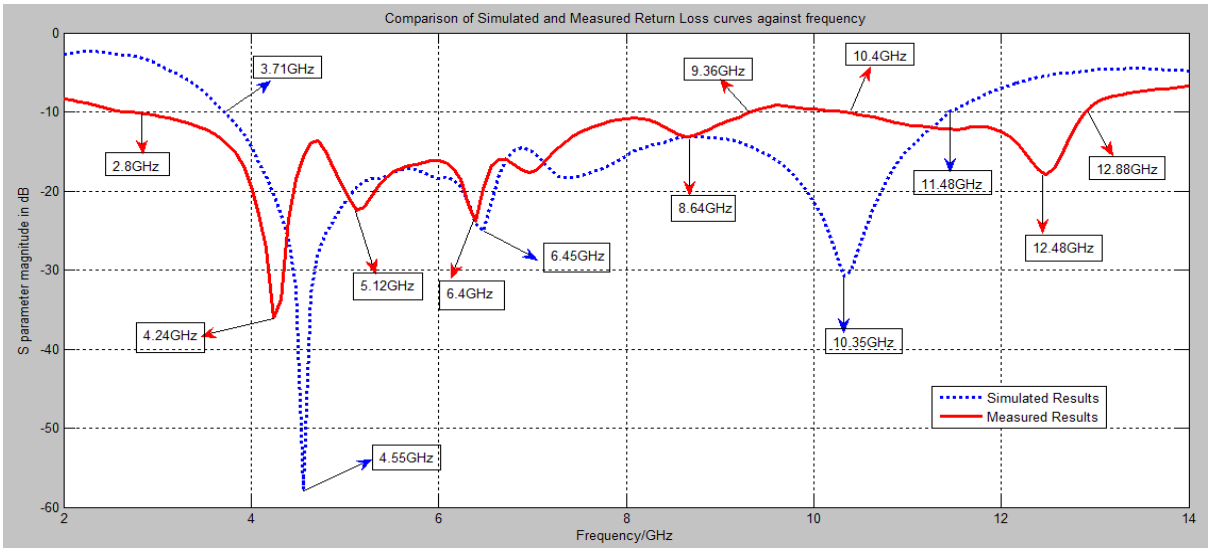

Figure 4.8 Comparison of Simulated and Measured S_{11}(dB) of the proposed antenna

Parameter	Simulated Results	Measured Results
Frequency range	3.71GHz to 11.48GHz	2.8GHz to 9.36GHz, 10.4GHz to 12.88GHz
Resonant Frequencies	4.55GHz,6.45GHz,10.35GHz	4.24GHz,5.12GHz,6.4GHz, 8.64GHz ,12.48GHz
Bandwidth	7.77 GHz	6.56GHz, 2.48GHz
Return loss	-57.71dB,-25.07dB, 30.75dB	-36dB,-22.48dB,-23.82dB, -13.15dB ,-17.88dB
Applications covered	UWB operation (3.7-10.6GHz) which makes the proposed antenna suitable for breast cancer detection, INSAT (4.5-4.8GHz), WLAN (5.15-5.535GHz , 5.725-5.825GHz), Radio Astronomy band (5.01-5.03GHz), STM band (6-6.17GHz) applications, Amateur radio operations (10-10.5GHz), Amateur satellite operations (10.45-10.5GHz)	UWB operation (3.1-9.36GHz) which makes the proposed antenna suitable for breast cancer detection, WiMAX (3.4-3.69GHz), IMT band (3.4-3.6GHz), INSAT (4.5-4.8GHz), WLAN (5.15-5.535GHz, 5.725-5.825GHz), Radio Astronomy band (5.01-5.03GHz), STM band (6-6.17GHz) applications, Amateur satellite operations (10.45-10.5GHz)

Table 4.3 Comparison of Simulated and Measured Results for Fork Shaped MSA

4.5 FABRICATION OF RECTANGULAR MSA LOADED WITH STUBS AND REDUCED DGS

Figure 4.9 shows the snapshot of the fabricated antenna which consists of a rectangular radiating patch joined with two stubs and a reduced ground plane with DGS.

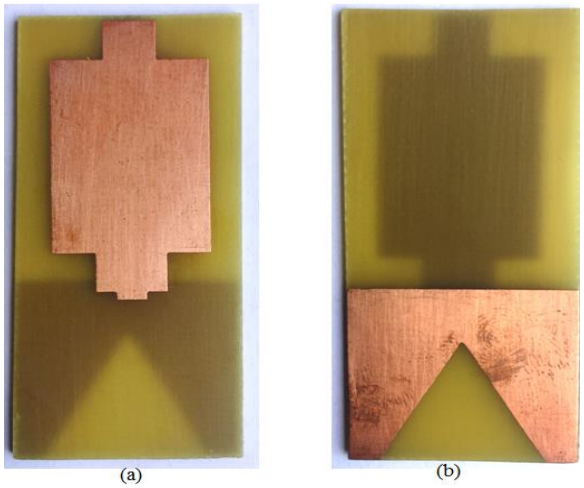

Figure 4.9 Fabricated antenna (a) Top view (b) Back view with Reduced DGS

4.5.1 Comparison of Simulated and Measured Results of the proposed MSA

Figure 4.10 shows the comparison between simulated and measured results of the proposed antenna in terms of S_{11}(dB) values with respect to frequency. It can be observed that the

simulated results show an impedance bandwidth of 7.08GHz for the frequency band from 0.17GHz to 7.25GHz and measured ones provide the impedance bandwidth of 4.14GHz and 0.8GHz for two frequency bands from 0.42GHz to 4.56GHz and 6.64GHz to 7.44GHz respectively. Table 4.4 illustrates this comparison. It can be seen that the proposed antenna exhibit an UWB behavior which can be employed for early diagnosis of breast cancer using microwave imaging systems.

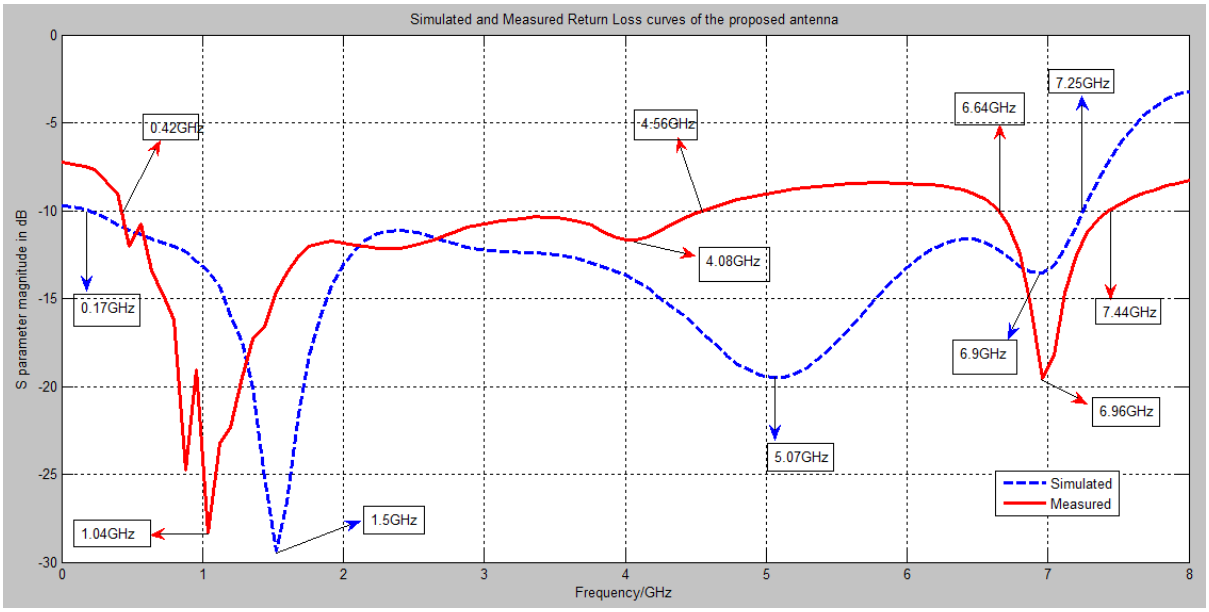

Figure 4.10 Comparison of Simulated and Experimentally Measured S_{11}(dB) of the proposed antenna

Parameters	Simulated Results	Measured Results
Frequency Range	0.17GHz to 7.25GHz	0.42GHz to 4.56GHz, 6.64GHz to 7.44GHz
Resonant Frequencies	1.5GHz, 5.07GHz, 6.9GHz	1.04GHz, 4.08GHz , 6.96GHz
Bandwidth	7.08GHz	4.14GHz, 0.8GHz
Return Loss	-29.74dB,-19.6dB,-14.04dB	-28.35dB, -11.69dB ,-19.57 dB
Applications Covered	UWB operation (3.1-7.25GHz) which makes the proposed antenna suitable for breast cancer detection, GSM mobile phones (800-900MHz,1800-1900MHz), WLAN applications (2.4-2.485GHz, 5.15-5.535GHz, 5.725-5.825GHz), Bluetooth (2.4-2.483 GHz), Microwave oven (2450MHz), Zig-Bee (2.4-2.485GHz), WiMaX (3.4-3.69GHz), IMT band (3.4-3.6GHz), INSAT (4.5-4.8GHz), Radio Astronomy Band (5.01-5.03GHz), STM band (6-6.17 GHz)	UWB operation (3.1-4.56GHz) which makes the antenna suitable for breast cancer detection, GSM mobile phones (800-900MHz, 1800-1900MHz), WLAN applications (2.4-2.485GHz), Bluetooth (2.4-2.483GHz), Microwave oven (2450MHz), Zig-Bee (2.42.485GHz), WiMaX (3.4-3.69GHz), IMT band (3.4-3.6GHz)

Table 4.4 Comparison of Simulated and Measured Results for Rectangular MSA

4.6 CONCLUSION

This chapter covers the fabrication and testing of four microstrip patch antennas that have been designed as UWB antennas and simulated using CST MWS'14 in chapter 3. The antennas are fabricated on commercially available FR4 substrate (ε_r= 4.4 and tan δ = 0.0024) using photolithography process. These antennas are experimentally tested for impedance bandwidth results on a VNA. The measured results in most of the cases are found to be quite satisfactory and matched with the simulated ones. A little variation in the measured results is seen because of the fabrication errors.

CHAPTER 5

SIMULATIONS FOR DETECTION OF BREAST CANCER

5.1 INTRODUCTION

This chapter presents the usage of designed and simulated microstrip antennas for the detection of breast cancer using simulations based on Radar based Microwave Imaging. A 3D planar breast phantom is modeled using CST MWS'14 software which is used for the fast and accurate electromagnetic analysis of high frequency devices. The mono-static radar based microwave imaging is employed to diagnose the presence of tumor inside the breast phantom when it is illuminated by the microwave signals. For this purpose, fork shaped microstrip patch antenna with a reduced DGS and rectangular microstrip patch antenna with a reduced DGS discussed in chapter 3 are utilized. These antennas exhibit high gain, miniaturization and UWB characteristics which makes them a good candidate for diagnosis of malignant tumors by microwave imaging technique. The distance between the breast phantom surface and UWB patch antenna is varied for recording scattering parameters (S_{11}) values.

5.2 DESIGN AND SIMULATION OF A PLANAR BREAST PHANTOM

Figure 5.1 show the perspective view of the designed 3D planar breast phantom. It is a two layer model where the first layer is the skin and second layer is the fatty tissue with different dielectric properties (permittivity and conductivity). The cancer cell is modeled as a spherical structure (radius of 10mm) which is embedded inside the breast phantom at the depth of 18.5mm. Table 5.1 shows different permittivity and conductivity values of designed breast phantom. The dimensions of the fat layer are selected as 148x86x36mm^3 and the dimensions of the skin layer are selected as 148x86x1mm^3 where the skin is placed over the fatty tissue.

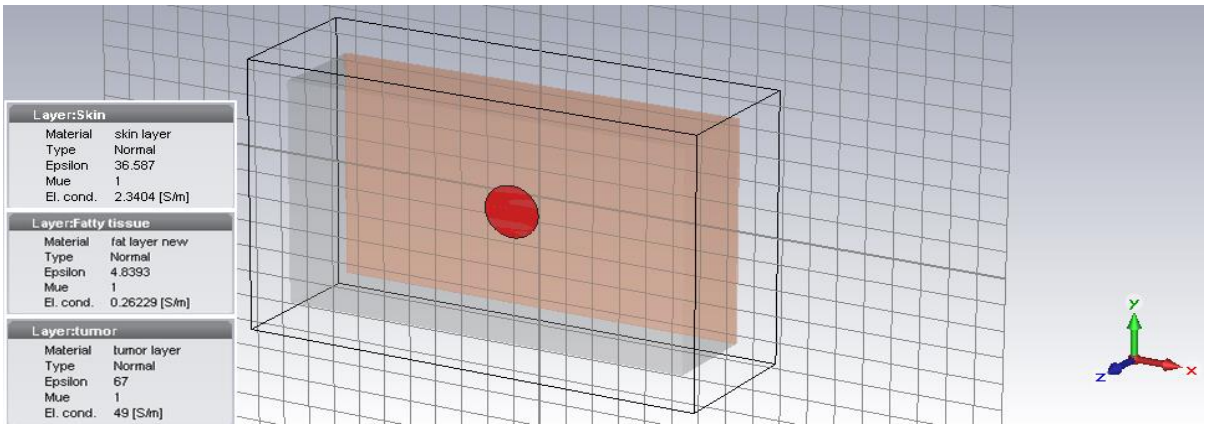

Figure 5.1 Perspective view of 3D planar breast phantom design in CST MWS'14

Tissue Type	Permittivity(ε_r)	Conductivity(σ) (S/m)
Skin layer	36.587	2.3404
Fatty tissue	4.8393	0.26229
Tumor	67	49

Table 5.1 Dielectric properties of breast tissues

5.3 SIMULATION SETUP FOR FORK SHAPED MICROSTRIP PATCH ANTENNA WITH REDUCED DGS FOR DETECTION OF BREAST CANCER

The designing, simulation and parametric analysis of a miniaturize fork shaped microstrip-fed patch antenna with reduced DGS has been discussed in chapter 3. The proposed antenna operates in the frequency range from 3.71GHz to 11.48GHz with bandwidth of 7.77GHz and peak return loss of -57.71dB at a frequency of 4.55GHz. It exhibits a peak gain of 5.82dB at a frequency of 11GHz. The proposed antenna satisfies the overall requirements for UWB operation which makes it acceptable for diagnosis of cancerous cell present in the breast phantom using mono-static radar based microwave imaging technique. The procedure is to place the antenna near the affected part of the breast. The antenna is then allowed to transmit and receive the backscattered signals. The simulations are carried out in CST MWS'14 for recording the backscattered signals by varying the distance between breast phantom surface and proposed UWB antenna for with and without tumor. Four cases are examined under this section using tumor radius of 10mm.

5.3.1 Direct Contact

The simulations are carried out when the proposed UWB antenna is placed in direct contact with the surface of the breast phantom in the absence and presence of tumor where the radius of tumor is 10mm.

Figure 5.2 View of y-z axis when there is a direct contact between breast phantom surface and the proposed antenna

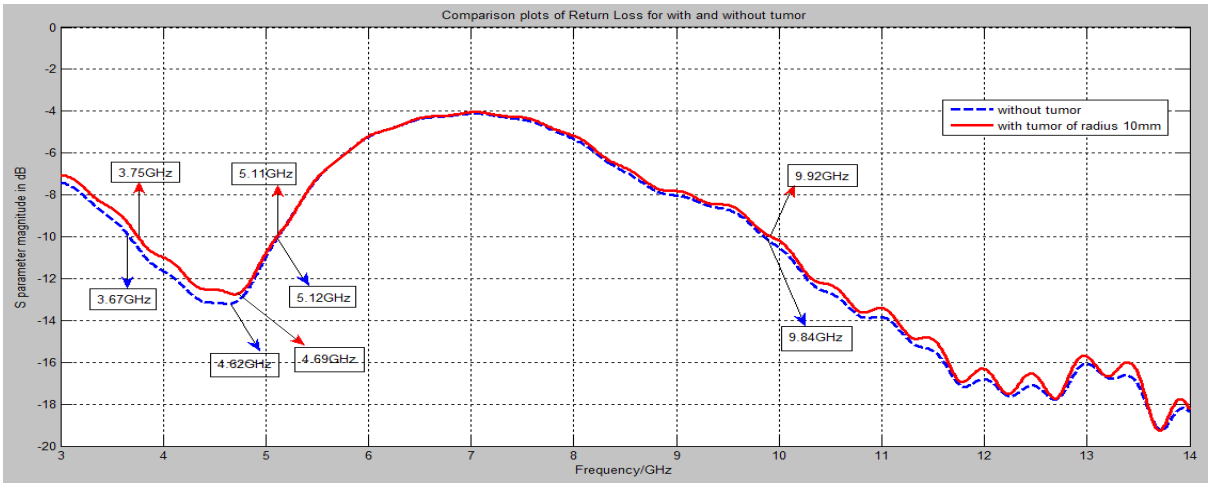

Figure 5.3 Comparison plots of S_{11} parameter values when proposed antenna is placed in direct contact with the breast phantom surface

Breast Phantom	Frequency Band	Return loss
No tumor	3.67-5.12GHz, 9.84-14GHz	-13.19dB at 4.62GHz
Tumor with radius of 10mm	3.75-5.11GHz, 9.92-14GHz	-12.75dB at 4.69GHz

Table 5.2 Comparison of Simulated results for direct contact

Table 5.2 shows that when the antenna is placed in direct contact with skin for two cases of breast phantom with and without tumor, the signals reflected back in the presence of tumor are more as compared to the case without tumor.

5.3.2 10mm distance

In order to further illustrate this fact that breast phantom with tumor will give more reflections, the simulations are carried out when the proposed UWB antenna is placed at the distance of 10mm from the surface of the breast phantom in the absence and presence of tumor where the radius of tumor is 10mm.

Figure 5.4 View of y-z axis where the proposed antenna is placed at the distance of 10mm from the breast phantom surface

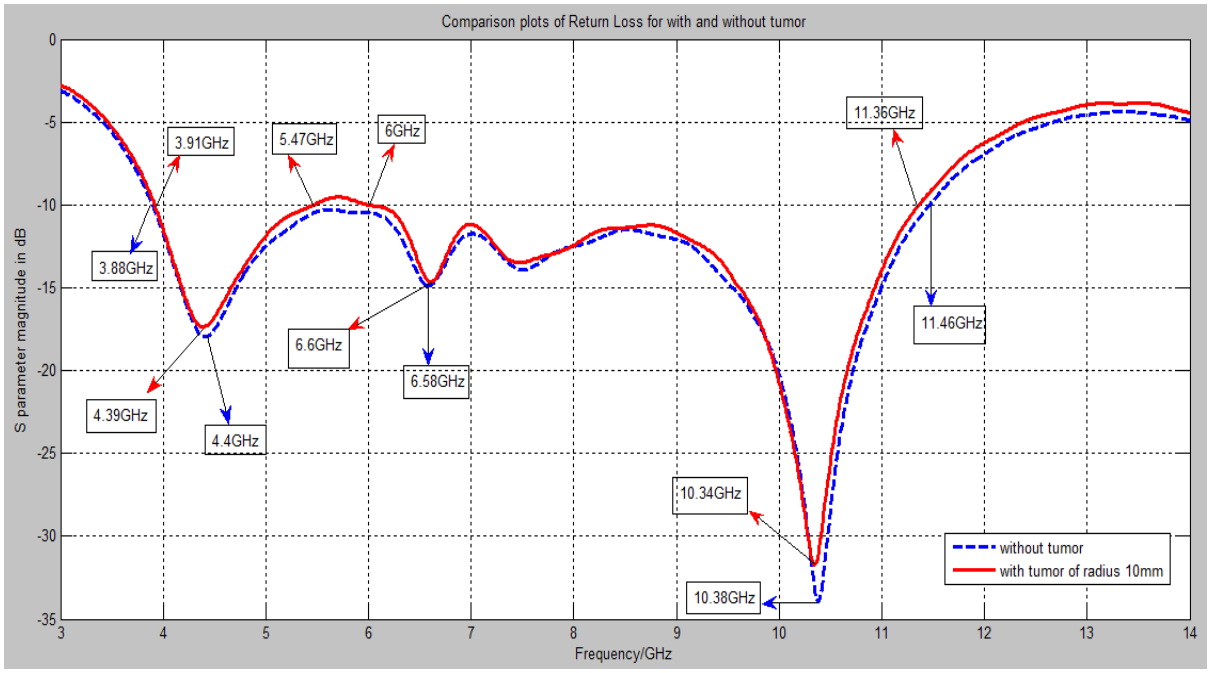

Figure 5.5 Comparison plots of S_{11} parameter values when proposed antenna is placed at a distance of 10mm from the breast phantom surface

Breast Phantom	Frequency Band	Return loss
No tumor	3.88-11.46GHz	-17.95dB at 4.4GHz, -14.87dB at 6.58GHz, -33.9dB at 10.38GHz
Tumor with radius of 10mm	3.91-5.47GHz, 6-11.36GHz	-17.37dB at 4.39GHz, -14.63dB at 6.6GHz, -31.73dB at 10.34GHz

Table 5.3 Comparison of Simulated results for 10mm distance

Table 5.3 shows that when the proposed UWB antenna is placed at a distance of 10mm from the skin layer for two cases of breast phantom with and without tumor, more signal reflections takes place which results in more return loss in presence of tumor as compared to the case without tumor.

5.3.3 20mm distance

To further validate the fact that breast phantom with tumor will give more reflections, the simulations are carried out when the proposed UWB antenna is placed at the distance of 20mm from the surface of the breast phantom in the absence and presence of tumor where the radius of tumor is 10mm.

Figure 5.6 View of y-z axis where the proposed antenna is placed at the distance of 20mm from the breast phantom surface

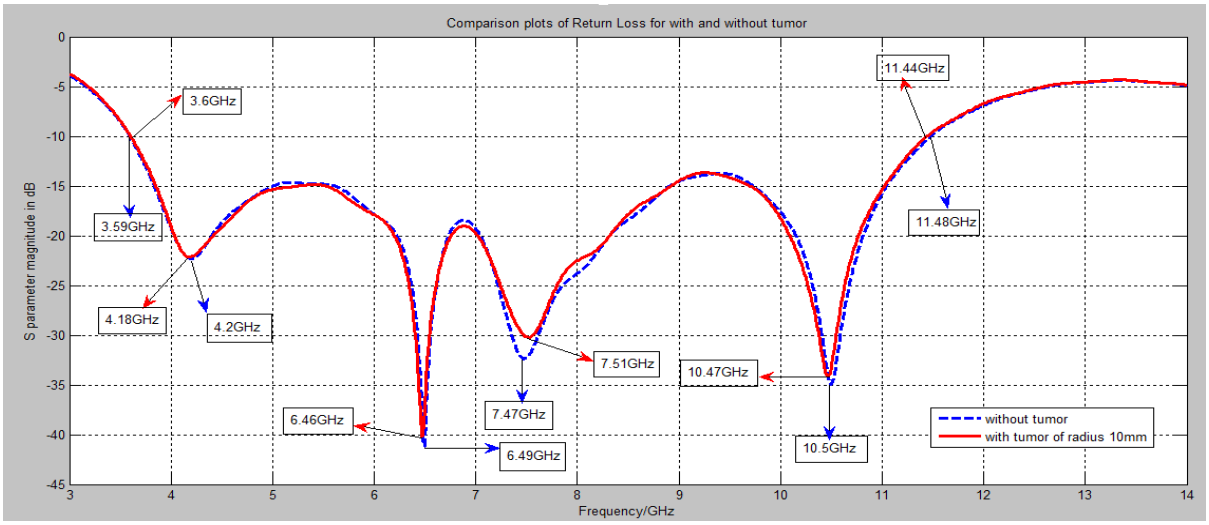

Figure 5.7 Comparison plots of S_{11} parameter values when proposed antenna is placed at a distance of 20mm from the breast phantom surface

Breast Phantom	Frequency Band	Return loss
No tumor	3.59-11.48GHz	-22.33dB at 4.2GHz, -41.13dB at 6.49GHz, -32.37dB at 7.47GHz, -34.97dB at 10.5GHz
Tumor with radius of 10mm	3.6-11.44GHz	-22.14dB at 4.18GHz, -40.19dB at 6.46GHz, -30.21dB at 7.51GHz, -34.13dB at 10.47GHz

Table 5.4 Comparison of Simulated results for 20mm distance

Table 5.4 shows that when the antenna is placed at a distance of 20mm from the skin layer for two cases of breast phantom with and without tumor, more loss of signal power takes place for malignant breast tissue as compared to the case of normal breast tissue.

5.3.4 30mm distance

To see the effect of varying distance of antenna for tumor detection, the simulations are carried out when the proposed UWB antenna is placed at the distance of 30mm from the surface of the breast phantom in the absence and presence of tumor where the radius of tumor is 10mm.

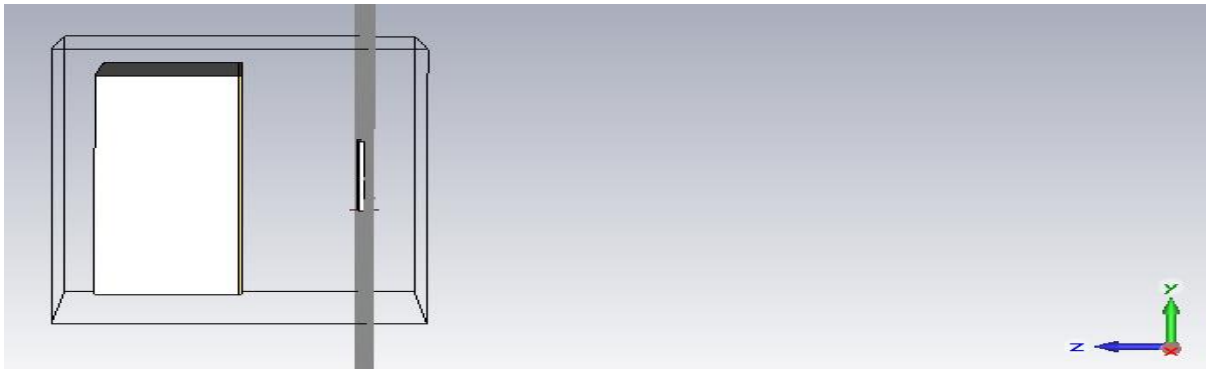

Figure 5.8 View of y-z axis where the proposed antenna is placed at the distance of 30mm from the breast phantom surface

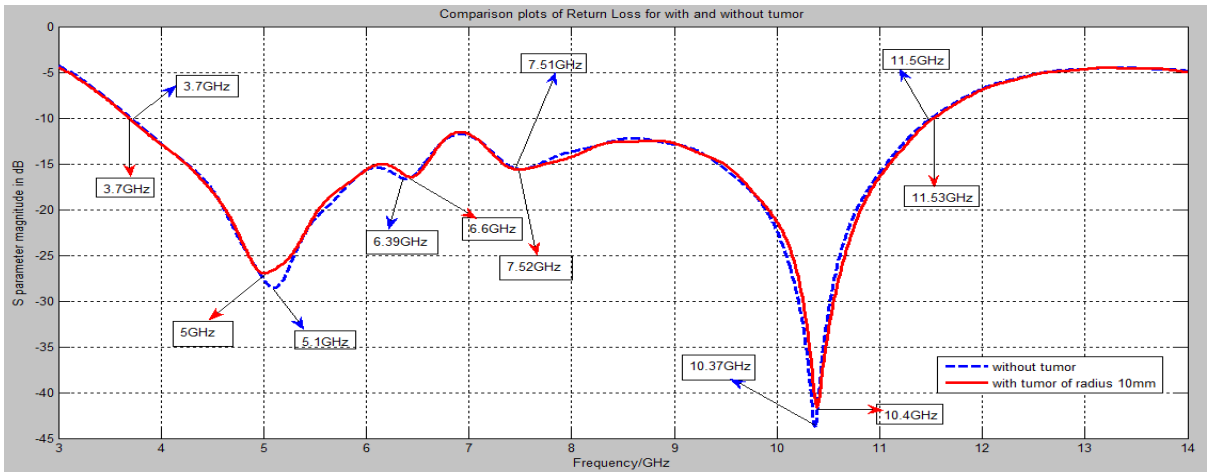

Figure 5.9 Comparison plots of S_{11} parameter values when proposed antenna is placed at a distance of 30mm from the breast phantom surface

Breast Phantom	Frequency Band	Return loss
No tumor	3.7-11.5GHz	-28.58dB at 5.1GHz, -16.62dB at 6.39GHz, -15.59dB at 7.51GHz, -43.81dB at 10.37GHz
Tumor with radius of 10mm	3.7-11.53GHz	-26.96dB at 5GHz, -16.43dB at 6.6GHz, -15.64dB at 7.52GHz, -41.59dB at 10.4GHz

Table 5.5 Comparison of Simulated results for 30mm distance

Table 5.5 shows that when the antenna is placed at a distance of 30mm from the skin layer for two cases of breast phantom with and without tumor, less significant variations in received reflected signals from the malignant and normal breast phantom is observed.

It can be seen that as the distance of antenna is increased beyond 20mm, the reflected signals received from the breast phantom with and without tumor are of almost same intensity. Therefore, for radar based microwave imaging, the proposed antenna should be placed at a distance of 20mm (maximum).

5.4 SIMULATION SETUP FOR RECTANGULAR MICROSTRIP PATCH ANTENNA AND A REDUCED DGS FOR DETECTION OF BREAST CANCER

The designing, simulation and parametric study of a compact rectangular microstrip patch antenna loaded with stubs and a reduced DGS has been discussed in chapter 3. The proposed antenna covers a frequency range from 0.17GHz to 7.25GHz with bandwidth of 7.08GHz. It exhibits a peak gain of 5.007dB at 7.25GHz frequency. The proposed antenna provides miniaturization, high gain and an optimum UWB operation which makes it appropriate for the detection of malignant breast phantom based upon mono-static radar based active microwave imaging technique. The designing of the breast phantom and simulations are carried out in CST MWS'14 for recording the reflected signals from the breast tissues by varying the distance between breast phantom surface and proposed UWB antenna for with and without tumor. Four cases are examined under this section using tumor radius of 10mm.

5.4.1 Direct Contact

The simulations are carried out when the proposed UWB antenna is placed in direct contact with the surface of the breast phantom in the absence and presence of tumor with tumor radius of 10mm.

Figure 5.10 View of y-z axis when there is a direct contact between breast phantom surface and the proposed antenna

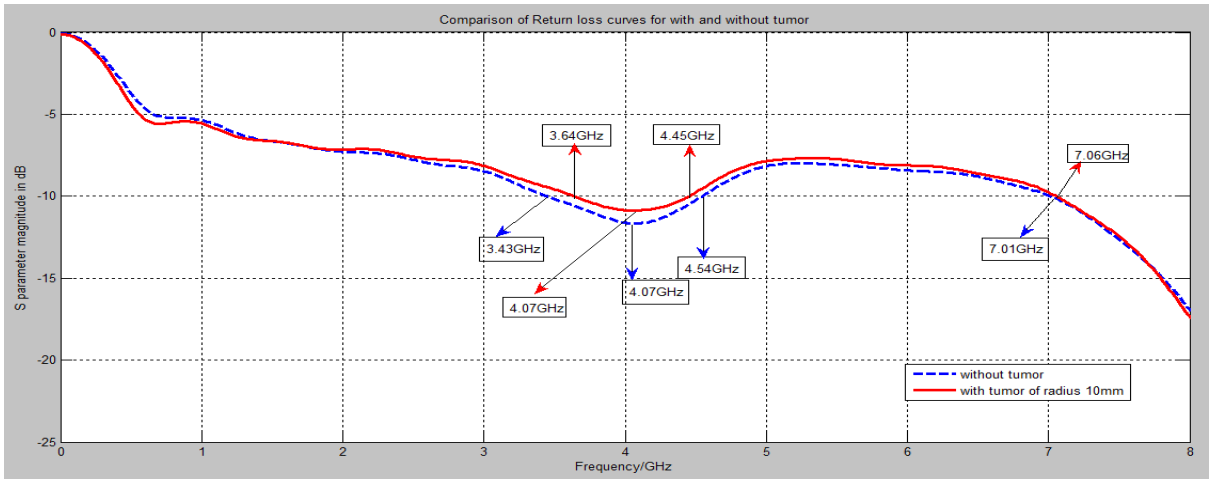

Figure 5.11 Comparison plots of S_{11} parameter values when proposed antenna is placed in direct contact with the breast phantom surface

Breast Phantom	Frequency Band	Return loss
No tumor	3.43-4.54GHz, 7.01-8GHz	-11.66dB at 4.07GHz
Tumor with radius of 10mm	3.64-4.45GHz, 7.06-8GHz	-10.86dB at 4.07GHz

Table 5.6 Comparison of Simulated results for direct contact

Table 5.6 illustrates that when the proposed antenna is placed in direct contact with the skin layer for two cases of breast phantom with and without tumor, the received reflected signals are more from the breast phantom with tumor as compared to the normal breast phantom.

5.4.2 10mm distance

To prove the validity of fact that more signal reflections takes place from malignant breast phantom, the simulations are carried out when the proposed UWB antenna is placed at the distance of 10mm from the surface of the breast phantom in the absence and presence of tumor where the radius of tumor is 10mm.

Figure 5.12 View of y-z axis where the proposed antenna is placed at the distance of 10mm from the breast phantom surface

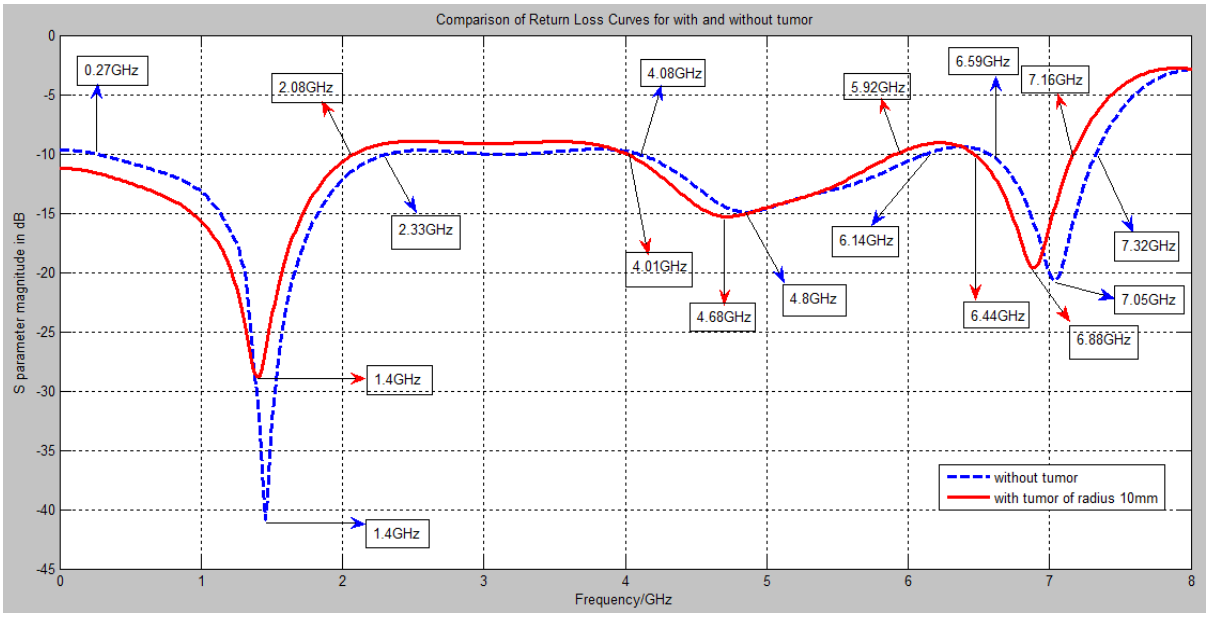

Figure 5.13 Comparison plots of S_{11} parameter values when proposed antenna is placed at a distance of 10mm from the breast phantom surface

Breast Phantom	Frequency Band	Return loss
No tumor	0.27-2.33GHz, 4.08-6.14GHz , 6.59-7.32GHz	-40.91dB at 1.45GHz, -15.13dB at 4.8GHz, -20.5dB at 7.05GHz
Tumor with radius of 10mm	0.17-2.08GHz, 4.01-5.92GHz , 6.44-7.16GHz	-28.86dB at 1.4GHz, -15.28dB at 4.68GHz, -19.61dB at 6.88GHz

Table 5.7 Comparison of Simulated results for 10mm distance

Table 5.7 shows that when the antenna is placed at a distance of 10mm from the skin layer for two cases of breast phantom with and without tumor, more signal reflections takes place from the malignant breast phantom. Hence, the return loss is more from the breast phantom with tumor as compared to the case of without tumor.

5.4.3 20mm distance

The simulations are carried out when the proposed UWB antenna is placed at the distance of 20mm from the surface of the breast phantom in the absence and presence of tumor with tumor radius of 10mm.

Figure 5.14 View of y-z axis where the proposed antenna is placed at the distance of 20mm from the breast phantom surface

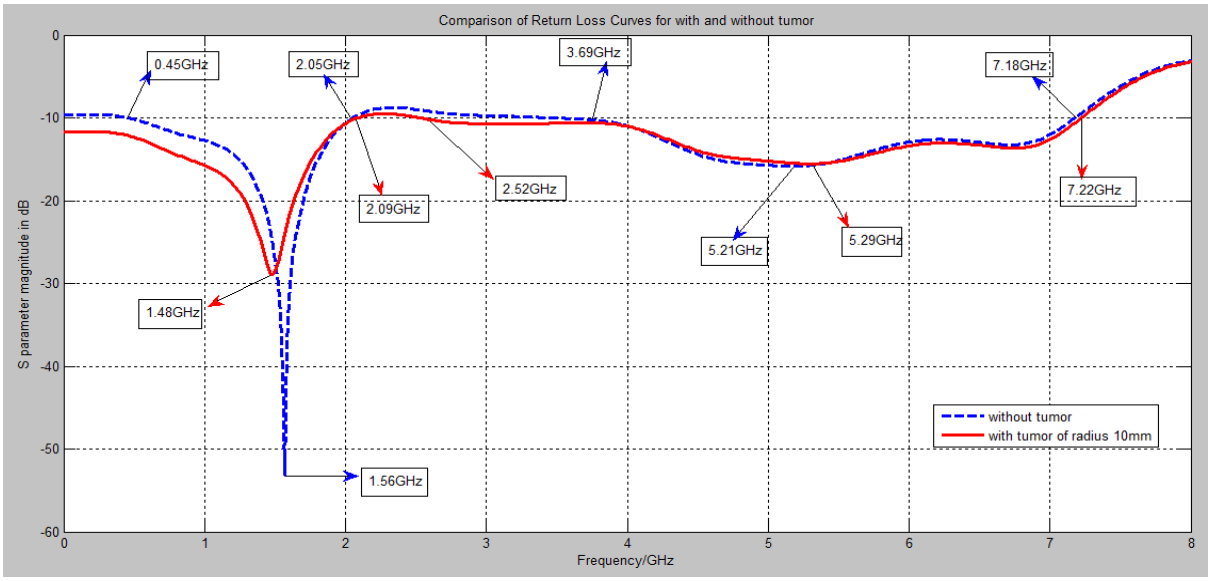

Figure 5.15 Comparison plots of S_{11} parameter values when proposed antenna is placed at a distance of 20mm from the breast phantom surface

Breast Phantom	Frequency Band	Return loss
No tumor	0.45-2.05GHz, 3.69-7.18GHz	-53.19dB at 1.56GHz, -15.82dB at 5.21GHz
Tumor with radius of 10mm	0.17-2.09GHz, 2.52-7.22GHz	-28.88dB at 1.48GHz, -15.54dB at 5.29GHz

Table 5.8 Comparison of Simulated results for 20mm distance

Table 5.8 shows that when the proposed UWB antenna is placed at a distance of 20mm from the skin layer for two cases of breast phantom with and without tumor, the peak return loss from malignant and normal breast phantom is -28.88dB and -53.19dB respectively. Hence, more signal reflections takes place in presence of tumor as compared to the case of without tumor.

5.4.4 30mm distance

The simulations are carried out when the proposed UWB antenna is placed at the distance of 30mm from the surface of the breast phantom in the absence and presence of tumor where the radius of tumor is 10mm.

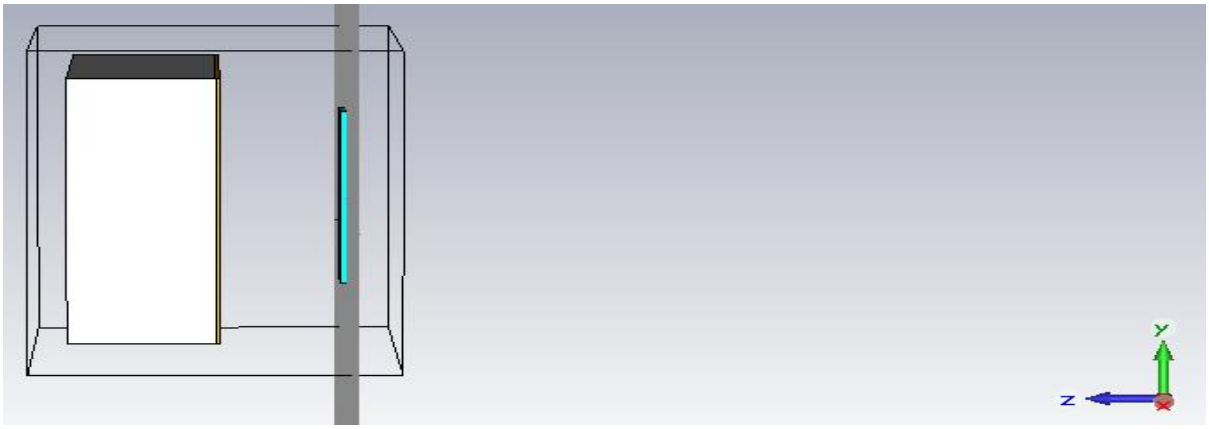

Figure 5.16 View of y-z axis where the proposed antenna is placed at the distance of 30mm from the breast phantom surface

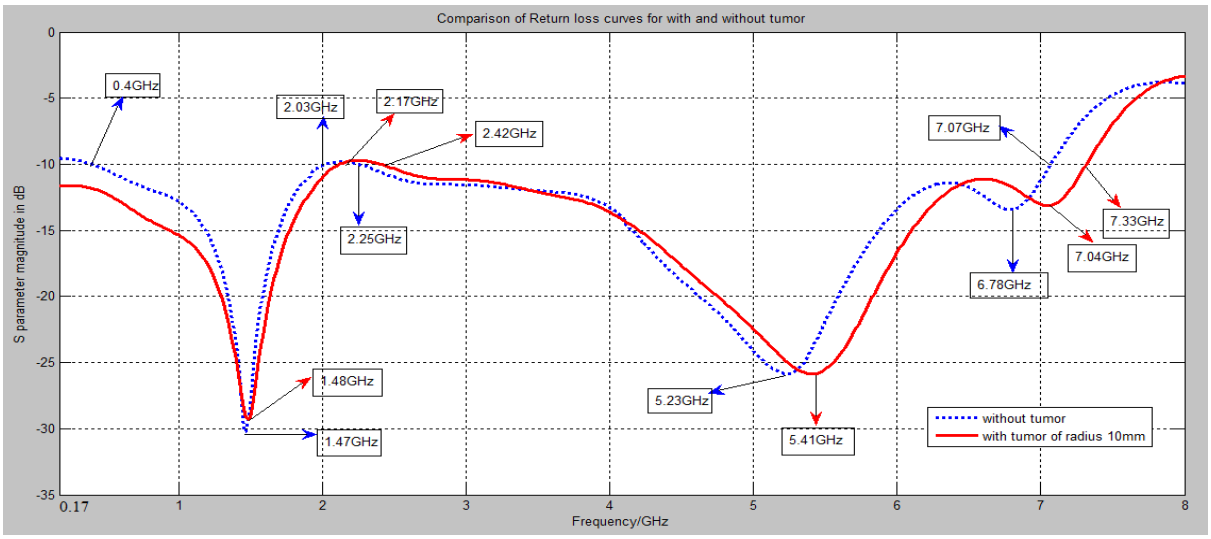

Figure 5.17 Comparison plots for Return Loss (S_{11}) values when proposed antenna is placed at a distance of 30mm from the breast phantom surface

Breast Phantom	Frequency Band	Return loss
No tumor	0.4-2.03GHz, 2.25-7.07GHz	-30.2dB at 1.47GHz, -25.82dB at 5.23GHz, -13.43dB at 6.78GHz
Tumor with radius of 10mm	0.17-2.17GHz, 2.42-7.33GHz	-29.3dB at 1.48GHz, -25.86dB at 5.41GHz, -13.1dB at 7.04GHz

Table 5.9 Comparison of Simulated results for 30mm distance

Table 5.9 shows that when the proposed antenna is placed at a distance of 30mm from the skin layer for two cases of breast phantom with and without tumor, the peak return loss from malignant and normal breast phantom is -29.3dB and -30.2dB respectively. Hence, less significant variations are observed between with and without tumor case.

5.5 CONCLUSION

Microwave signals are used for detecting the presence of cancerous cell in the breast phantom. It based upon the concept of tissue dependent microwave scattering and absorption in the breast phantom which helps to determine the significant contrast in the dielectric properties of cancerous and healthy breast tissue. It is widely assumed that high water content of malignant breast tissues causes larger microwave scattering as compared to the normal fatty breast tissue which have low water content. It is because malignant breast tissues are characterized by a high relative permittivity and conductivity whereas as normal breast tissue posses low relative permittivity and conductivity at microwave frequencies. Based upon the comparison plots of the recorded return loss values for with and without tumor as shown in Figures 4.3, 4.5, 4.7, 4.9, 4.11, 4.13, 4.15 and 4.17 and simulated data presented in Tables 4.2, 4.3, 4.4, 4.5, 4.6, 4.7, 4.8 and 4.9, it is can be concluded that in the presence of tumor (with radius of 10mm) the received reflected signal is more which results in poor impedance matching and poor return loss characteristics as compared to the normal breast phantom.

Another point that can be observed is that the designed UWB antennas provides best results to detect the presence of a cancerous cell only up to a distance of 20mm from the breast phantom surface. So the setup used for microwave imaging should be placed at a maximum distance of 20mm for the detection of small tumors up to the size of 10mm.

CHAPTER 6

CONCLUSION AND FUTURE WORK

6.1 CONCLUSIONS

- The thesis work begins with the general discussion on global scenario of breast cancer and various techniques for its early diagnosis out of which Microwave UWB imaging is regarded as the most promising technology. The main objective of the thesis was to design and fabricate microstrip patch antennas with both miniaturization and UWB characteristics which can employed for Radar based Active Microwave imaging for breast cancer detection.
- Chapter 2 deals with the literature review done in regard with microstrip patch antennas for UWB operation which can be employed for breast cancer detection using microwave imaging technique.
- Chapter 3 presents the design and simulation of four UWB microstrip patch antennas with microstrip feeding. A parametric study of various antenna design parameters such as slots, notches and tuning stubs are investigated to enhance the bandwidth of antenna. The simulation results are analyzed in terms of return loss, bandwidth, gain and current distribution. The first design is a small staircase shaped slotted microstrip patch antenna with a reduced DGS for UWB applications. It covers the operational band from 3.11GHz to 12.93GHz with bandwidth (S_{11}<-10dB) of 9.82GHz. The second design is a half circular patch antenna with an extended length and a partial ground plane with an inverted T-shaped slot and dual right angled isosceles triangular notches is designed to achieve both miniaturization and UWB behavior. It covers a frequency range from 3.09GHz to 9.7GHz with impedance bandwidth of 6.61GHz. The third design is a compact fork shaped microstrip patch antenna with a reduced DGS for UWB applications. The proposed antenna covers a wide frequency band from 3.71GHz to 11.48GHz with impedance bandwidth of 7.77GHz and show a peak gain of 7.16dB at a frequency of 12.6GHz which makes it a good candidate for UWB microwave imaging systems. The fourth design is a compact rectangular microstrip patch antenna combined with two stubs and a reduced ground plane with DGS. It covers the frequency band from 0.17GHz to 7.25GHz with impedance bandwidth of 7.08GHz and a peak gain of 5.007dB is achieved at a frequency of 7.25GHz. Table 6.1 presents the simulated results in terms of frequency range, bandwidth, resonant frequencies, peak return loss and peak gain values of all four UWB patch antennas.

Design	Frequency range	Bandwidth	Resonant Frequencies	Peak Return Loss (dB)	Peak Gain (dB)
Staircase Shaped Slotted MPA with Reduced DGS	3.11GHz-12.93GHz	9.82GHz	3.77GHz, 6.8GHz, 8.47GHz, 11.9GHz	-30.72dB at 8.47GHz	7.16dB at 12.6GHz
Extended Semi-circular MPA with Reduced DGS	3.09GHz-9.7GHz	6.61GHz	4.4GHz,6.6GHz, 8.8GHz	-26.05dB at 4.4GHz	4.58dB at 7.6GHz
Fork Shaped MPA with Reduced DGS	3.71GHz-11.48GHz	7.77GHz	4.55GHz,6.45GHz, 10.35GHz	-57.71dB at 4.55GHz	5.82dB at 11GHz
Stub loaded RMSA and Reduced DGS	0.17GHz-7.25GHz	7.08GHz	1.5GHz, 5.07GHz, 6.9GHz	-29.74dB at 1.5GHz	5dB at 7.25GHz

Table 6.1 Simulated results of all antenna designs

- In chapter 4, all four antennas designed and simulated in chapter 3 are fabricated using photolithography process and experimentally tested using VNA to validate the results of proposed antennas for UWB applications. The comparison is made between the simulated and measured S_{11} parameter values for all antenna designs. There is a good match and slight variation between simulated and tested results. The shift in the tested results along with reduced bandwidth is observed which may be due to the connector misalignment and environmental characteristics.
- In chapter 5, the designed and tested UWB antennas are simulated for detection of breast cancer based upon radar based microwave imaging technology. Here a 3D planar breast phantom is designed with specific values of permittivity and conductivity for skin layer and fatty tissue. A cancerous cell is inserted in this phantom and the antenna is placed in front of the breast. Simulations are done on the basis of signals transmitted to this phantom and received by the same antenna. It is observed that the affected area gives more reflections and less return loss for the same band. Thus, the presence of tumor can be easily diagnosed.

6.2 FUTURE WORK

The work and methodology adopted in this thesis for design of UWB patch antennas for breast cancer detection using microwave imaging can be in future extended to:

- Optimization Techniques: Inbuilt optimizer in CST MWS'14 can be used for carrying out the optimization of various antenna design parameters by using optimization

techniques such as genetic algorithm, PSO (Particle Swarm Optimization) etc which helps the antenna to achieve optimized results in terms in gain and bandwidth. Genetic algorithm can also be employed in feature selection for identifying the location of tumor in the breast phantom.

- Array Configuration: Suitable antenna array configurations can be used to achieve high gain, high power handling capacity and high reliability.
- Other Feeding Techniques: The microstrip patch antennas can be energized using other feeding techniques such as aperture-coupled, proximity coupled, coaxial cable and CPW for bandwidth enhancement.
- Metamaterials: It is an artificially constructed material which exhibits EM properties not found in nature as they depend upon the internal atomic structure. Metamaterial structure is composed of split ring resonators and thin wire elements to produce negative values of permittivity and permeability respectively. Such structures act as a lens for a microstrip patch antenna which helps to achieve an enhanced gain, better radiation pattern for greater coverage, broadband and miniaturization characteristics.
- Fabrication of Tissue Mimic Breast Phantom based on Gelatin Oil Technology: Measured results can be obtained by fabricating the breast phantom using gelatin oil technology. The fabricated breast phantom can be of a planar or hemi-spherical geometry. For carrying out the experimental study, a planar breast phantom can be fabricated in a simple cuboid container. The hemi-sphere breast phantom presents more realistic model but uses a complicated mould where the most difficult part is depositing the skin layer. The chemical mixture prepared for the skin layer is poured into the base and is covered for 2-3 days to solidify the skin layer. The cover should be removed very carefully as the skin layer is very thin and gets damaged easily. Then the fat layer mixture can be poured onto the skin layer in the same container. The fabricated tumor mixture can be cut into the required spherical radius and can be placed at the desired position before the fat layer solidifies. The skin layer formed is flexible and off-white in colour whereas the fat layer is flaccid and pale yellow in colour. The fabricated breast phantom can be employed for practical measurements.
- Signal processing: Various signal processing methods need to be investigated to determine the tumor size and exact location of tumor in breast phantom. For diagnosis, signal processing techniques also removes all the unwanted parts in obtained reflected signal to obtain high resolution images.

REFERENCES

[1] Ali. I., Wani, W.A. and Saleem, K. (2011). Cancer Scenario in India with Future Perspectives, *Cancer Therapy*, 8(8), 56-70

[2] MacMohan, B. (2006). Epidemiology and the Causes of Breast Cancer. *International Journal of Cancer*, 118(10), 2373-2378.

[3] Tabar, L. *et al.* (1996). Tumor development, histology and grade of breast cancers: Prognosis and progression, *International Journal of Cancer*, 66(4), 413-419.

[4] Palantei, E. *et al.* (2015). Early stage cancer detection technique considering the reflected power from breast tissues, *ARPN Journal of Engineering and Applied Sciences*, 10(17), 7361-7367.

[5] Moore, S.K. (2001). Better breast cancer detection, *IEEE Spectrum*, 38(5), 50-54.

[6] Karli, R. and Ammor, H. (2014). Miniaturized UWB Microstrip Patch Antenna with T-slot for Detecting Malignant Tumors by Microwave Imaging, *International Journal of Microwave and Optical Technology*, 9(3), 214-220.

[7] Bohra, S. and Shaikh, T. (2016). UWB Microstrip Patch Antenna for Breast Cancer Detection. *International Journal of Advanced Research in Electronics and Communication Engineering*, 5(1), 88-91.

[8] Calistan, R. *et al.* (2015). A Microstrip patch antenna Design for Breast Cancer Detection, *World Conference on Technology, Innovation and Entrepreneurship* [2nd: Istanbul, Turkey: 2015], pp. 2905-2911.

[9] Banu, S. *et al.* (2013). Performance analysis of circular patch antenna for breast cancer detection, *International Conference on Computing, Communications and Networking Technologies* [4th: Tiruchengode, India: 2013], pp. 1-7.

[10] Sam, A. and Jone, A.A. (2013). Ultra wideband Radar Based Breast Cancer Detection using Stacked Patch and Wide slot Antenna. *International Journal of Electronics Signals and Systems*, 3 (1), 36-40.

[11] Hassan, N.A *et al.* (2016). Basic Evaluation of Antennas used in Microwave Imaging for Breast Cancer Detection, *International Conference on Computer Science and Engineering* [3rd : Dubai,UAE:2016], pp. 55-63.

[12] Afyf, A. *et al.* (2015). A Novel Low Cost UWB Antenna for Early Breast Cancer Detection, *American Journal of Electromagnetics and Applications*, 3(5), 31-37.

[13] Lazaro, A., Villarino, R. and Girbau, D. (2011). Design of Tapered Slot Vivaldi Antenna for UWB Breast Cancer Detection, *Microwave and Optical Technology Letters*, 53(3), 639-643.

[14] Rufus, E., Alex, Z.C. and Chaitanya, P.V. (2008).A modified Bow-Tie Antenna for Microwave Imaging Applications, *Journal of Microwaves, Optoelectronics and Electromagnetic Applications*, 7(2), 115-122.

[15] Amineh, R.K. *et al.* (2009). Ultra Wideband TEM horn antenna for Microwave Imaging of the Breast, *International Symposium on Antenna Technology and Applied Electromagnetics and the Canadian Radio Science Meeting* [13th: Toronto,Canada:2009], pp. 1-4.

[16] Adnan, S. *et al.* (2010). A Compact UWB Antenna Design for Breast Cancer Detection, *PIER Letters*, 6(2), 129-132.

[17] Mahmud, M.Z., Islam, M.T. and Samsuzzaman, M. (2016). A High Performance UWB antenna design for Microwave Imaging System, *Microwave and Optical Technology Letters*, 58(8), 1824-1831.

[18] Singh, I. and Tripathi, V.S. (2011). Microstrip Patch Antenna and its Applications: a Survey, *International Journal of Computer Applications in Technology*, 2(5), 1595-1599.

[19] Balanis C.A., *Antenna Theory-Analysis and Design (3rd Edition)*, USA: John Wiley & Sons Inc., 2005, 811-846.

[20] Kumar, A., Gupta, N. and Gautam, P.C. (2016). Gain and Bandwidth Enhancement Techniques in Microstrip Patch Antennas: A Review. *International Journal of Computer Applications*, 148(7), 9-14.

[21] Nasr, M.A., Ouda, M.K. and Ouda, S.O. (2013). Design of Star-Shaped Microstrip Patch Antenna for Ultra Wideband Applications, *International Journal of Wireless and Mobile Networks*, 5(4), 65-73.

[22] Majidzadeh, M. and Ghobadi, C. (2012). Compact Microstrip Fed monopole Antenna with Modified Slot Ground plane for UWB Applications, *Applied Computational Electromagnetics Society Journal*, 27(10), 801-807.

[23] Kaur, A., Khanna, R. and Kartikeyan, M.V. (2015). A Stacked Sierpinski Gasket Gasket Fractal Antenna with a Defected Ground Structure for UWB/WLAN/Radio Astronomy/STM Link Applications, *Microwave and Optical Technology Letters*, 57(12), 2786-2792.

[24] Werner, D.H. *et al.* (2014). A review of high performance ultra wideband antenna array layout design, *European Conference on Antennas and Propagation* [8th: The Hague, Netherland: 2014], pp. 3128-3131.

[25] Mandal, T. and Das, S. (2013), Microstrip Feed Spanner Shape Monopole Antennas for Ultra Wideband Applications, *Jouranl of Microwaves, Optoelectronics and Electromagnetic Applications*, 12(1), 15-22.

[26] Dheyab, A.A. and Hamad, K.A. (2011). Improving Bandwidth Rectangular Patch Antenna using Different Thickness of Dielectric Substrate, *ARPN Journal of Engineering and Applied Sciences*, 6(4), 16-21.

[27] Gonzalo, R., Maagt, P.D. and Srolla, M. (1999). Enhanced patch antenna performance by suppressing surface waves using photonic band gap structures, *IEEE Transactions on Microwave Theory and Techniques*, 47(11), 2131-2138.

[28] Garg, R. *et al.*, *Microstrip Antenna Design Handbook*, Boston: Artech House, 2001, 3.

[29] Pozar, D.M. (1992). Microstrip antennas, *Proceedings of the IEEE*, 80(1), 79-91.

[30] Jung, J., Choi, W. and Choi, J. (2005). A Small Wideband Microstrip-fed Monopole Antenna, *IEEE Microwave and Wireless Components Letters*, 15(10), 703-705.

[31] Kaur, S. and Khanna, R. (2015). Design and analysis of stair-shape antenna with flowery DGS, *International Journal of Microwave and Wireless Technologies*, 7(1), 53-60.

[32] Ping, L.C *et al.* (2009). Design of Ultra Wideband slotted microstrip patch antenna, *Malaysia International Conference on Communications* [9th: Kuala Lumpur, Malaysia: 2009], pp.41-45.

[33] Azim, R. *et al.* (2011). Planar UWB antenna with multi-slotted ground plane, *Microwave and Optical Technology Letters*, 53(5), 966-968.

[34] Vuong, T.P. *et al.* (2007). Design and Characteristics of a Small U-slotted Planar Antenna for IR-UWB, *Microwave and Optical Technology Letters*, 49(7), 1727-1731.

[35] Kaur, A. *et al*. (2017). A Compact Staircase Slotted Microstrip Patch Antenna with DGS for UWB application, *International Conference on Advancements in Engineering and Technology* [5th: Sangrur, India: 2017], pp.66-68.

[36] Ghassemi, N. *et al*. (2007). Investigation of Multilayer Probe-Fed Microstrip Antenna for Ultra Wideband Operation, *Asia Pacific-Microwave Conference* [Bangkok, Thailand: 2007], pp. 1-4.

[37] Kasi, B., Ping, L.C. and Chakrabarty, C.K. (2011). A Compact Microstrip Antenna for Ultra Wideband Applications, *European Journal of Scientific Research*, 67(1), 45-51.

[38] Elkorany, A.S. *et al*. (2015). UWB integrated microstrip patch antenna with unsymmetrical opposite slots, *APS Topical Conference on Antennas and Propagation in Wireless Communications* [5th: Turin, Italy: 2015], pp.426-429.

[39] Yaccoub M.H *et al*. (2013). Rectangular Ring Microstrip patch antenna for Ultra Wideband Applications, *International Journal of Innovation and Applied Studies*, 4(2), 441-446.

[40] Liu, L. *et al*. (2011). A Compact Circular Ring Antenna for Ultra Wideband Applications, *Microwave and Optical Technology Letters*, 53(10), 2283-2288.

[41] Koohestani, M. and Golpour, M. (2010), U-shaped microstrip patch antenna with novel parasitic tuning stubs for ultra wideband applications, *IET Microwaves, Antennas and Propagation*, 4(7), 938-946.

[42] George, N. and Lethakumary, B. (2015). A Compact Microstrip Antenna for UWB Applications, *Microwave and Optical Technology Letters*, 57(3), 621-624.

[43] Djalal, Z.K. and Mouhamed, M.S. (2012).New Diamond Antenna for Ultra Wideband Applications, *International Journal of Computer Science Issues*, 9(4), 387-390.

[44] Dastranj, A., Imani, A. and Moghaddasi, M.N. (2008). Printed Wide-Slot Antenna for Wideband Applications, *IEEE Transactions on Antennas and Propagation*, 56(10), 3097-3102.

[45] Choi, S.H. *et al*. (2004). A New Ultra Wideband Antenna for UWB Applications, *Microwaves and Optical Technology Letters*, 40(5), 399-401.

[46] Telsang, T.M. and Kakade, A.B. (2014). Ultra Wideband Slotted Semicircular Patch Antenna, *Microwave and Optical Technology Letters*, 56(2), 362-369.

[47] Zhang, H. *et al*. (2010). Designs of Ultra Wideband Printed Elliptical Monopole antennas with slots, *Microwave and Optical Technology Letters*, 52(2), 466-471.

[48] Ping, L.C., Chakrabarty, C.K. and Khan, R.A. (2010). Enhanced Bandwidth of Impulse-Ultra Wideband Slotted Rectangular Patch Antenna with Partial Ground Plane, *International Journal of Electronics, Computer and Communications Technologies*, 1(1), 21-25.

[49] Beigi, P. *et al*. (2015). Bandwidth Enhancement of Small Square Monopole Antenna with Dual Band Notch Characteristics using U-Shaped Slot and Butterfly Shape Parasitic Element on Backplane for UWB applications, *Applied Computational Electromagnetics Society Journal*, 30(1), 78-85.

[50] Wu, C.M., Chen, Y.L. and Wen, C.L. (2012). A Compact Ultra Wideband Slotted Patch Antenna for Wireless Dongle Application, *IEEE Antennas and Wireless Propagation Letters*, 11, 596-599.

[51] Kaur, A. and Kaur, A. (2017). An Extended Semi-circular Microstrip Patch Antenna with DGS for UWB Applications, Journal of Microwave Engineering and Technology, 4(1), 13-18.

[52] Lee, C.P., and Chakrabarty, C.K. (2011). Ultra Wideband Microstrip Diamond Slotted Patch Antenna with Enhanced Bandwidth, *International Journal of Communications, Network and System Sciences*,4(7), 468-474.

[53] Moghadasi, M.N. *et al.* (2009). Ultra wideband square slot antenna with a novel diamond open-ended microstrip feed, *Microwave and Optical Technology Letters*, 51(4), 1075-1080.

[54] Hanapi, K.M. *et al*. (2014). An elliptically planar UWB monopole antenna with step slots defective ground structure, *Microwaves and Optical Technology Letters*, 56(9), 2084-2088.

[55] Arya, A.K., Patnaik, A. and Kartikeyan, M.V. (2013). Gain Enhancement of Microstrip patch antenna using Dumbbell shaped Defected Ground Structure, *International Journal of Scientific Research Engineering and Technology*, 2(4), 184-188.

[56] Arya, A.K., Kartikeyan, M.V. and Patnaik, A. (2010). Defected Ground Structure in the perspective of Microstrip Antennas: A Review, *Frequenz, International Journal of RF-Engineering and Telecommunication*, 64(5-6), 79-84.

[57] Reddy, B.R. and Vakula, D. (2014). Compact Zigzag Shaped Slit Microstrip Antenna with Circular Defected Ground Structure for Wireless Applications, *IEEE Antennas and Wireless Propagation Letters*, 14, 678-681.

[58] Toshniwal, S. *et al*. (2015), Compact Design of rectangular Patch Antenna with Symmetrical U-slots on Partial Ground for UWB Applications, *International Conference on Innovations in Bio-Inspired Computing and Applications*[6th: Kochi, India: 2015], pp.535-542.

[59] Seong, H.L., Park, J.K. and Jung, N.L. (2004). A Novel CPW fed Ultra Wideband Antenna Design, *Microwave and Optical Technology Letters*, 44(5), 393-396.

[60] Matin, M.A., Sharif, B.S. and Tsimenidis, C.C. (2007). Dual layer Stacked Rectangular Microstrip Patch Antenna for UWB Applications, *IET Microwaves, Antennas & Propagation*, 1(6), 1192-1196.

[61] Maity, S. and Gupta, B. (2013). Accurate resonant frequency of isosceles right-angled triangular patch antenna, *Microwave and Optical Technology Letters*, 55(6), 1306-1308.

[62] Chen, W., Lee, K.F. and Dahele, J.S. (1992). Theoretical and Experimental Studies of Resonant Frequencies of the Equilateral Triangular Microstrip Antenna, *IEEE Transactions on Antennas and Propagation*, 40(10), 1253-1256.

LIST OF PUBLICATIONS

PUBLISED

- Kaur, A. *et al.* (2017). A Compact Staircase Shaped Slotted Microstrip Patch Antenna with DGS for UWB Applications, *International Conference on Advancements in Engineering and Technology*, [5th: Sangrur: India, 2015], pp. 66-69.
- Kaur, A. and Kaur, A. (2017). An Extended Semi-circular Microstrip Patch Antenna with DGS for UWB applications, *Journal of Microwave Engineering &Technology*, 4(1), 13-18.

COMMUNICATED

- Kaur, A. and Kaur, A. (2017). A Miniature Fork Shaped Microstrip Patch Antenna with L-Shaped Tuning Stubs and a Reduced DGS for UWB/WLAN/STM/INSAT Applications, *International Journal of Microwave and Wireless Technologies*
- Kaur, A. and Kaur, A. (2017). A Compact UWB Microstrip Patch Antenna loaded with Stubs and Defected Partial Ground Structure for Breast Cancer Detection, *Wireless Personal Communications*

Thesis

ORIGINALITY REPORT

%19	%9	%16	%0
SIMILARITY INDEX	INTERNET SOURCES	PUBLICATIONS	STUDENT PAPERS

PRIMARY SOURCES

1	bradscholars.brad.ac.uk Internet Source	%1
2	aut.researchgateway.ac.nz Internet Source	%1
3	Proceedings of the International Conference on Recent Cognizance in Wireless Communication & Image Processing, 2016. Publication	%1
4	Lee Chia Ping. "Design of Ultra Wideband slotted microstrip patch antenna", 2009 IEEE 9th Malaysia International Conference on Communications (MICC), 12/2009 Publication	<%1
5	"Handbook of Antenna Technologies", Springer Nature, 2016 Publication	<%1
6	Lecture Notes in Electrical Engineering, 2015. Publication	<%1
7	Kaur, Amanpreet, Rajesh Khanna, and	<%1